การสังเคราะห์ไทรเอซีนที่มีพอร์ไฟรินเพื่อเป็นสารประกอบไวแสงสำหรับเซลล์สุริยะ

นายอริย์ธัช ลือชัย

วิทยานิพนธ์นี้เป็นส่วนหนึ่งของการศึกษาตามหลักสูตรปริญญาวิทยาศาสตรมหาบัณฑิต
สาขาวิชาปิโตรเคมีและวิทยาศาสตร์พอลิเมอร์
คณะวิทยาศาสตร์ จุฬาลงกรณ์มหาวิทยาลัย
ปีการศึกษา 2553
ลิขสิทธิ์ของจุฬาลงกรณ์มหาวิทยาลัย

SYNTHESIS OF TRIAZINES CONTAINING PORPHYRIN AS PHOTOACTIVE COMPOUNDS FOR SOLAR CELLS

Mr. Arithat Luechai

A Thesis Submitted in Partial Fulfillment of the Requirements
for the Degree of Master of Science Program in Petrochemistry and Polymer Science
Faculty of Science
Chulalongkorn University
Academic Year 2010
Copyright of Chulalongkorn University

Thesis Title	SYNTHESIS OF TRIAZINES CONTAINING PORPHYRIN AS PHOTOACTIVE COMPOUNDS FOR SOLAR CELLS
By	Mr. Arithat Luechai
Field of Study	Petrochemistry and Polymer Science
Thesis Advisor	Associate Professor Amorn Petsom, Ph.D.
Thesis Co-advisor	Assistant Professor Patchanita Thamyongkit, Ph.D.

Accepted by the Faculty of Science, Chulalongkorn University in Partial Fulfillment of the Requirements for the Master's Degree

…… Dean of the Faculty of Science
(Professor Supot Hannongbua, Dr.rer.nat.)

THESIS COMMITTEE

…… Chairman
(Associate Professor Supawan Tantayanon, Ph.D.)

…… Thesis Advisor
(Associate Professor Amorn Petsom, Ph.D.)

…… Thesis Co-advisor
(Assistant Professor Patchanita Thamyongkit, Ph.D.)

…… Examiner
(Associate Professor Voravee P. Hoven, Ph.D.)

…….External Examiner
(Nantanit Wanichacheva, Ph.D.)

อริย์ธัช ลือชัย : การสังเคราะห์ไทรเอซีนที่มีพอร์ไฟรินเพื่อเป็นสารประกอบไวแสงสำหรับเซลล์สุริยะ. (SYNTHESIS OF TRIAZINES CONTAINING PORPHYRIN AS PHOTOACTIVE COMPOUNDS FOR SOLAR CELLS) อ.ที่ปรึกษาวิทยานิพนธ์หลัก : รศ. ดร. อมร เพชรสม, อ.ที่ปรึกษาวิทยานิพนธ์ร่วม : ผศ. ดร.พัชณิตา ธรรมยงค์กิจ, 86 หน้า.

พอร์ไฟรินในฐานะตัวเก็บเกี่ยวแสงในอุปกรณ์อิเล็กโทรนิกทางแสง เป็นสารที่มีประโยชน์มากในการดูดกลืนแสง การส่งผ่านประจุที่ดีเยี่ยม และง่ายต่อการปรับเปลี่ยนโครงสร้าง งานวิจัยนี้เกี่ยวข้องกับการสังเคราะห์สารประกอบพอร์ไฟริน การศึกษาสมบัติทางเคมีไฟฟ้า สมบัติทางแสงเชิงกายภาพ และการประดิษฐ์และประเมินผลของเซลล์สุริยะที่มีสารประกอบพอร์ไฟรินเป็นองค์ประกอบ สารประกอบพอร์ไฟรินเป้าหมายประกอบด้วยพอร์ไฟริน 2–3 หน่วย ซึ่งเชื่อมต่อกันผ่านหน่วยไทรเอซีน ในส่วนของสารประกอบที่มีพอร์ไฟริน 2 หน่วย ตำแหน่งที่เหลือบนวงไทรเอซีนจะถูกเชื่อมต่อด้วยหมู่ 4-carboxy phenyl, 4-(2-carboxy-2-cyanoethynyl)phenyl หรือหมู่คาร์บามิล การใช้พอร์ไฟรินที่มากกว่าหนึ่งวงช่วยเพิ่มประสิทธิภาพในการเก็บเกี่ยวแสง ในขณะที่ไทรเอซีนเป็นที่รู้จักกันดีในฐานะตัวส่งผ่านประจุที่ดี ไซคลิกโวลแทมเมตรีถูกใช้พิจารณาระดับพลังงาน HOMO และ LUMO ของสารประกอบเหล่านี้ ลักษณะทางสัณฐานวิทยาของฟิล์มก็ถูกศึกษาด้วยเช่นกัน โดยอาศัยผลการศึกษาเบื้องต้นเหล่านี้ เซลล์สุริยะถูกเตรียมเพื่อนำมาประเมินประสิทธิภาพการเปลี่ยนแปลงพลังงานแสงให้เป็นพลังงานไฟฟ้าต่อไป

สาขาวิชา...ปิโตรเคมีและวิทยาศาสตร์พอลิเมอร์ ลายมือชื่อนิสิต.....

ปีการศึกษา……2553…….. ลายมือชื่ออ.ที่ปรึกษาวิทยานิพนธ์หลัก.....

ลายมือชื่ออ.ที่ปรึกษาวิทยานิพนธ์ร่วม.....

5172546723 : PETROCHEMISTRY AND POLYMER SCIENCE
KEYWORDS: PORPHYRIN / TRIAZINE / PHOTOACTIVE COMPOUND / BULK HETEROJUNCTION SOLAR CELLS / DYE-SENSITIZED SOLAR CELLS

ARITHAT LUECHAI : SYNTHESIS OF TRIAZINES PORPHYRIN AS PHOTOACTIVE COMPOUNDS FOR SOLAR CELLS ADVISOR : ASSOC. PROF. AMORN PETSOM, Ph.D., CO-ADVISOR : ASST. PROF. PATCHANITA THAMYONGKIT, Ph.D., 86 pp.

Porphyrins as light harvesters in optoelectronic device are useful for their extremely high potential absorption coefficients excellent change mobility, and relative ease with which a variety of covalent and non-covalent bonding possibilities. This research described the synthesis of a series of porphyrinic compounds, investigation of their electrochemical and photophysical properties, and fabrication/evaluation of solar cells based on these compounds. The target molecules include two or three porphyrin macrocycles connected via triazine units. When two porphyrin macrocycles are presented, the remaining peripheral position on the triazine ring is taken by a 4-carboxyphenyl group or 4-(2-carboxy-2-cyanoethenyl)phenyl anchoring group or carbamyl group. Introduction of more than one porphyrin macrocycle enhances the light-harvesting efficiency of these compounds. Triazines are known to be good charge transporters. Cyclic voltammograms of these compounds were recorded to obtain HOMO-LUMO energy levels, and the film morphology was investigated as well. According to finding from these studies, organic photovoltaic cells were prepared and light-to-electrical energy conversion efficiencies of the resulting devices were evaluated.

Field of study:..Petrochemistry and Polymer science Student's signature:……..

Academic year: ……2010…… Advisor's signature:……..

Co-advisor's signature:….....

ACKNOWLEDGEMENTS

I would like to begin by thanking Associate Professor Dr. Amorn Petsom and Assistant Professor Dr. Patchanita Thamyongkit for being the best advisors anyone could ever ask for. There no words that can express the depth of gratitude that I have toward them. They have supported me in everything that I set out to improve the synthetic skills, believe in me even at the moment of my life when I was down and help me to get back on my feet.

I also grateful to Associate Professor Dr. Supawan Tuntayanon, for serving as the chairman, Associate Professor Dr. Voravee P. Hoven and Dr. Nantanit Wanichacheva for serving as the members of my thesis committee, respectively, for their valuable suggestion and comments.

I would like to thank Marie Curie international incoming fellowship (PIIF-GA-2008-220272), Thailand Research Fund-Master research grants-Window II (TRF-MAG-WII525S022), the Center of Excellent of Petroleum, Petrochemicals and Advance Material, and graduate school of Chulalongkorn university for partial financial support of this research.

I also thank Research Centre for Bioorganic Chemistry (RCBC) for warm welcome into their family, great experience and laboratory facilities. I feel blessed and privileged to have joined a group with great members who supported me throughout this course.

Finally, I am grateful to my family and my friends for their love, understanding and great encouragement the entire course of my study.

CONTENTS

Page

ABSTRACT (THAI)..... iv

ABSTRACT (ENGLISH)..... v

ACKNOWLEDGEMENTS..... vi

CONTENTS..... vii

LIST OF FIGURES..... ix

LIST OF SCHEMES..... xii

LIST OF CHARTS..... xiii

LIST OF ABBREVIATIONS..... xiv

CHAPTER I INTRODUCTION..... 1

1.1 Objectives of this research..... 2

1.2 Scope of this research..... 3

CHAPTER II THEORY AND LITERATURE REVIEWS..... 4

THEORY..... 4

2.1 Organic Solar Cell..... 4

2.2 Bulk Heterojunction Solar Cells..... 7

2.3 Dye-sensitized Solar Cells..... 9

2.4 Porphyrin..... 9

2.5 Triazine..... 11

LITERATURE REVIEWS..... 12

CHAPTER III EXPERIMENTAL..... 16

3.1 Chemicals..... 16

3.2 Analytical Instruments..... 17

3.3 Experimental Procedure..... 18

Part 1: Synthesis of triazine-porphyrin derivatives for bulk heterojunction solar cells..... 18

Page

3.3.1 5-(4-nitrophenyl)-10,15,20-triphenylporphyrin (**5**)…..……... 18
3.3.2 5-(4-aminophenyl)-10,15,20-triphenylporphyrin (**6**)..…….. 18
3.3.3 Compound **Zn-1**..... 19
3.3.4 Compound **Zn-8**……..... 20
Part 2: Synthesis of triazine-porphyrin derivatives for dye-sensitized solar cells..... 21
3.3.5 3-(4-aminophenyl)-2-cyano acrylic acid (**10**).....…….. 21
3.3.6 Compound **Zn-2**.....…… 21
3.3.7 Compound **2**..... 22
CHAPTER IV RESULTS AND DISCUSSION……... 23
4.1 Synthesis of Triazine-porphyrin Derivatives for Bulk Heterojunction Solar Cell...…… 23
4.2 Synthesis of Triazine-porphyrin Derivatives for Dye-sensitized Solar Cells……... 26
4.3 Electrochemical and Photophysical Properties……... 30
4.3.1 Compound **Zn-1**..... 30
4.3.2 Compound **Zn-2**..... 32
CHAPTER V CONCLUSION……... 34
REFFERENCES…...…… 35
APPENDIX…..... 38
VITA……...…… 86

LIST OF FIGURES

Figure		Page
1-1	Molecular structures of compounds **Zn-1–4**.....	2
2-1	Principle operation of bilayer organic solar cell…..……..	4
2-2	Primary structure of organic solar cell……...	5
2-3	Current density-voltage curve……	5
2-4	The different morphorogies of heterojunctions…….	7
2-5	Working principle of bulk heterojunction solar cells.....……..	8
2-6	Operation principle of dye-sensitized solar cells.....	9
2-7	Schematic bulk heterojunction structure.....	15
4-1	Comparative energy diagram of compound **Zn-1**–based bulk heterojunction.....	30
4-2	Result of photoluminescence study of the films.....	31
4-3	A schematic cell structure of a bulk heterojunction solar cell based on **Zn-1**.....	31
4-4	Comparative energy diagram of compound **Zn-2**–based dye-sensitized.....	33
1	^{1}H-NMR spectrum of compound **5**.....	39
2	^{13}C-NMR spectrum of compound **5**.....	40
3	MALDI-TOF mass spectrum of compound **5**.....	41
4	^{1}H-NMR spectrum of compound **6**.....	42
5	^{13}C-NMR spectrum of compound **6**.....	43
6	MALDI-TOF mass spectrum of compound **6**.....	44
7	MALDI-TOF mass spectrum of compound **7**.....	45
8	MALDI-TOF mass spectrum of compound **8**.....	46
9	^{1}H-NMR spectrum of compound **Zn-1**.....	47
10	^{13}C-NMR spectrum of compound **Zn-1**.....	48
11	IR spectrum of compound **Zn-1**.....	49

Figure **Page**

12 MALDI-TOF mass spectrum of compound **Zn-1**..... 50

13 UV-Vis spectrum of compound **Zn-1**..... 51

14 Calibration curve for quantitative determination of compound **Zn-1** in toluene (λ_{abs} = 431 nm)..... 52

15 Calibration curve for quantitative determination of compound **Zn-1** in toluene (λ_{abs} = 552 nm)..... 53

16 Calibration curve for quantitative determination of compound **Zn-1** in toluene (λ_{abs} = 601 nm)..... 54

17 Fluorescence spectrum of compound **Zn-1**..... 55

18 ^{1}H-NMR spectrum of compound **Zn-8**..... 56

19 ^{13}C-NMR spectrum of compound **Zn-8**..... 57

20 IR spectrum of compound **Zn-8**..... 58

21 MALDI-TOF mass spectrum of compound **Zn-8**..... 59

22 UV-Vis spectrum of compound **Zn-8**..... 60

23 Calibration curve for quantitative determination of compound **Zn-8** in toluene (λ_{abs} = 422 nm)..... 61

24 Calibration curve for quantitative determination of compound **Zn-8** in toluene (λ_{abs} = 554 nm)..... 62

25 Calibration curve for quantitative determination of compound **Zn-8** in toluene (λ_{abs} = 599 nm)..... 63

26 Fluorescence spectrum of compound **Zn-8**..... 64

27 ^{1}H-NMR spectrum of 3-(4-aminophenyl)-2-cyano acrylic acid (**10**)... 65

28 ^{13}C-NMR spectrum of 3-(4-aminophenyl)-2-cyano acrylic acid (**10**). 66

29 ^{1}H-NMR spectrum of compound **Zn-2**..... 67

30 ^{13}C-NMR spectrum of compound **Zn-2**..... 68

31 IR spectrum of compound **Zn-2**..... 69

Figure **Page**

32 MALDI-TOF mass spectrum of compound **Zn-2**..... 70

33 UV-Vis spectrum of compound **Zn-2**..... 71

34 Calibration curve for quantitative determination of compound **Zn-2** in THF (λ_{abs} = 422 nm)..... 72

35 Calibration curve for quantitative determination of compound **Zn-2** in THF (λ_{abs} = 557 nm)..... 73

36 Calibration curve for quantitative determination of compound **Zn-2** in THF (λ_{abs} = 595 nm)..... 74

37 Fluorescence spectrum of compound **Zn-2**..... 75

38 ^{1}H-NMR spectrum of compound **2**..... 76

39 ^{13}C-NMR spectrum of compound **2**..... 77

40 MALDI-TOF mass spectrum of compound **2**..... 78

41 UV-Vis spectrum of compound **2**..... 79

42 Calibration curve for quantitative determination of compound **2** in THF (λ_{abs} = 419 nm)..... 80

43 Calibration curve for quantitative determination of compound **2** in THF (λ_{abs} = 515 nm)..... 81

44 Calibration curve for quantitative determination of compound **2** in THF (λ_{abs} = 550 nm)..... 82

45 Calibration curve for quantitative determination of compound **2** in THF (λ_{abs} = 587 nm)..... 83

46 Calibration curve for quantitative determination of compound **2** in THF (λ_{abs} = 650 nm)..... 84

47 Fluorescence spectrum of compound **2**..... 85

LIST OF SCHEMES

Scheme **Page**

2-1 Principle synthesis of substituent triazine..... 11

4-1 Synthesis of porphyrin-triazine **Zn-1**..... 24

4-2 Synthesis of porphyrin-triazine **2**..... 26

4-3 Synthesis of porphyrin-triazine **Zn-2**..... 27

4-4 Synthesis of porphyrin-triazine **Zn-3**..... 28

4-5 Synthesis of porphyrin-triazine **Zn-4**..... 29

LIST OF CHARTS

Chart		Page
2-1	Structure of 5,10,15,20-tetrakis(4-carboxyphenyl) porphinatozinc II....	10
2-2	Triazine-containing carbozole structure.....	12
2-3	Triazine-based compounds.....	13
2-4	1,3,5–triazine with electron-donating groups.....	13
2-5	Triazine based electron-donating group.....	13
2-6	4,4’-bis-[2-(4,6-diphenyl-1,3,5-triazinyl)]-1,1’-biphenyl (**2**).....	14
2-7	Structure of **3**.....	14
2-8	Zn-porphyrin derivatives with anchoring group.....	15

LIST OF ABBREVIATIONS

λ_{abs}	:	absorption wavelength
calcd	:	calculated
^{13}C-NMR	:	carbon-13 nuclear magnetic resonance spectroscopy
δ	:	chemical shift
J	:	coupling constant
ºC	:	degree Celsius
$CDCl_3$	:	deuterated chloroform
d	:	doublet (NMR)
g	:	gram (s)
^{1}H-NMR	:	proton nuclear magnetic resonance spectroscopy
Hz	:	hertz (s)
h	:	hour (s)
IR	:	Infrared spectroscopy
MS	:	mass spectrometry
MALDI-MS	:	matrix-assisted laser desorption ionization mass spectrometry
λ_{ex}	:	excitation wavelength
λ_{em}	:	emission wavelength
CH_2Cl_2	:	methylene chloride
mL	:	milliliter (s)
mmol	:	millimole (s)
ε	:	molar absorptivity
m	:	multiplet (NMR)
nm	:	nanometer
NMR	:	nuclear magnetic resonance spectroscopy
obsd	:	observed
OLED	:	organic light emitting diode
ppm	:	parts per million
PEDOT:PSS	:	Polyethylenedioxythiophene:polystyrenesulfonate

PLED	:	Polymer light-emitting diodes
P3HT	:	poly(3-hexyl thiophene)
PCBM	:	Phenyl-C61-butyric acid methyl ester
THF-d_8	:	Deuterated tetrahydrofuran
t	:	triplet (NMR)
HOMO	:	the highest occupied molecular orbital
LUMO	:	the lowest unoccupied molecular orbital
UV-Vis	:	ultraviolet and visible spectroscopy
cm^{-1}	:	unit of wavenumber (IR)

CHAPTER I

INTRODUCTION

The expectations of decreasing fossil oil usage and increasing environmental concern have encouraged the research on inexpensive renewable energy source. Solar energy is the largest energy source available on the earth. Harvesting energy directly from sunlight using photovoltaic (PV) cells is broadly recognized as a promising approach to future global energy production. Nowadays, inorganic solar cell is dominating the present market, while organic solar cell has been developed for recent years. Compared with inorganic solar cells, organic solar cells have several advantages to increase energy conversion efficiency by various methods.[1–3]

Organic solar cells based on heterojunction blending of electron donating and accepting materials in which nanoscale phase separation is created to achieve both quantitative charge generations after photo-excitation and effective collection of these charge. Therefore, the interesting for bulk heterojunction solar cells are radically increasing because of low-cost cell fabrication, ease of modification of photoactive compound, and possibility for making flexible devices. While the bulk-heterojunction solar cells are greatly developed, dye-sensitized solar cell is one of the most popular organic solar cells. Its primary structure consists of the metal electrode, photoactive compound binding on TiO_2 surface and electrolyte. According to recent studies, anchoring groups that exhibit its electronic property as electron withdrawing group such as carboxylate, phosphonate or cyano acrylate group are essential for photoactive compound to bind to TiO_2 surface and increase electron transfer efficiency.[1–4]

Porphyrin derivatives which have been widely known as highly absorptive organic compounds due to its characteristic, such as high absorptivity in visible wavelength and high photo-, thermal- and chemical stability, become promising photoactive compounds for organic solar cell application. According to recent studies, triazine derivatives have high electron affinity and have been broadly explored as building blocks for electron-transporting materials (ETMs) for organic light-emitting diodes (OLEDs).[1–4]

To integrate these beneficial properties of porphyrin and triazine compounds, this research aims to develop a porphyrin-triazine derivative bearing three porphyrin macrocycle connected to each other in three-branch fashion via a triazine core unit for bulk heterojunction solar cells. For dye-sensitized solar cells, two porphyrin and anchoring groups will be connected via triazine core unit. The target molecules will be observed essential properties for solar cells devices for instance electrochemical and photophysical properties and are expected to have high absorptivity and satisfactory charge transfer properties.

1.1 Objectives of this research

The objectives of this research are synthesizing porphyrin-triazine compounds **Zn-1–4** as photoactive compounds for bulk heterojunction and dye-sensitized solar cells.

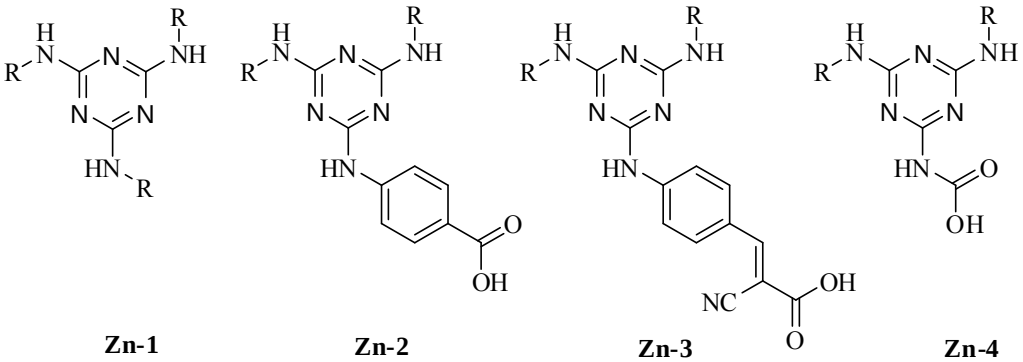

Zn-1 **Zn-2** **Zn-3** **Zn-4**

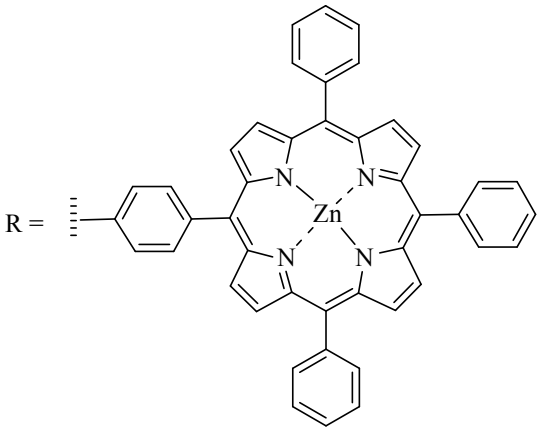

Chart 1-1. Molecular structures of compounds **Zn-1–4**.

1.2 Scope of this research

The scope of this research covers the synthesis of porphyrin-trazine derivatives bearing three and two porphyrin macrocycles. These photoactive compounds will be fully characterized by various spectroscopic techniques such as mass spectrometry, ^{1}H-NMR and ^{13}C-NMR spectroscopy, ATR-FTIR spectrophotometry and UV-Vis and Fluorescence spectrophotometry. To determine the potential use of the target compounds in organic solar cells, photoluminescence and electrochemical properties of the compounds and energy conversion efficiency of the resulting solar cells will be investigated as well.

CHAPTER II
THEORY AND LITERATURE REVIEWS

THEORY

2.1 Organic Solar Cell

Organic solar cells have been of interest as one of the most promising alternative energy source. The first organic solar cell with 1% power conversion efficiency was invented in 1980s. Its characteristic was based on bilayer made of donor and acceptor materials. In principle, the cell operation starts from light absorption primarily by a donor material to generate photo-excited electrons and positive counterparts (hole). The excitons, pairs of excited electrons and holes, diffuse within donor toward the interface to the acceptor material which has stronger electronegativity. Then, holes stay on donor material and move towards an anode while electrons diffuse through acceptor to a cathode to generate electrical current in an external circuit (Figure 2-1).[1,6,7,9]

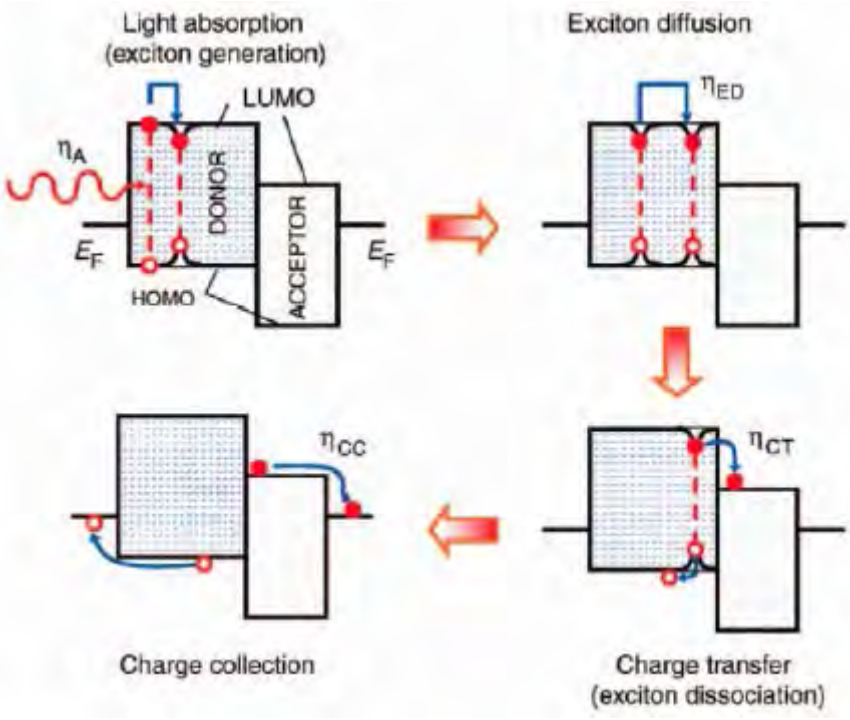

Figure 2-1. Principle operation of bilayer organic solar cell.

In practice, this organic solar cell contains 4 primary components as shown in Figure 2-2. A glass is coated by ITO layer which is a transparent electrode layer(s). On top of the ITO layer, a film of an organic photosensitizer or a blend of photoactive compounds is placed before a metal electrode, which is aluminum in this case, is evaporated on top of the organic layer.

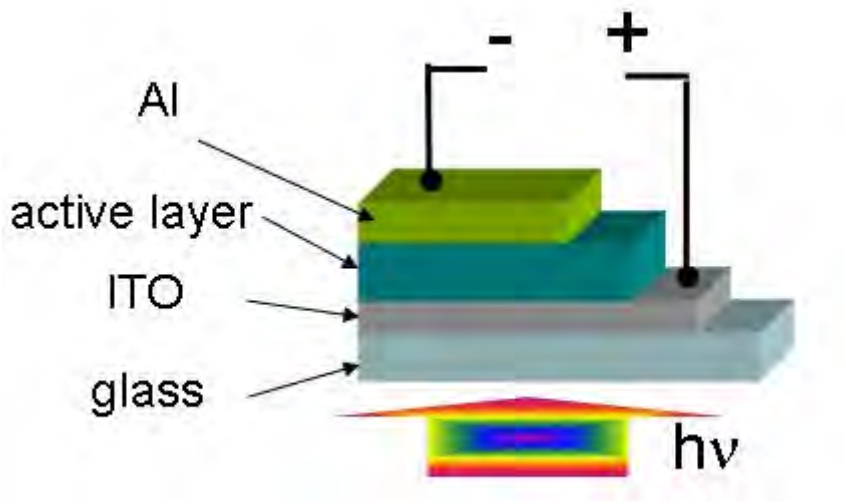

Figure 2-2. Primary structure of organic solar cell.

The basic parameters describing the performance of photovoltaic cell *i.e.* maximum power point (P_{mp}), fill factor (FF), energy-conversion efficiency (η_e) and incident photon to converted electron efficiency (IPCE) can be extracted from a current-voltage curve (Figure 2-3). The plot exhibits external electrical current which is measured as a function of externally applied voltage.

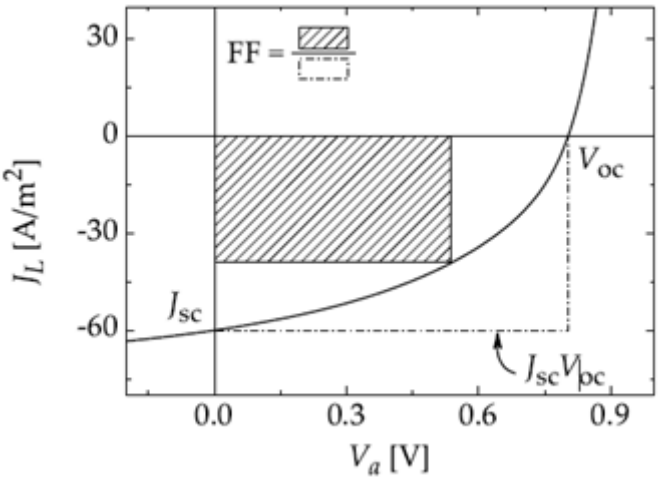

Figure 2-3. Current density-voltage curve.

The point where this power is maximized is called the *maximum power point* (P_{mp}) and is given by Equation (1).

$$P_{mp} = I_{mp} \cdot V_{mp} \quad (1)$$

Where I_{mp} is maximum current point and V_{mp} is maximum voltage point and P_{mp} corresponds to the area of rectangle under I-V curve.

Two other important parameters exhibited are short-circuit current (I_{sc}) and open-circuit voltage (V_{oc}). I_{sc} is the electric current flowing through the circuit under illumination without external applied voltage (V = 0 V). Since a measurement of I_{sc} depends on area of photovoltaic cells, it is commonly reported as the short-circuit current density (J_{sc}). V_{oc} is the value of bias applied without the external current flowing toward the circuit under illumination (I = 0 A).

From the I-V curve with analogous to the coordinate of the maximum power point, the second rectangle can be indicated by I_{sc} and V_{oc} points. The ratio of two rectangles indicates the quality of the shape of I-V characteristic called *fill factor* (FF). It defines the ration of the actual maximum power extracted to the theoretical upper limit from I_{sc} and V_{oc} as shown in Equation (2).

$$FF = \frac{P_{mp}}{V_{oc} \cdot I_{sc}} = \frac{V_{mp} \cdot I_{mp}}{V_{oc} \cdot I_{sc}} \quad (2)$$

Furthermore, these parameters relate to efficiency of a cell called *energy-conversion efficiency* (η) whose the calculation is described by Equation (3).

$$\eta = \frac{P_{mp}}{P_{in}} = \frac{V_{mp} \cdot I_{mp}}{P_{in}} = \frac{V_{oc} \cdot I_{sc} \cdot FF}{P_{in}} \quad (3)$$

The overall efficiency can be described by incident photon to converted electron efficiency (IPCE). The IPCE is calculated by number of electron leaving the device under short circuit condition per time and area divided by the number of photons incident per time and area

$$\text{IPCE} = \frac{\#\ \text{extracted electrons}}{\#\ \text{incident photons}} \qquad (4)$$

The IPCE is a measurement of the external quantum efficiency, meaning that losses due to reflection at surface or transmission through the device are included in the IPCE value. Subtracting these two loss channels would lead to the internal quantum efficiency, which is rarely used to compare solar cells.

For effective comparison, all parameters must be observed under standard illumination conditions. The standard test condition (STC) of solar cell is the Air Mass 1.5 spectrum (AM 1.5G), an incident power density of 1000 $W \cdot m^{-2}$, which is defined as a standard "1 sun" value at ambient temperature of 25 °C.[7]

2.2 Bulk Heterojunction Solar Cells.

Bulk heterojunction solar cell is classified to be in the third generation of photovoltaic devices. The concept of energy conversion is based on donor-acceptor heterojunction. In heterojunction solar cell, there are four primary modes of realizing the inner structure of heterojunction, which have been developed and named as a) two-layer heterojunction, b) bulk heterojunction, c) molecular heterojunction and d) double-cable polymers (Figure2-4).

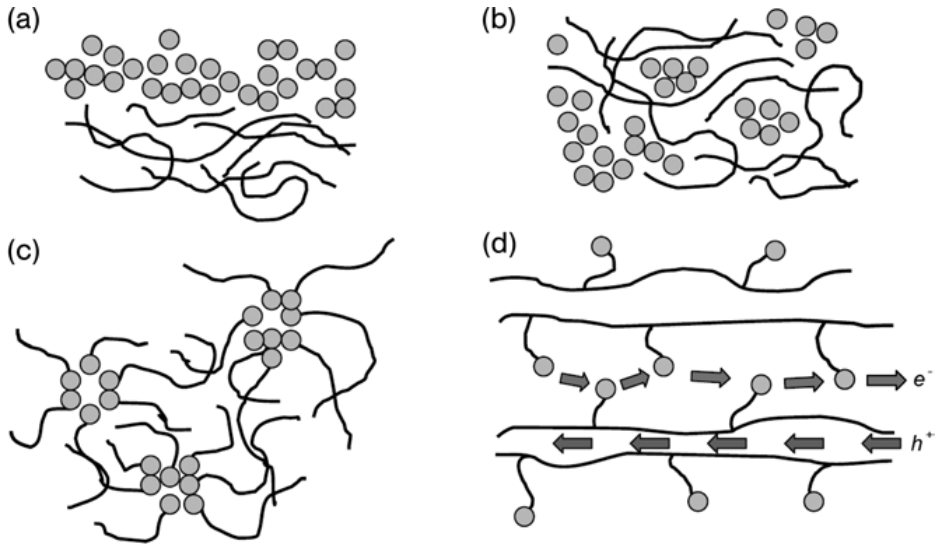

Figure 2-4. The different morphologies of heterojunctions:
(a) two-layer heterojunction, (b) bulk heterojunction, (c) molecular heterojunction and (d) double-cable polymers

The different between bi-layer (two-layer) and bulk heterojunction is the increase in interfacial contact between donor and acceptor material. However, a drawback of the bulk heterojunction structure is that a percolating pathway for the hole and electron transporting phase to the electrode is needed in order that the separated charge carriers can reach their corresponding electrodes.[9,7]

Under illumination of the bulk heterojunction solar cell, the donor molecules are excited by the sunlight photons absorbed, leading to the formation of excitons. In reality, the acceptor phase can also absorb light, but for simplicity only the photons that are absorbed by the donor phase are taken into consideration here. The excitons start to diffuse within the donor phase until they reach the interface with the acceptor where fast charge separation takes place. The resulting metastable electron-hole pairs across the donor/acceptor interface may still be coulombically bound and an electric field is needed to separate them into free charges. However, if the individual layer thicknesses (in case of a bilayer structure) or phase separated domains (in case of a blend layer) is larger than diffusion length of exciton, most of the excitons may recombine in donor phase (Figure2-5). In another word, if the excitons are generated in close proximity to an interface, they have chance to be separated into free charge carriers which might diffuse to the corresponding electrodes.[10]

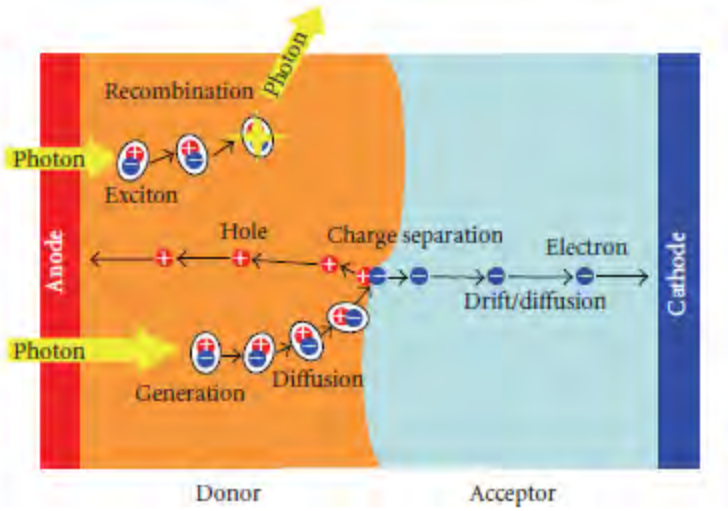

Figure 2-5. Working principle of bulk heterojunction solar cells

2.3 Dye-sensitized Solar Cells

The working mechanism of dye-sensitized solar cell (DSSC) relies on optical absorption and the charge separation processes by association of a sensitizer as light absorbing material with wide band gap semiconductor of nanocrystalline morphology. As shown in Figure 2-6, DSSC consists of five primary components, *i.e.* transparent conducting glass, TiO_2, dye, electrolyte and metal electrode. The heart of the system is a mesoporous oxide layer composed of nanometer-sized particles allowing the electronic conduction to take place. Attached to the surface of the nanocrystalline film is a monolayer of the dye. Photo-excitation of the sensitizer provided electron injection into conduction band of mesoporous oxide semiconductor. Then, electrons pass through the metal oxide to the electrode. The dye or sensitizer molecule is regenerated by redox reaction from counter electrode by electron passed through the electrolyte which is commonly used I^-/I_3^- solution.

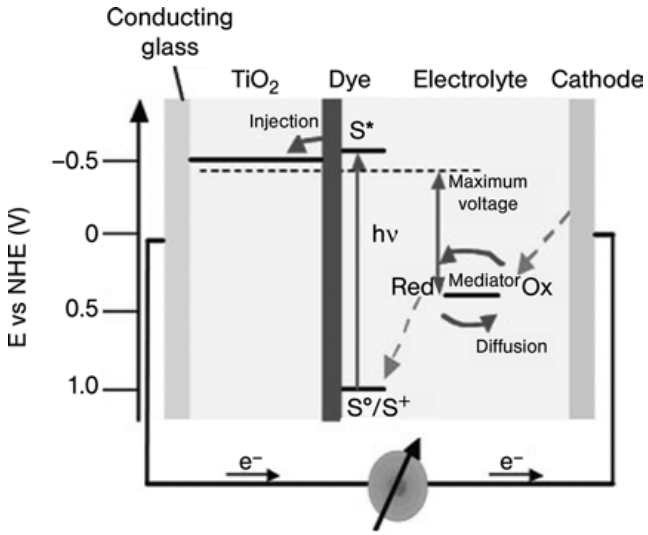

Figure 2-6. Operation principle of dye-sensitized solar cells.

The voltage generated under illumination corresponds to the difference between the Fermi level of the electron in the solid and the redox potential of the electrolyte. Overall the device generates electric power from sun light without suffering any permanent chemical transformation.[11,12]

2.4 Porphyrin

Porphyrins are interesting biochemical compound. In nature, they present in several forms including chlorophyll, myoglobins, hemes and several others. In

photosynthesis processes, porphyrins are one of the most important compounds. In common life, porphyrins are generally used in various applications in chemical and medical research. For example:

1. Solar energy conversion
2. Catalysis and photocatalysis
3. Sensoring and biosensoring
4. Photodynamic therapy (PDT)

Various porphyrins have been demonstrated as photosensitizer in solar cells, especially DSSCs. The most common porphyrins being investigated are the free-base and zinc derivatives of 5,10,15,20-tetra(4-carboxyphenyl) porphyrin (TCPP and Zn-TCPP, Chart 2-1), because theses porphyrins exhibit long-live π* singlet excited states and only weak singlet/triplet mixing. They have an appropriate LUMO energy level that resides above the conduction band of the TiO_2 and a HOMO energy level that lies below the redox couple in the electrolyte solution, required for charge separation at the solar cell dye/electrolyte surface. The relative LUMO and HOMO energy levels have been estimated for a wide range of dyes including TCPP and Zn-TCPP bound to TiO_2 using a UV photoemission technique.[13]

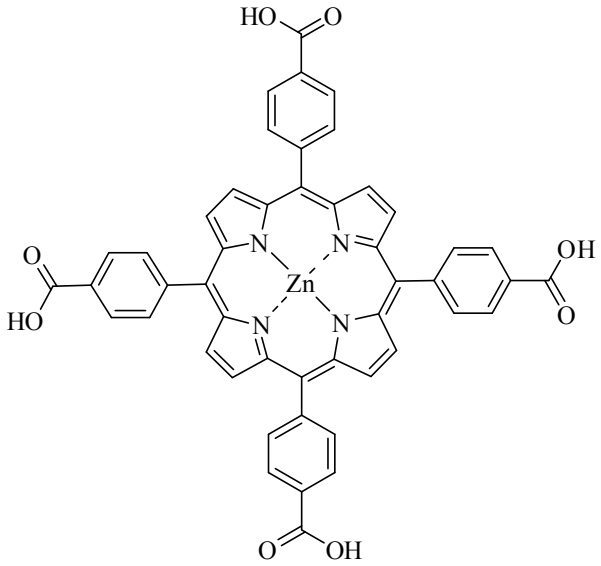

Zn-TCPP

Chart 2-1. Structure of 5,10,15,20-tetrakis(4-carboxyphenyl) porphinatozinc II (Zn-TCPP)

In heterojunction solar cell, porphyrin macrocycle and metallo porphyrin complex are used as donor material. They have an appropriate LUMO energy level

that lies atop the LUMO energy level of acceptor and conduction band of metal electrode. Because of long-live π* singlet excited states, they have enough time to generate charge separation from exciton and negative charge may diffuse to acceptor and metal electrode to generate electrical current.[14]

2.5 Triazine

Substituted 1,3,5-triazine derivatives have been known for widespread application in pharmaceutical, plastic, textile and rubber industries. They are also used as pesticides, dyes, optical bleaches, explosives and surface active agents. Because of their symmetrical enriched nitrogen atom structure, triazine derivatives have strong electronegativity property. In the recent studies, triazine derivatives have been proven to be good electron acceptors for optoelectronic applications, such as OLED or PLED. Furthermore, triazine derivatives are usually used as building blocks for electron transporting materials (ETMs) in OLEDs.[15]

Substituted 1,3,5-triazine are usually prepared by nucleophilic aromatic substitution between cyanuric chloride (CC) and various nucleophile. The substitution pattern depends on the nucleophilicity of nucleophile, their basic strength and steric factor. By controlling the mole ratio of nucleophile, temperature, time and optimization of variables, such as solvent and base, the substituent triazine can be formed in various forms by one-pot synthesis.

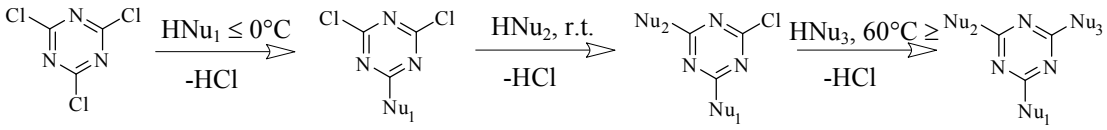

Scheme 2-1. Principle synthesis of substituent triazine.

Tommaso Carfiglo *et al*. achieved 1,3,5 substituted triazine with porphyrin by nucleophilic substitution of cyanuric chloride and porphyrin derivatives in one-pot synthesis.[16]

LITERATURE REVIEWS

Hiroko Inomata *et al*. synthesized a triazine-containing carbazole derivative (**1**, Chart 2-2) for organic light-emitting diodes.[17]

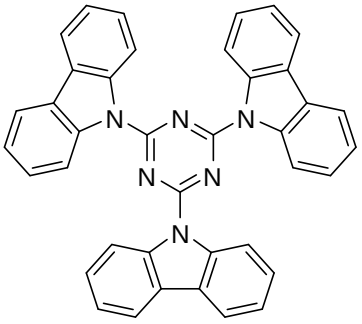

1

Chart 2-2. Triazine-containing carbozole structure.

Compound **1** exhibited high external electroluminescent (EL) quantum efficiency and energy conversion efficiency. Triazine core unit showed its characteristic properties that are strong electron-accepting and high electron transfer ability.

Hongliang Zhong *et al.* reported the application of triazine-based compounds **1**–**4** (Chart 2-3) in OLED as a hole-blocking material.[18]

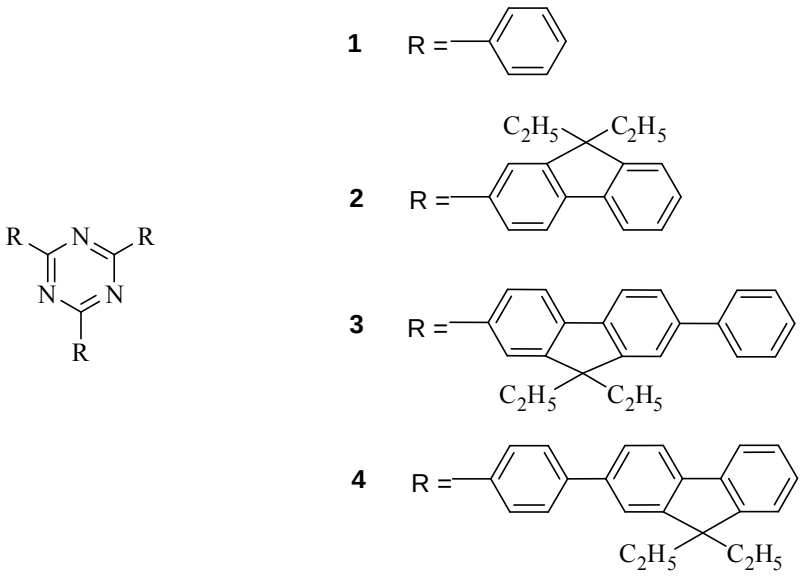

Chart 2-3. Triazine-based compounds.

The result of electroluminescences support the concept for molecular design that introducing more electron-donating groups and extended π-conjugation into a triazine ring can turn the optimal energy levels and band of the molecules, resulting in the improvement of optoelectronic properties of the molecules.

Michael M. Rothmann *et al.* synthesized substituted 1,3,5–triazine with different electron-donating groups.[19] The general structure is shown in chart 2-4

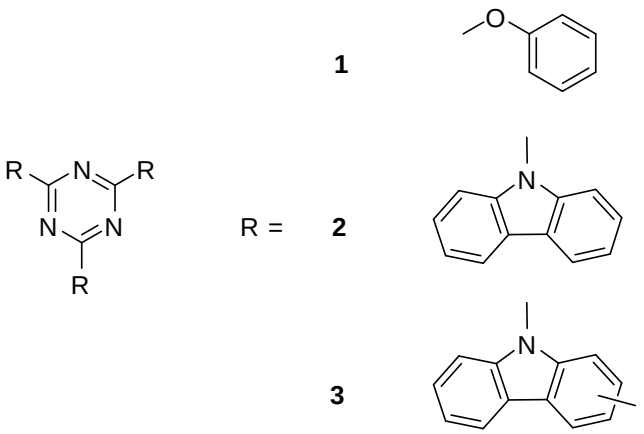

Chart 2-4. 1,3,5–Triazine with different electron-donating groups.

These substituted triazine compounds exhibited blue phosphorescence and exhibited great potential for being used as host transport material for OLEDs.

Krzysztof R. Idzick *et al.* prepared donor-acceptor materials based on 1,3,5-triazine derivatives **1**–**5**[20] (Chart 2-5) via palladium-catalyzed cross-coupling reaction

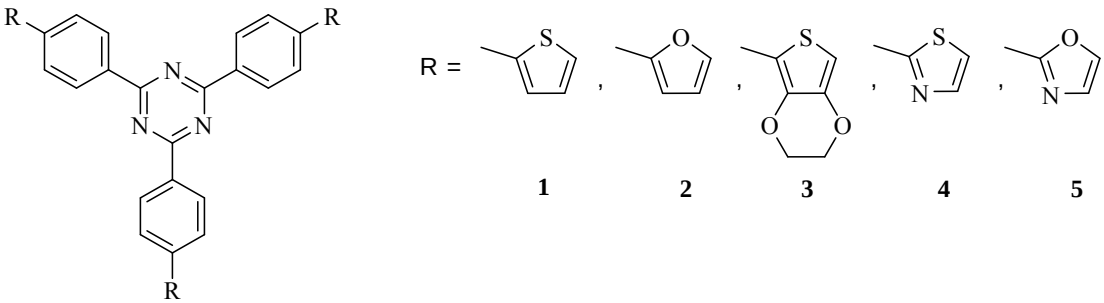

Chart 2-5. Triazine based electron-donating group

Richard A. Klenkler *et al.* synthesized 4,4'-bis-(2-(4,6-diphenyl-1,3,5-triazinyl))-1,1'-biphenyl (**2**) that exhibited higher electron mobility than AlQ_3 which is widely known as electron transporting material for OLED.[21]

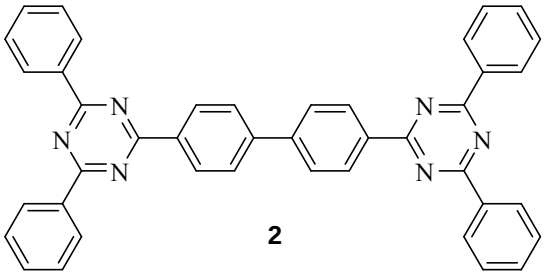

Chart 2-6. 4,4'-bis-(2-(4,6-diphenyl-1,3,5-triazinyl))-1,1'-biphenyl (**2**)

(6) John A. Mikroyannidis *et al.* reported the synthesis and use of compound **3** (Chart 2-7) for bulk heterojunction solar cell.[22]

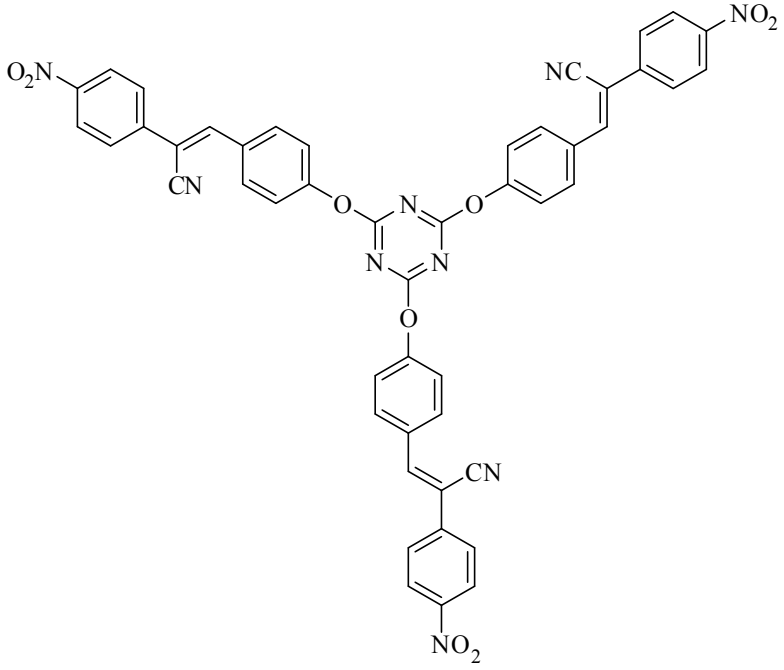

Chart 2-7. Structure of **3**.

The target molecule exhibited low energy band gap and a device based on this compound showed 1.43% energy conversion efficiency. Because triazine unit was proved to lower a LUMO level of the compound.

Chang-Wei Lee *et al.* synthesized a big series of Zn-porphyrin derivatives **1**–**12** for dye-sensitized solar cells.[23] The cells with up to 6.0% energy conversion efficiency was obtained.

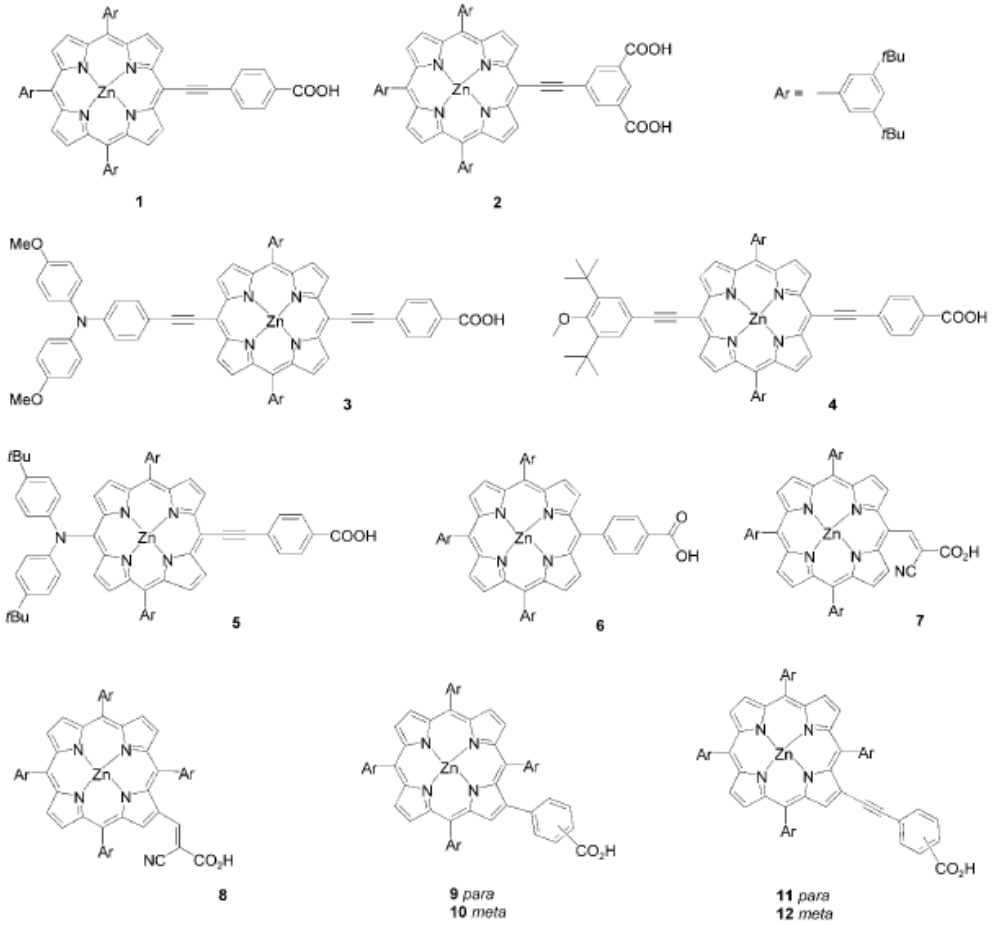

Chart 2-8. Zn-porphyrin derivatives with anchoring group.

Takeo Oku *et al.* fabricated a ZnTPP (Zn-Tetraphenylporphyrin)-based bulk heterojunction solar cell with the following structure (Figure 2-7).[23] The device showed the maximum η of 0.078%.

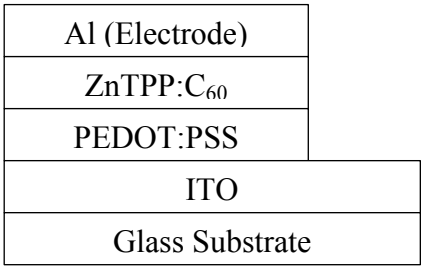

Figure 2-7. Schematic bulk heterojunction structure.

CHAPTER III
EXPERIMENTAL

3.1 Chemicals

All chemicals are purchased from commercial sources and used as received, unless noted otherwise.

1. Aniline : Merck
2. Potassium Carbonate : Carlo-Erba
3. Tetrahydrofuran : RCI Lab-Scan
4. Benzaldehyde : Merck
5. 4-Nitrobenzaldehyde : SigmAldrich
6. Pyrrole : Merck
7. 2,3-dichloro-5,6-dicyano benzoquinone : SigmAldrich
8. Methylene Chloride : Distilled from commercial grade
9. Hexanes : Distilled from commercial grade
10. Silica gel : Merck
11. Boron triflouride diethyletherate : Fluka
12. Tin(II) chloride dihydrate : Merck
13. Hydrochloric acid : Merck
14. Ammonium hydroxide : RCI Lab-Scan
15. Ethanol : RCI Lab-Scan
16. Sized-exclusion resin 200-400 mesh : Bio-Rad Laboratories
17. Deuterated Chloroform : Cambridge Isotope
18. Deuterated Dimethyl sulfoxide-d_6 : Cambridge Isotope
19. 4-Nitrobenzoic acid : SigmAldrich
20. Zinc(II) acetate dihydrate : SigmAldrich
21. 4-Amino benzaldehyde : Pi Chemical
22. Cyano acetic acid : Merck
23. Methyl carbamate : SigmAldrich
24. Sodium hydroxide : Merck
25. Ethyl acetate : Distilled from commercial grade
26. Deuterated Tetrahydrofuran-d_8 : Cambridge Isotope

3.2 Analytical Instruments

All reagents were purchased and used as received without further purification. ^{1}H-NMR and ^{13}C-NMR were obtained in $CDCl_3$ or THF-d_8 at 400 MHz for ^{1}H nuclei and 100 MHz for ^{13}C nuclei (Varian Company, USA). Chemical shifts (δ) are reported in parts per million (ppm) relative to the residual $CHCl_3$ peak (7.26 ppm for ^{1}H-NMR and 77.0 for ^{13}C-NMR). Coupling constant (J) are reported in Hertz (Hz). Mass spectra were obtained by using matrix-assisted laser desorption ionization mass spectrometry (MALDI-TOF) and dithranol as a matrix. Absorption spectra were measured in toluene using a Hewlett-Packard 8453 spectrophotometer and absorption extinction coefficient (ε) was reported in L/mol·cm. Fluorescence spectra were measured in toluene or THF using a Perkin-Elmer LS45 luminescence spectrometer. FT-IR spectra were measured by ATR-FTIR technique using Nicolet 6700 and were reported in wave number (cm^{-1}).

3.3 Experimental Procedure

Part 1 : Synthesis of triazine-porphyrin derivatives for bulk heterojunction solar cells.

3.3.1 5-(4-nitrophenyl)-10,15,20-triphenylporphyrin (5)

Following a previously published procedure[24] with slight modification, a mixture of 4-nitrobenzaldehyde (592 mg, 3.92 mmol), benzaldehyde (1.13 ml, 11.1 mmol) and pyrrole (1.04 ml, 15.0 mmol) were dissolved in CH_2Cl_2 (756 mL). $BF_3 \cdot OEt_2$ (0.20 ml, 1.6 mmol) was then added and the reaction mixture was stirred at room temperature for 1 h. After that, DDQ (0.83 g, 3.7 mmol) was added and the reaction was continued additional for 1 h. Then, solvent was removed under vacuum and the resulting crude was purified by column chromatography [silica, Hexanes:CH_2Cl_2, (1:1)] to give compound **1** which was eluted as a second band (0.6058 g, 35.3%). ^{1}H-NMR δ –2.78 (s, 2H), 7.70–7.83 (m, 9H), 8.22 (d, *J* = 6.4 Hz, 6H), 8.40 (d, *J* = 7.2 Hz, 2H), 8.64 (d, *J* = 7.2 Hz, 2H,), 8.74 (d, *J* = 4.4 Hz, 2H), 8.81–8.93 (m, 6H) (**Figure 1**); ^{13}C-NMR δ 116.6, 120.7, 121.1, 121.9, 126.7, 126.8, 127.9, 134.5, 141.9, 142.0, 147.7, 149.2 (**Figure 2**); MALDI-TOF-MS m/z obsd 613.416 [$(M\text{-}NO_2)^+$], 659.382 [M^+], calcd 659.733 (M = $C_{44}H_{29}N_5O_2$) (**Figure 3**).

3.3.2 5-(4-aminophenyl)-10,15,20-triphenylporphyrin (6)

Following a previously published procedure[24] with slight modification, a mixture of compound **1** (457 mg, 0.693 mmol) and $SnCl_2 \cdot 2H_2O$ (393 mg, 2.07 mmol) in concentrated HCl (12 N, 15 ml) was stirred at 65 °C for 4 h. After cooling down to room temperature, reaction mixture was poured into water (100 mL) and was adjusted to pH 8 by 30% NH_4OH. The resulting purple mixture was extracted by CH_2Cl_2 (3 × 200 mL) until an aqueous layer was colorless. Organic fractions were combined, dried over anhydrous Na_2SO_4 and concentrated to dryness. The resulting crude was purified by column chromatography (silica, CH_2Cl_2) to give compound **6** as a second band (0.381 g, 65%). ^{1}H-NMR δ –2.75 (s, 2H), 4.03 (br, 2H), 7.07 (d, *J* = 8.0 Hz, 2H), 7.71–7.81 (m, 9H), 8.00 (d, *J* = 8.0 Hz, 2H), 8.22 (d, *J* = 7.2 Hz, 6H), 8.84 (s, 6H), 8.95 (d, *J* = 4.4 Hz, 2H) (**Figure 4**); ^{13}C-NMR δ 113.5, 119.7, 120.0, 120.8, 126.7, 127.7, 132.4, 134.6, 135.7, 142.2, 142.3, 146.0 (**Figure 5**); MALDI-TOF-MS m/z obsd 630.121 [$M+H^+$], calcd 629.750 (M = $C_{44}H_{31}N_5$) (**Figure 6**).

3.3.3 Compound Zn-1

Following published literatures[25,26] with slight modification, compound **6** (0.2317 g, 0.3684 mmol) and K_2CO_3 (0.5103 g, 0.3692 mmol) were dissolved in THF (5 mL). Cyanuric chloride (0.0175 g, 0.0949 mmol) was added and the resulting solution was refluxed for 8 h. Then, the reaction mixture was cooled down to room temperature and solvent was removed under reduced pressure. The residue was purified by a silica column using 1% EtOH in CH_2Cl_2 as an eluent and the purple fractions were collected. Compound **7** was isolated from the porphyrinic byproducts by subsequent size-exclusion column chromatography using THF as eluent. After that, compound **7** and **8** were purified again by a silica column using 1% EtOH in CH_2Cl_2 as an eluent and obtained as a purple solid (0.1036 g, 56%). MALDI-MS m/z obsd 1964.342 [M^+], calcd 1964.280 (M = $C_{135}H_{90}N_{18}$) (**Figure 7**). Compound **8**: MALDI-MS m/z obsd 1371.742 [$M+H^+$], calcd 1370.990 (M = $C_{135}H_{90}N_{18}$) (**Figure 8**). The yield of compound **8** was optimized as described below. Both compounds were used directly in the next step without further purification.

Compound **7** was redissolved in THF (10 mL) and treated with a solution of $Zn(OAc)_2 \cdot 2H_2O$ (0.1743 g, 0.5263 mmol) in MeOH (10 mL). The reaction mixture was stirred at room temperature for 8 h and refluxed for additional 2 h. After cooling down to room temperature, the mixture was concentrated to dryness and redissolved in CH_2Cl_2. The resulting solution was washed with water, dried over anhydrous Na_2SO_4 and concentrated to dryness. The crude was purified by a silica column using 1% EtOH in CH_2Cl_2 as an eluent to give compound **1** as a purple solid (0.1007 g, 89 %). ^{1}H-NMR δ 6.47 (s, 3H), 7.29–7.59 (m, 6H), 7.60–7.75 (m, 27H), 7.75–7.88 (m, 6H), 7.90–8.29 (m, 18H), 8.76–8.97 (m, 18H), 8.97–9.15 (m, 6H) (**Figure 9**); ^{13}C-NMR δ 119.0, 120.7, 121.1, 124.3, 126.4, 126.5, 127.3, 127.4, 132.0, 134.4, 134.9, 137.7, 138.0, 142.7, 142.8, 143.1, 150.1, 150.2, 15.03, 163.9 (**Figure 10**); ν_{max}: 1595, 1564, 1479, 1439, 1404, 1362, 1338, 1310, 1225, 1204, 1177, 1068 (**Figure 11**); MALDI-TOF-MS m/z obsd 2154.516 [M^+] calcd 2154.462 (M = $C_{135}H_{84}N_{18}Zn_3$) (**Figure 12**); $\lambda_{abs}(\varepsilon)$ 431(643,506), 552(23,817), 601(9,209) nm (**Figure 13–16**); λ_{em} (λ_{ex} = 431 nm) 611 nm (**Figure 17**).

3.3.4 Compound Zn-8

In the similar manner to the synthesis of compound **7** except that the reaction mixture was stirred at room temperature for 10 h, compound **8** was obtained as a purple solid (0.2337 g, 68%). A solution of compound **8** (0.0577 g, 0.0421 mmol) in THF (10 mL) was reacted with a solution of $Zn(OAc)_2 \cdot 2H_2O$ (0.0943 g, 0.421 mmol) in MeOH (5 mL). The mixture was stirred at room temperature for 8 h. After the removal of solvent under reduced pressure, the resulting residue was redissolved in CH_2Cl_2, washed with water, dried over Na_2SO_4, and concentrated to dryness. The crude was purified by column chromatography [silica, CH_2Cl_2:EtOAc (4:1)], leading to give compound **Zn-8** (0.0675 g, 91%). ^{1}H-NMR δ 6.47 (s, 2H), 7.50–7.81 (m, 22H), 7.92–8.26 (m, 16H), 8.68–9.02 (m, 16H) (**Figure 18**); ^{13}C-NMR δ 121.1, 126.5, 127.5, 131.7, 131.9, 134.3, 134.4, 135.0, 142.8, 143.1, 150.2 (**Figure 19**); ν_{max} (cm^{-1}): 1608, 1595, 1564, 1489, 1440, 1417, 1405, 1386, 1339, 1234, 1205, 1177, 1071, 1001, 992 (**Figure 20**); MALDI-MS m/z obsd 1498.714 [$M+H^+$], calcd 1497.778 (M = $C_{91}H_{56}ClN_{13}Zn_2$) (**Figure 21**); $\lambda_{abs}(\varepsilon)$ 422(553,288), 554(28,717), 599(13,226) nm (**Figure 22–25**); λ_{em} (λ_{ex} = 422 nm) 608 nm (**Figure 26**).

Part 2 : Synthesis of triazine-porphyrin derivatives for dye-sensitized solar cells

3.3.5 3-(4-aminophenyl)-2-cyano acrylic acid (10)

Following a previously published procedure[28], a solution of 4-amino benzaldehyde (0.5043 g, 4.168 mmol), cyano acetic acid (0.3511 g, 4.131 mmol) and NH_4OAc (0.3182 g, 4.132 mmol) in glacial acetic acid (15 mL) was refluxed for 8 h. After cooled down to room temperature, the solution was concentrated to dryness and redissolved in hot EtOH. The mixture was filtered off and the resulting filtrate was kept in refrigerator for precipitation. The precipitate was filtered off, washed with cold EtOH and left to dryness to give compound **11** as yellow solid (0.2351 g, 34%). ^{1}H-NMR δ 7.34(br, 2H), 7.68(d, *J* = 8.0, 2H), 7.83(d, *J* = 8.0, 2H), 10.31(s, 1H) (**Figure 27**) ^{13}C-NMR δ 119.2, 120.0, 127.9, 131.0, 142.2, 148.2, 169.3 (**Figure 28**).

3.3.6 Compound Zn-2

A solution of compound **Zn-8** (0.0541 g, 0.0361 mmol) and K_2CO_3 (0.0058 g, 0.042 mmol) in THF (5 mL) was reacted with 4-Amino benzoic acid (**9**, 0.0454 g, 0.36 mmol) under reflux for 8 h. After the completion of the reaction (TLC-monitoring), the solvent was removed under reduced pressured and the resulting crude was redissolved in CH_2Cl_2, washed with water, dried over anhydrous Na_2SO_4 and concentrated to dryness. Purification by column chromatography [silica, CH_2Cl_2:EtOAc (4:1)] afforded compound **Zn-2** (0.0275 g, 47%) as a purple solid. ^{1}H-NMR δ 7.18–7.56 (m, 4H), 7.56–7.86 (m, 26H), 7.86–8.35 (m, 16H), 8.73–8.94 (m, 12H), 8.94–9.21 (m, 4H), 10.88 (s, 1H) (**Figure 29**); ^{13}C-NMR δ 116.4, 117.1, 118.4, 118.6, 118.8, 124.3, 125.2.4, 128.3, 129.5, 132.7, 135.6, 137.8, 141.7, 141.8, 142.6, 148.1, 148.5, 163.1, 163.3, 164.6 (**Figure 30**); ν_{max} (cm^{-1}): 1687, 1594, 1563, 1478, 1403, 1337, 1269, 1203, 1174, 1067, 992 (**Figure 31**); MALDI-TOF-MS m/z obsd 1599.636 [M+H$^+$], calcd 1598.453 (M = $C_{98}H_{63}N_{14}O_2Zn_2$) (**Figure 32**); λ_{abs}(ε) 422(814,117), 557(49,699), 595(23,620) nm (**Figure 33–36**); λ_{em} (λ_{ex} = 422 nm) 605 nm (**Figure 37**).

3.3.7 Compound 2

Following a previously published procedure,[29] a mixture of compound **8** (0.1682 g, 1.227 mmol) and **9** (0.5317 g, 3.881 mmol) was refluxed in glacial acetic acid for 30 min. After cooling down to room temperature, the resulting reaction mixture was poured into water, filtered off and washed with water. The residue was purified by silica column [10% MeOH in CH_2Cl_2], leading to compound **2** (0.0148 g, 0.82%) as a purple solid. ^{1}H-NMR δ –2.79 (s, 4H), 7.11 (s, 3H), 7.33–7.77 (m, 26H), 7.79–8.00 (m, 16H), 8.00–8.33 (m, 12H), 8.59–9.01 (m, 4H), 10.60 (s, 1H) (**Figure 38**); ^{13}C-NMR δ 111.5, 119.6, 120.1, 124.0, 124.8, 126.5, 126.6, 127.5, 127.6, 128.5, 130.2, 131.1, 132.3, 134.4, 134.5, 135.0, 136.3, 137.8, 142.0, 142.1, 143.0, 164.0, 169.9 (**Figure 39**); MALDI-TOF-MS m/z obsd 1473.531 [M+H$^+$], calcd 1471.665 (M = $C_{98}H_{66}N_{14}O_2$) (**Figure 40**); $\lambda_{abs}(\varepsilon)$ 419(746,440), 515(33,411), 550(16,046), 587(3,520), 650(1,966) nm (**Figure 41–46**); λ_{em} (λ_{ex} = 419 nm) 653 nm (**Figure 47**).

CHAPTER IV

RESULTS AND DISCUSSION

In this research, a series of the porphyrin-triazine derivatives was synthesized for using as photoactive compounds in organic photovoltaic cells. The molecule includes two or three porphyrin macrocycles linked via triazine units. When two porphyrin macrocycles are presented, the remaining peripheral position on the triazine ring is occupied by a 4-carboxyphenyl, a 4-(2-carboxy-2-cyanoethenyl)phenyl or a carboxyl anchoring group. The synthesis relied on the aryl amination between triazine unit containing a chloro group and an amino precursor. These compounds will be employed in the dye-sensitized solar cells, while the one with three porphyrin macrocycles will be investigated as a photosensitizer in the bulk heterojunction solar cells.

4.1 Synthesis of Triazine-porphyrin Derivatives for Bulk Heterojunction Solar Cells.

Synthesis of compound **Zn-1** for bulk heterojunction solar cells and **Zn-8** as a precursor for compound **Zn-2–Zn-4** for dye-sensitized solar cells are illustrated in Scheme 4-1.

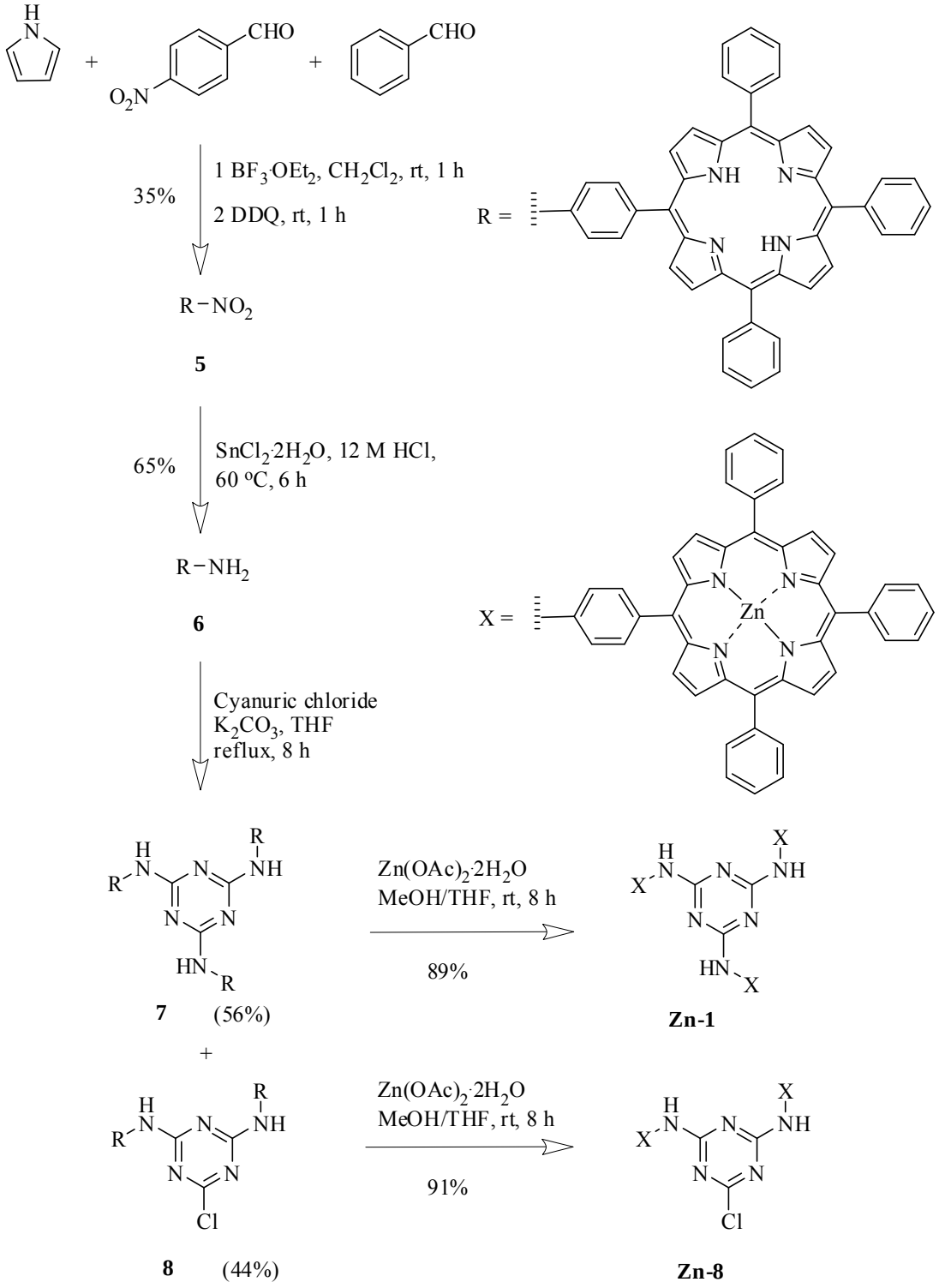

Scheme 4-1. Synthesis of porphyrin-triazine **Zn-1**.

As shown in scheme 4-1, compound **5** was prepared in 35% yield from a statistical condensation of pyrrole, 4-nitrobenzaldehyde and benzaldehyde in the presence of $BF_3 \cdot OEt_2$, followed by oxidation with DDQ. Due to a distinctive polarity resulted from its nitro group, compound **5** was easily isolated by column chromatography. In its ^{1}H-NMR spectrum, a characteristic peak of inner proton of compound **5** appears as a singlet at δ–2.79 ppm. In regard to the solubility, compound **5** is soluble in several common organic solvents, such as toluene, CH_2Cl_2 and THF.

Reduction of the nitro group of compound **5** was carried out by the reaction of **5** with $SnCl_2 \cdot 2H_2O$ in conc. HCl, leading to amino derivative **6** in 65% yield. Based on^{1}H-NMR spectroscopic analysis, aromatic proton signals of the peripheral phenyl ring bearing an amino group was observed in the upfielded region compared to those in compound **5** due to electron donating effect of the amino group. The amino and inner protons appeared as singlet signals at 3.91 and –2.83 ppm, respectively.

Compounds **7** and **8** were synthesized by arylamination of compound **5** and cyanuric chloride in the presence of K_2CO_3 in refluxing THF and were obtained 56% and 44% yield, respectively. Three-column process is required to purify the target compounds. Firstly, the silica column was used to remove unreacted compound **6** and other polar byproducts. Secondly, sized-exclusion chromatography (SEC) separated compounds **7**, **8** and smaller byproducts from each other. Finally, another silica column was used for removal of impurities incoming from SEC. Mass spectra confirmed the formation of compounds **7** and **8** by showing their molecular ion peaks at m/z 1964.342 and 1371.742, respectively. When the reaction was performed under room temperature, compound **8** became a major product with the yield of 68% and the lower yield of **7** (4%). In regard to the solubility, compound **7** is more soluble than compound **8** in low polar organic solvents. Compound **7** is soluble in toluene, CH_2Cl_2 and THF, while compound **8** is readily soluble in THF and slightly soluble in CH_2Cl_2.

Zn-metallation of compound **7** with $Zn(OAc)_2 \cdot 2H_2O$ led to compound **Zn-1** quantitatively. The disappearance of the singlet signal at δ –2.84 ppm in the ^{1}H-NMR spectrum and an emission peak at ~720 nm indicated the completion of the reaction. In its absorption spectrum, **Zn-1** exhibited intense B-band at 431 nm and Q-bands at 556 and 601 nm, while the emission spectrum showed a peak at 611 nm. Compound **Zn-8** was prepared in the same manner as the preparation of **Zn-1**. Beside the

disappearance of a ^{1}H-NMR peak at –2.84 ppm and an emission peak at ~720 nm, the formation of **Zn-8** was proved by MALDI-MS that exhibited a molecular ion peak at m/z 1498.786. Solubilty on **Zn-8** was found to be better than that of compound **8**. **Zn-8** is soluble in several common organic solvent, *e.g.* THF, CH_2Cl_2 and toluene.

4.2 Synthesis of Porphyrin-triazine Derivatives for Dye-sensitized Solar Cells.

In dye-sensitized solar cells, the efficient electronic communication stems from the covalent binding of the photoactive molecules with the TiO_2 surface via the surface anchoring group. In this study, the carboxyl group was introduced to the porphyrin-triazine compound.

Following a published procedure,[29] compound **2** was obtained in 0.82% yield from reaction of compound **9**[27] and **8** as shown in Scheme 4-2.

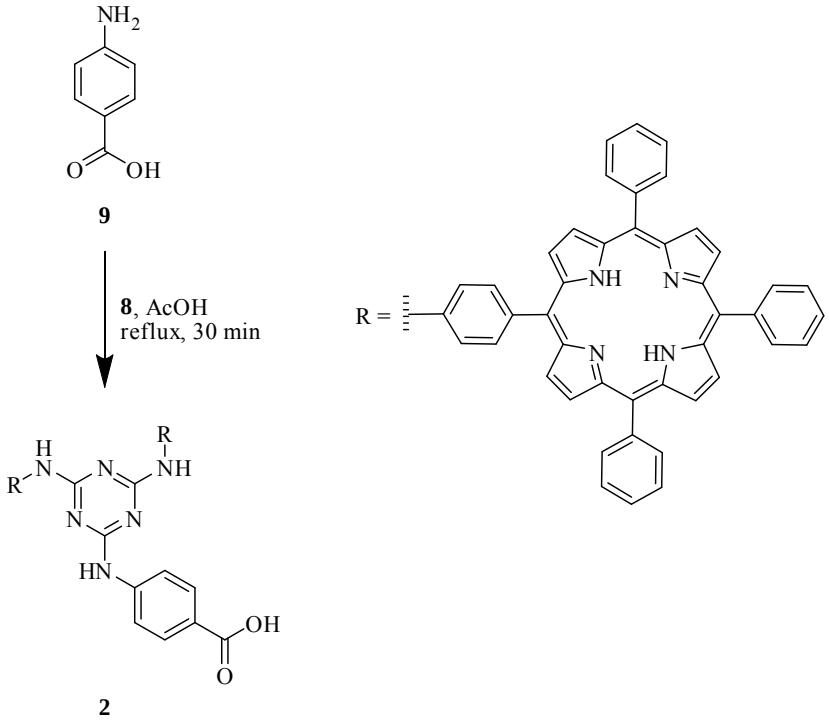

Scheme 4-2. Synthesis of porphyrin-triazine compound **2**.

Mass spectrometry confirmed the formation on compound **2** by showing its molecular ion peak at m/z 1473.531. Due to the steric hindrance in **8** resulted from the bulky porphyrin macrocycles together with the limited nucleophilicity of the amino group on compound **9** as a result of the carboxyl group, the reaction required an excess amount of compound **10** (10 equivalents) and the refluxing condition. In regard to the solubility, compound **2** is soluble in organic solvents such as THF.

In the similar manner, compound **Zn-2** was obtained in 47% from a reaction of compounId **9**[27] and **Zn-8** as shown in Scheme 4-3.

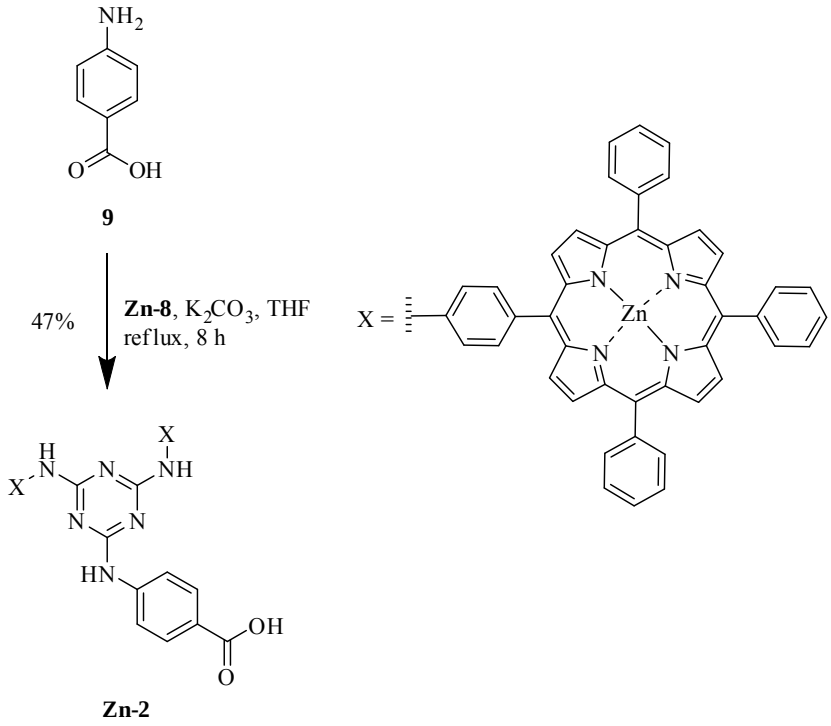

Scheme 4-3. Synthesis of porphyrin-triazine compound **Zn-2**.

Mass spectrometry confirmed the formation of **Zn-2** by showing its molecular ion peak at m/z 1599.636. In regard to the solubility, compound **Zn-2** is soluble in organic solvents such as THF and CH_2Cl_2.

To increase electron injection from the dye molecule to the TiO_2 surface in DSSCs, the use of a cyano acrylic anchoring group is a popular strategy. Therefore, synthesis of surface anchoring group unit **10** was pursued (Scheme 4-3).

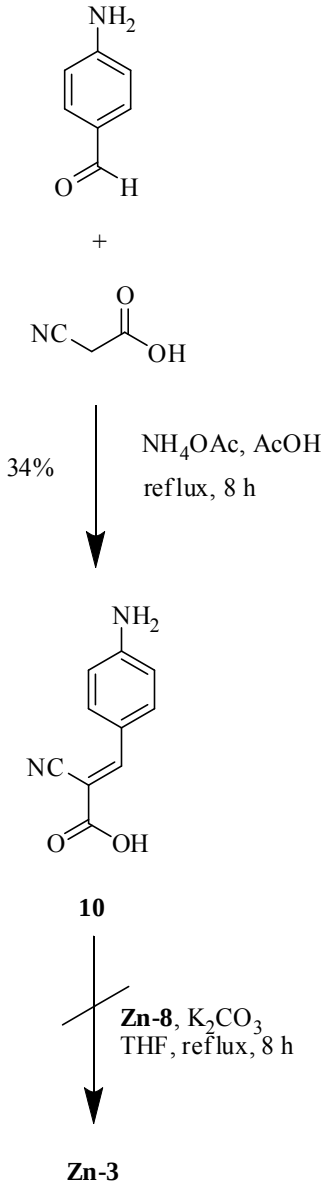

Scheme 4-4. Synthesis of porphyrin-triazine compound **Zn-3**.

Compound **10** was obtained in 34% yield from the known reaction of commercial 4-aminobenzaldehyde and cyano acetic acid in presence of NH_4OAc in refluxing glacial acetic acid.[28] The structure of **10** was confirmed by NMR spectroscopy which showed a characteristic $–NH_2$ peak at 7.34 ppm in the ^{1}H-NMR spectrum and a –CN peak at 120.0 ppm in the ^{13}C-NMR spectrum. However, the attempt to perform the reaction of **10** and **Zn-8** under the same condition as that employed in the synthesis of both **2** and **Zn-2** was failed to give compound **Zn-3**. It is attributed to two factors: (1) the low nucleophilicity of the amino group of compound **10** due to the strong electron withdrawing effect of the cyano acrylic moiety, and (2)

the limited solubility of compound **10** in the reaction media. Therefore, the synthesis of compound **Zn-3** was not continued.

An alternative to enhance the electronic communication between the dye and the electrode surface is to shorten the distance between the chromophore and the electrode surface. Hence, the carboxyl group was designed to directly attach to the triazine unit as shown in the structure of compound **Zn-4**. In the similar manner, the reaction of **Zn-8** and commercial methyl carbamate in the present of K_2CO_3 ใn refluxing THF.

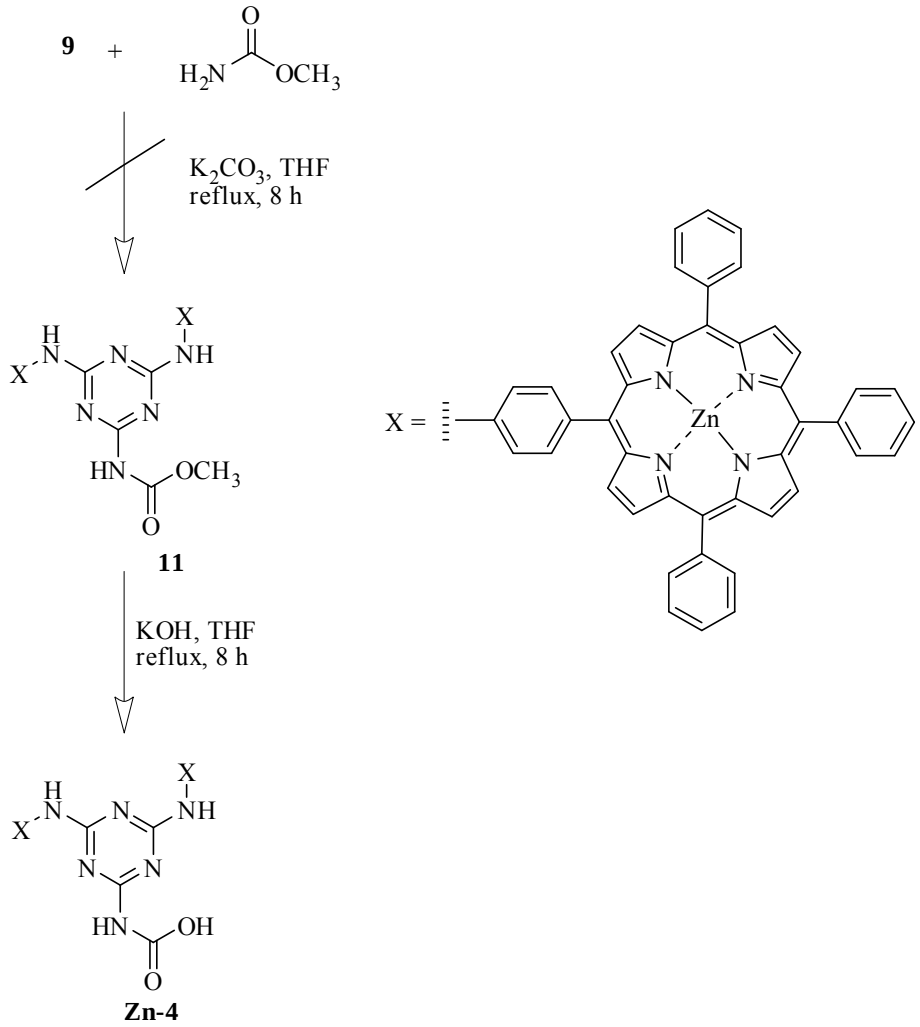

Scheme 4-5. Synthesis of porphyrin-triazine compound **Zn-4**.

4.3 Electrochemical and Photophysical Properties

4.3.1 Compound Zn-1

Electrochemical properties of compound **Zn-1** was determined by cyclic voltammetry in MeCN containing 0.1 M Bu_4NPF_6 by using a ITO-coated glass working electrode, Pt wire counter electrode and Ag/AgCl quasi-reference electrode (QRE) with scan rate of 50 mV/s. The resulting redox potentials were externally calibrated with ferrocene/ferrocenium couple of which the potential of 0.40 V vs NHE was used. The result from cyclic voltammetry indicated that the estimated energy gap of compound **Zn-1** was 1.9 eV with the HOMO level of –5.4 eV and the LUMO level of –3.5 eV. When consider together with ITO conduction band (CB), PEDOT:PSS Fermi level (FL), HOMO-LUMO level of P3HT and PCBM and Al work function (WF), the HOMO-LUMO level of **Zn-1**, the HOMO-LUMO levels of **Zn-1** should be able to serve both as donor or acceptor for the solar cells as illustrated in Figure 4-1.

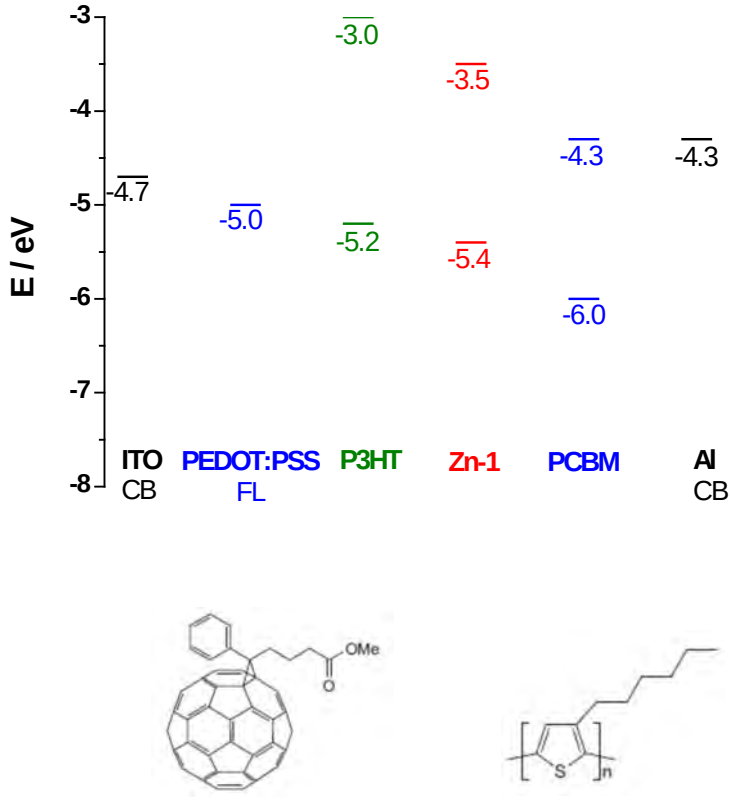

PCBM P3HT

Figure 4-1. Comparative energy diagram of compound **Zn-1**–based bulk heterojunction solar cells.

In order to improve the ability of compound **Zn-1** for serving as a donor or an acceptor material, a photoluminescence study of compound **Zn-1**:PCBM (1:1) and P3HT:compound **Zn-1** (1:1) blended films was performed. The result shown in Figure 4-2 revealed that porphyrin emission was completely quenched by PCBM, indicating the efficient electron transfer from compound **Zn-1** (donor) to PCBM (acceptor). Such emission quenching was not observed in the case of a P3HT:**Zn-1** film, indicating that the charge transfer from P3HT (donor) to **Zn-1** (acceptor) was not efficient. Therefore, the PCBM:**Zn-1** blended film was employed as a photoactive layer in the bulk heterojunction solar cell, whose fabrication and study are explained below.

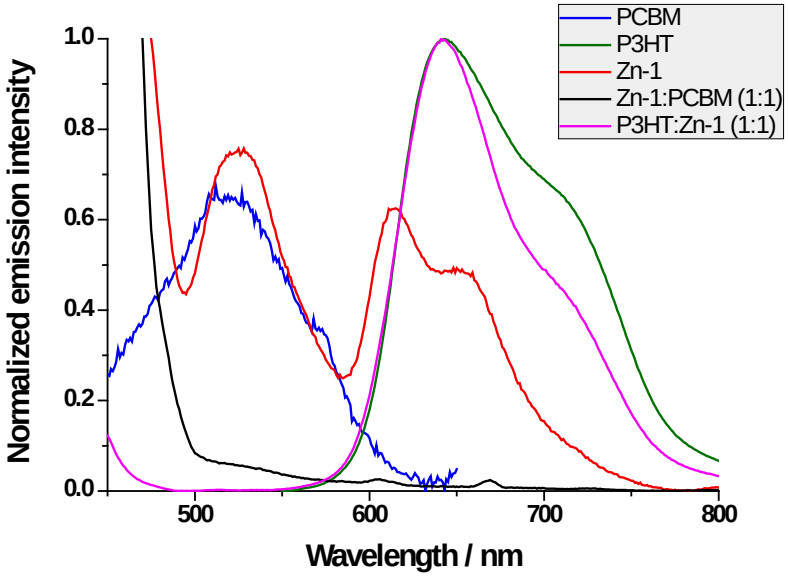

Figure 4-2. Result of photoluminescence study of the films.

Following published literature[30] with slight modification, The bulk heterojunction solar cells containing the **Zn-1**:PCBM was fabricated in the schematic structure shown in Figure 4-3.

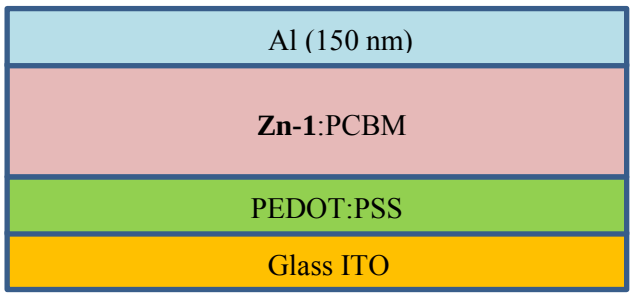

Figure 4-3. A schematic cell structure of a bulk heterojunction solar cell based on **Zn-1**.

With the fixed film thickness and type of a metal top contact, PEDOT:PSS and ITO-coated glass, the **Zn-1**:PCBM ratio was varied to optimize the device efficiency. As a result, the η was found to be the highest at 0.5% when **Zn-1**:PCBM weight ratio was 1:10. Based on Atomic Force Microscopy (AFM) film measurement, the roughness of the resulting film was less than 10 nm with the thickness of ~80 nm. Varying of film thickness by using the different concentration of **Zn-1**:PCBM solution mixture in the film formation process was failed to improve the cell efficiency. Further improvement of the device efficiency can be expected when other cell parameters, for example, types of top contact and PEDOT:PSS, and film formation technique is optimized.

4.3.2 Compound Zn-2

Electrochemical properties of compound **Zn-2** was determined by cyclic voltammetry in MeCN containing 0.1 M Bu_4NPF_6 by using a ITO-coated glass working electrode, Pt wire counter electrode and Ag/AgCl quasi-reference electrode (QRE) with scan rate of 50 mV/s. The resulting redox potentials were externally calibrated with ferrocene/ferrocenium couple of which the potential of 0.40 V vs NHE was used. The result from cyclic voltammetry indicated that the estimated energy gap of compound **Zn-2** was 2.1 eV with the HOMO level of 0.7 eV and the LUMO level of –1.4 eV. When consider together with TiO_2 CB and redox potential of I^-/I_3^- electrolyte ($E_{1/2}$), HOMO-LUMO level of **Zn-2** and **2** should enable the electron transport in the solar cells (Figure 4-4). The device fabrication and evaluation still have yet to be done.

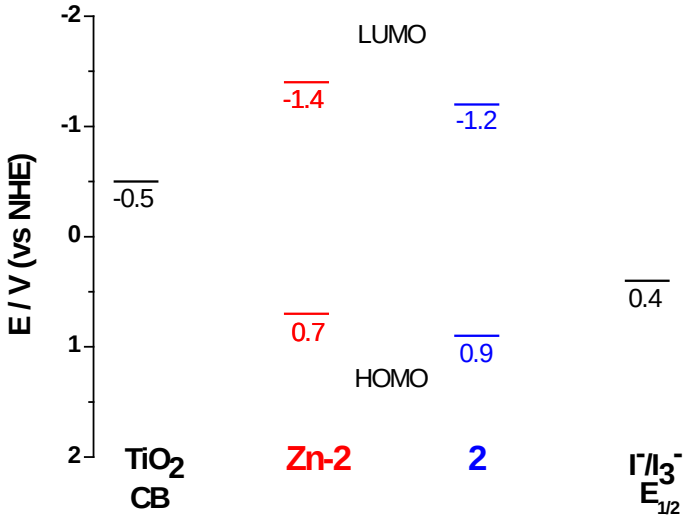

Figure 4-4. Comparative energy diagram of compound **Zn-2**–based dye-sensitized solar cells.

CHAPTER V

CONCLUSION

A series of target porphyrin-triazine compounds were synthesized fully characterized by spectroscopic techniques. Based on cyclic voltammetry analysis, HOMO-LUMO levels of these compounds should enable the electron transport in the solar cells. Photoluminescence study of the blended containing **Zn-1** confirmed the efficient charge transfer from the compound (as a donor) and PCBM (as an acceptor). Bulk heterojunction solar cells based on **Zn-1** gave up to 0.5% energy conversion efficiency.

REFERENCES

[1] Lee, C., and others. Novel Zinc Porphyrin Sensitizer for Dye-Sensitized solar cells: Synthesis and spectral, Electrochemical, and Photovoltaic Properties. Chem. Eur. J. 15 (December 2009): 1403–1412.

[2] Ling, Y., et al. For the Bright Future—Bulk Heterojunction Polymer Solar Cells with Power Conversion Efficiency of 7.4%. Adv. Mater. 22 (Janurary 2010): E135–E138.

[3] Roncali, J. Molecular Bulk Heterojunctions: An Emerging Approach to Organic Solar Cells. Acc. Chem. Res. 42 (November 2009): 1719–1730.

[4] Shang, X., et al. The Effect of Anchoring Group Number on The Performance of Dye-sensitized Solar Cells. Dyes Pigm. 87 (April 2010): 249–256.

[5] Mihailetchi, V. D. "Device Physics of Organic Bulk Heterojunction solar Cells" (Ph.D.-thesis Physics of Organic Semiconductors of the Material Science University of Groningen Netherlands, 2005).

[6] Liu, J. "P3HT:PCBM Bulk Heterojunction Organic Solar cell:Performance Optimization & Application of Inkjet Printing" (Thesis Department of Science and Technology Linköping University Sweden 2008).

[7] Pagliaro, M., Palmisano G., and Ciriminna, R. Flexible Solar Cells Federal Republic of Germany: WILEY-VCH Verlag GmbH & Co., 2008.

[8] Tang, W., et al. Recent Development of Conjugated Oligomers for High-efficiency Bulk Heterojunction Solar Cells. Sol Energ Mat Sol C. 94 (July 2010): 1963–1979.

[9] Hoppe, H., and Sariciftci, N. S. Organic Solar Cells: An Overview. J. Mater. Res. 4 (July 2004): 1924–1945.

[10] Kietzke, T. Recent Advances in Organic Solar Cells. Adv. Optoelectron. (November 2007): 1–15.

[11] Grätzel, M. Dye-sensitized Solar Cells. J. Photochem. Photobiol, A. Rev. 4 (October 2003): 145–153.

[12] Grätzel, M. Solar Energy Conversion by Dye-sensitized Photovoltaic Cells. Inorg. Chem. 44 (September 2005): 6841–6851.

[13] Puangmalee S. “Synthesis of Porphyrinic Derivatives from Cardanol as Petroleum Fluorescenct Marker” (Thesis: Petrochemistry and Polymer science Program Faculty of Science Chulalongkorn University, 2007)

[14] Campbell, W. M., Burrell, A. K., Officer, D. L., and Jolley, K. W. Porphyrin as Light Harvesters in The Dye-sensitized TiO2 Solar Cell. Coord. Chem. Rev. 248 (June 2004): 1363–1379.

[15] Blotny, G. Recent Applications of 2,4,6-Trichloro-1,3,5-Triazine and Its Derivatives in Organic Synthesis. Tetrahedron 62 (August 2006): 9507–9522.

[16] Carfiglo, T., Varotto, A., and Tonellato, U. One-Pot Synthesis of Cyanuric Acid-Bridged Porphyrin-Porphyrin Dyads. J. Org. Chem. 69 (March 2004): 8121–8124.

[17] Inomata, H., and others High-Efficiency Organic Electrophosphorescent Diodes Using 1,3,5-Triazine Electron Transport Materials. Chem. Mater. 16 (March 2004): 1285–1291.

[18] Zhong, H., Lai, H., and Fang, H. New Conjugated Triazine Based Molecular Materials for Application in Optoelectronic Devices: Design, Synthesis, and Properties. J. Phys. Chem. C 115 (December 2011): 2423–2427.

[19] Rothmann, M. M., Haneder, S., Como, E. D., Lennartz, C., Schildknecht, C., and Strohriegl, P. Donor-Substituted 1,3,5-Triazines as Host Materials for Blue Phosphorescent Organic Light-Emitting Diodes. Chem. Mater. 22 (March 2010): 2403–2410.

[20] Idzick, K. R., Papta, P., Cywinski, P. J., Beckert, R., and Dunsch L. Synthesis and Electrochemical Characterization of New Optoelectronic Material Based on Conjugated Donor-Acceptor System Containing Oligo-tri(heteroaryl)-1,3,5-Triazines. Electrochim. Acta. 55 (April 2010): 4858–4864.

[21] Klenkler, R. A., Aziz, H., Tran, A., Popovic, Z. D., and Xu, G. High Electron Mobility Triazine for Lower Driving Voltage and Higher Efficiency Organic Light Emitting Devices. Org. Electron. 9 (December 2008): 285–290.

[22] Mikroyannids, J. A., Sharma, S. S.; Vijay, Y. K., and Sharma G. D. Novel Low Band Gap Small Molecule and Phenylenevinylene Copolymer with Cyanovinylene 4-Nitrophenyl Segment: Synthesis and Application for Efficient Bulk Heterojunction Solar Cells. ACS Appl. Mater. Interfaces 71 (December 2010): 551–555.

[23] Oku, T., Noma, T., Suzuki, A., Kikuchi, K., and Kikuchi, S. Fabrication and Characterization of Fullerene/porphyrin Bulk Heterojunction Solar Cells. J. Phys. Chem. Solid 71 (April 2010): 551–555.

[24] Yan, G., Bischa, D., and Bottle, S. E. Synthesis and properties of novel porphyrin spin probes containing isoindoline nitroxide. Free Radical. Biol. Med. 43 (April 2007): 111–116.

[25] Ichihara K., and Naruta Y. New and Efficient Synthesis of Oligomeric Porphyrins via Stepwise Nucleophilic Substitution of Aminoporphyrins to Cyanuric chloride. Chem. Lett. (August 1995): 631–632.

[26] Jiao, J., Thamyongkit, P., Schmidt, I., Lindsey J. S., and Bocian, D. F. Characterization of Porphyrin Surface Orientation in Monolayers on Au(111) and Si(100) Using Spectroscopically Labeled Molecules. J. Phys. Chem. C 111 (August 2007): 12693–12704.

[27] Bellamy, F.D., and Ou K. Selective reduction of aromatic nitro compounds with stannous chloride in non acidic and non aqeous medium. Tetrahedron Lett. 25 (February 1984): 839–842.

[28] Zhou, W., Li, H., Xia, C., Zheng, X., and Hu, W. The Synthesis and Biological evaluation of some caffeic acid amide derivatives: *E*-2-Cyano-(3-substituted phenyl) acrylamide. Bioorg. Med. Chem. Lett. 19 (February 2009): 1861–1865.

[29] Kolmakov, K. A. An Efficient, "Green" Approach to Aryl Amination of Cyanuric Chloride Using Acetic Acid as Solvent. J. Heterocyclic Chem. 45 (March 2008): 533–539.

[30] Pavel, A. T., et. al. Material Solubility-Photovoltaic Performance Relationship in the Design of Novel Fullerene Derivatives for Bulk Heterojunction Solar Cells. Adv. Funct. Mater. 19 (February 2009): 779–788.

Appendix

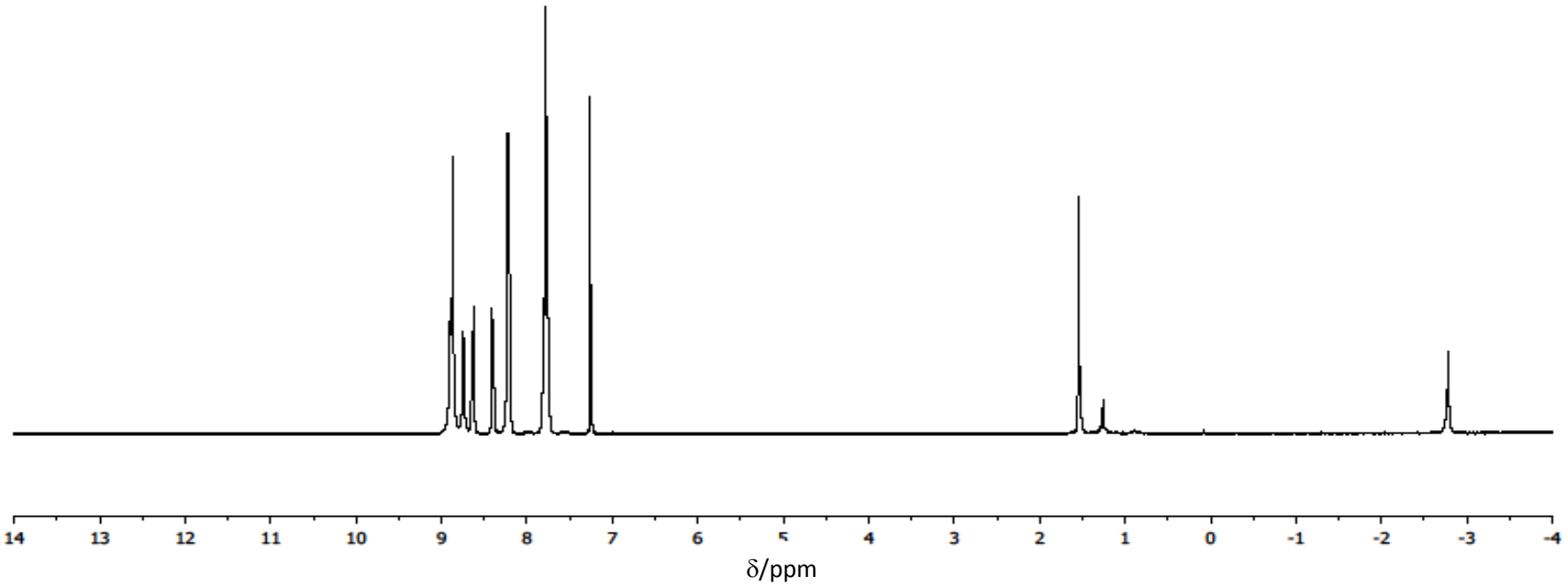

Figure 1. ^{1}H-NMR spectrum of compound **5**.

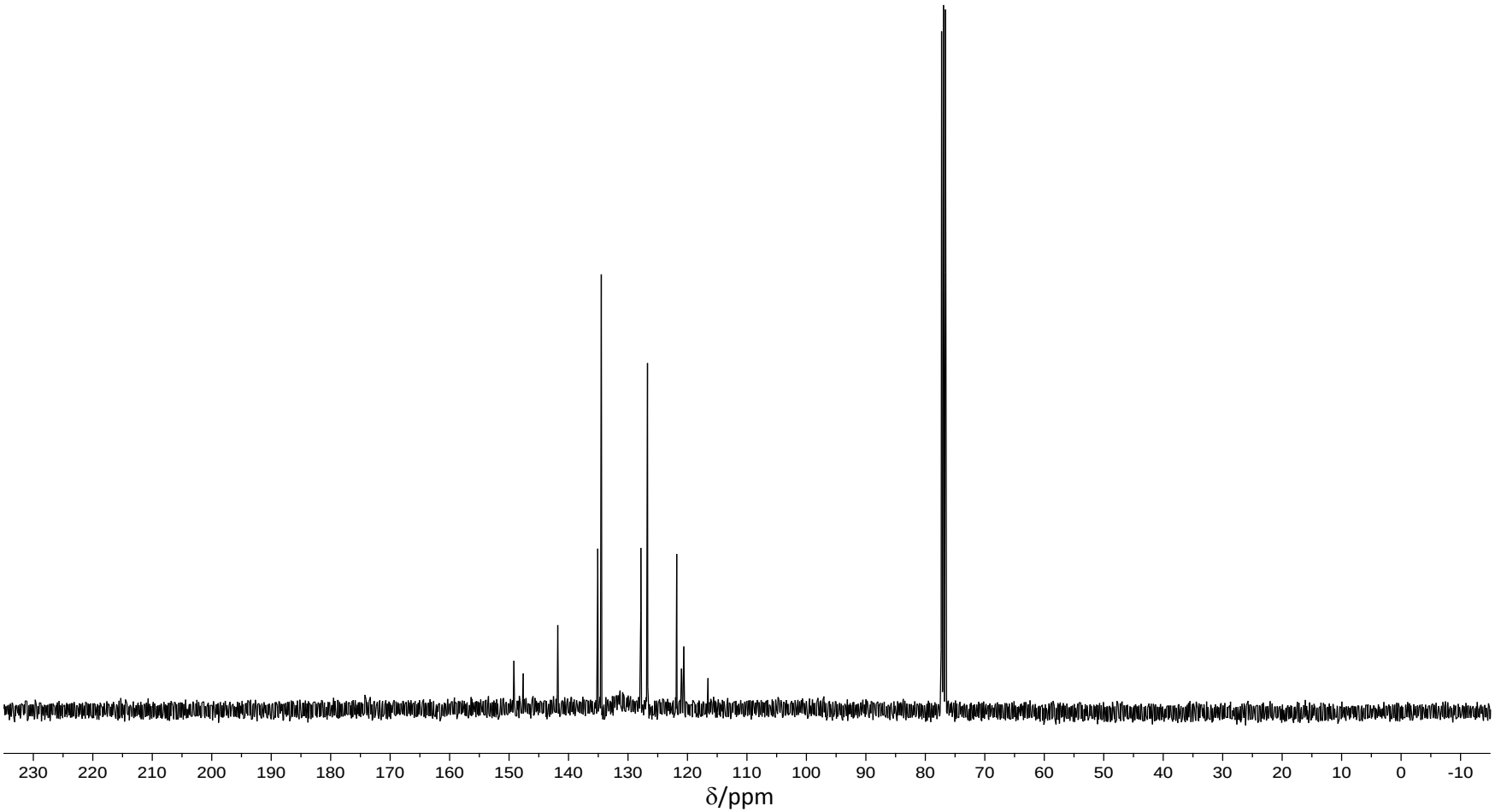

Figure 2. ^{13}C-NMR spectrum of compound **5**.

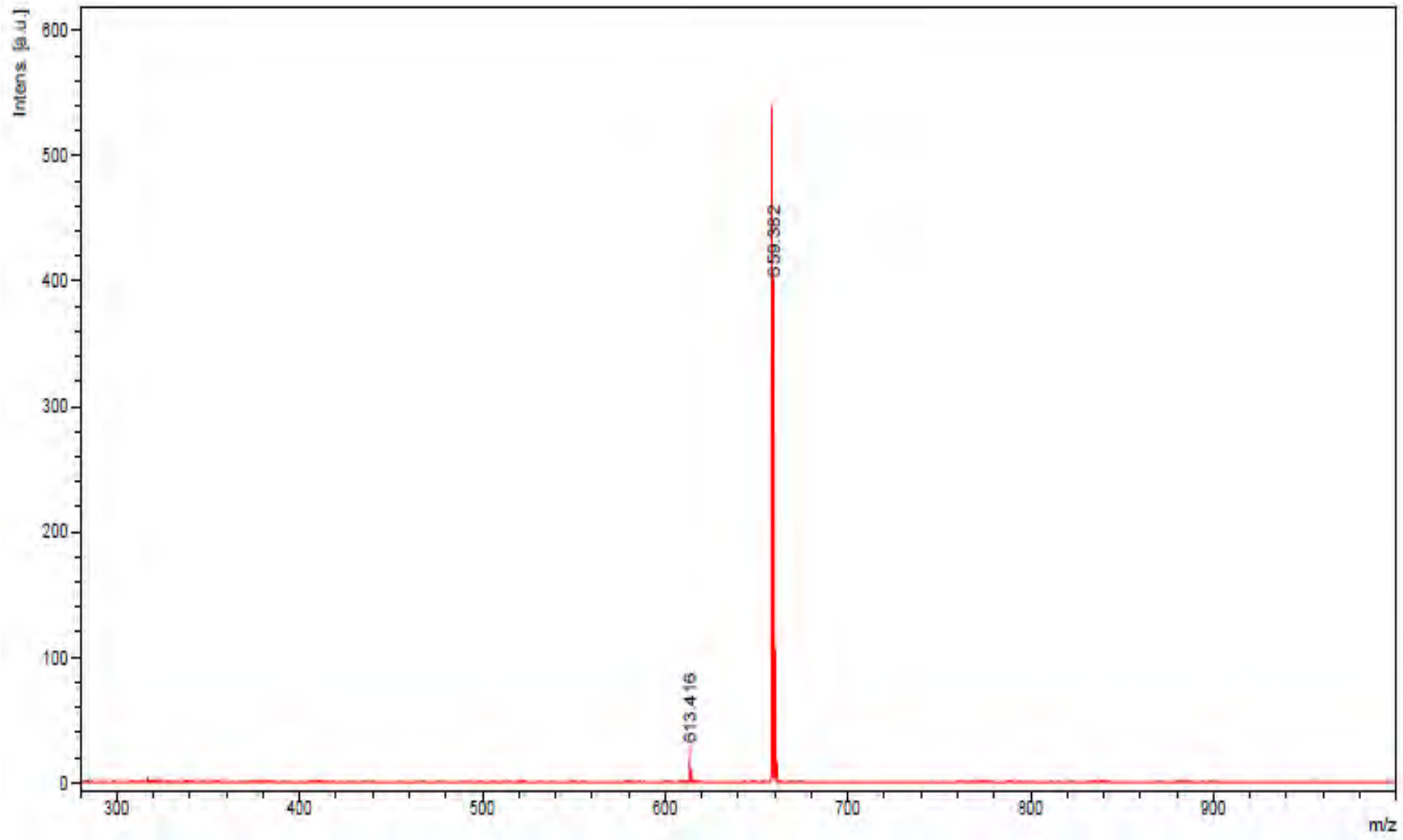

Figure 3. MALDI-TOF mass spectrum of compound **5**.

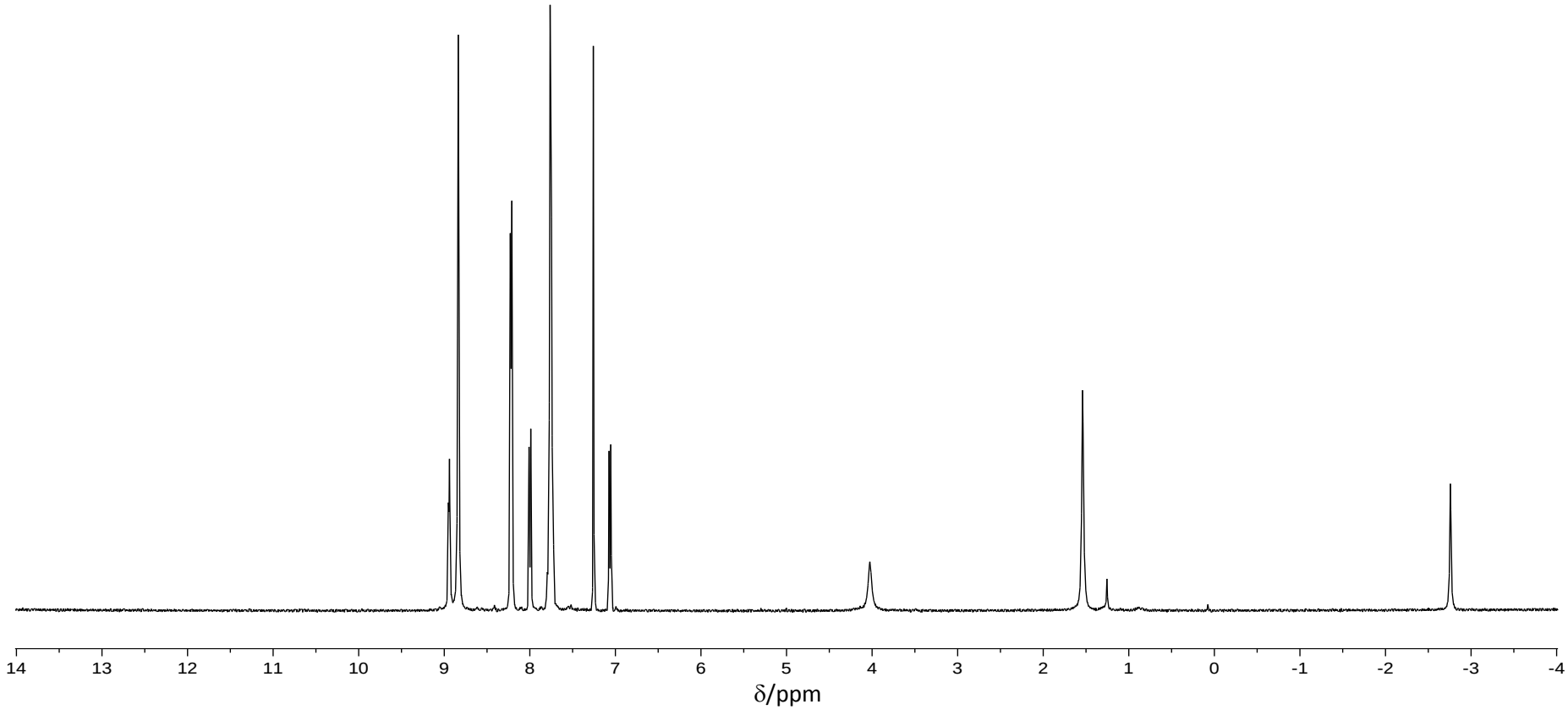

Figure 4. ^{1}H-NMR spectrum of compound **6**.

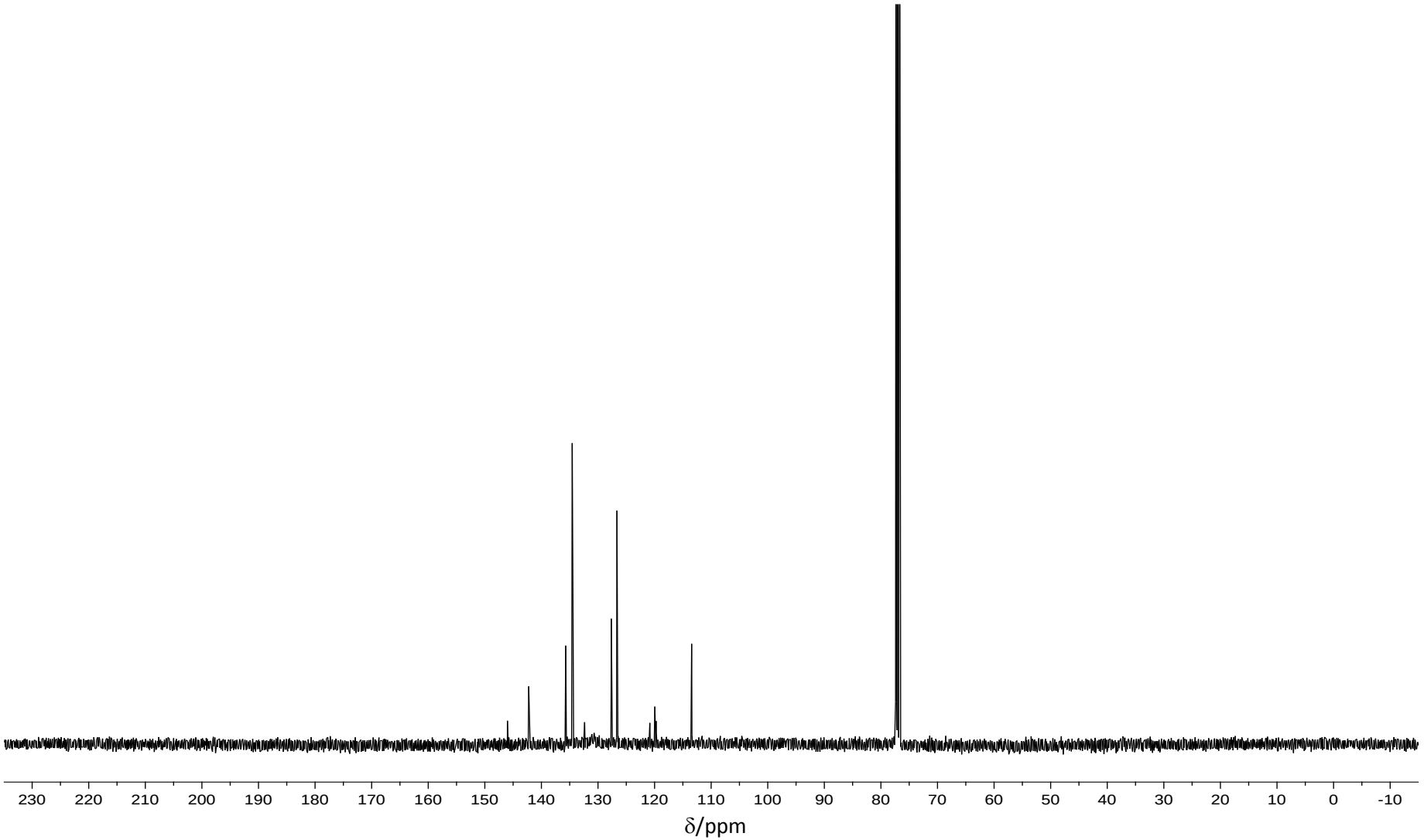

Figure 5. ^{13}C-NMR spectrum of compound **6**.

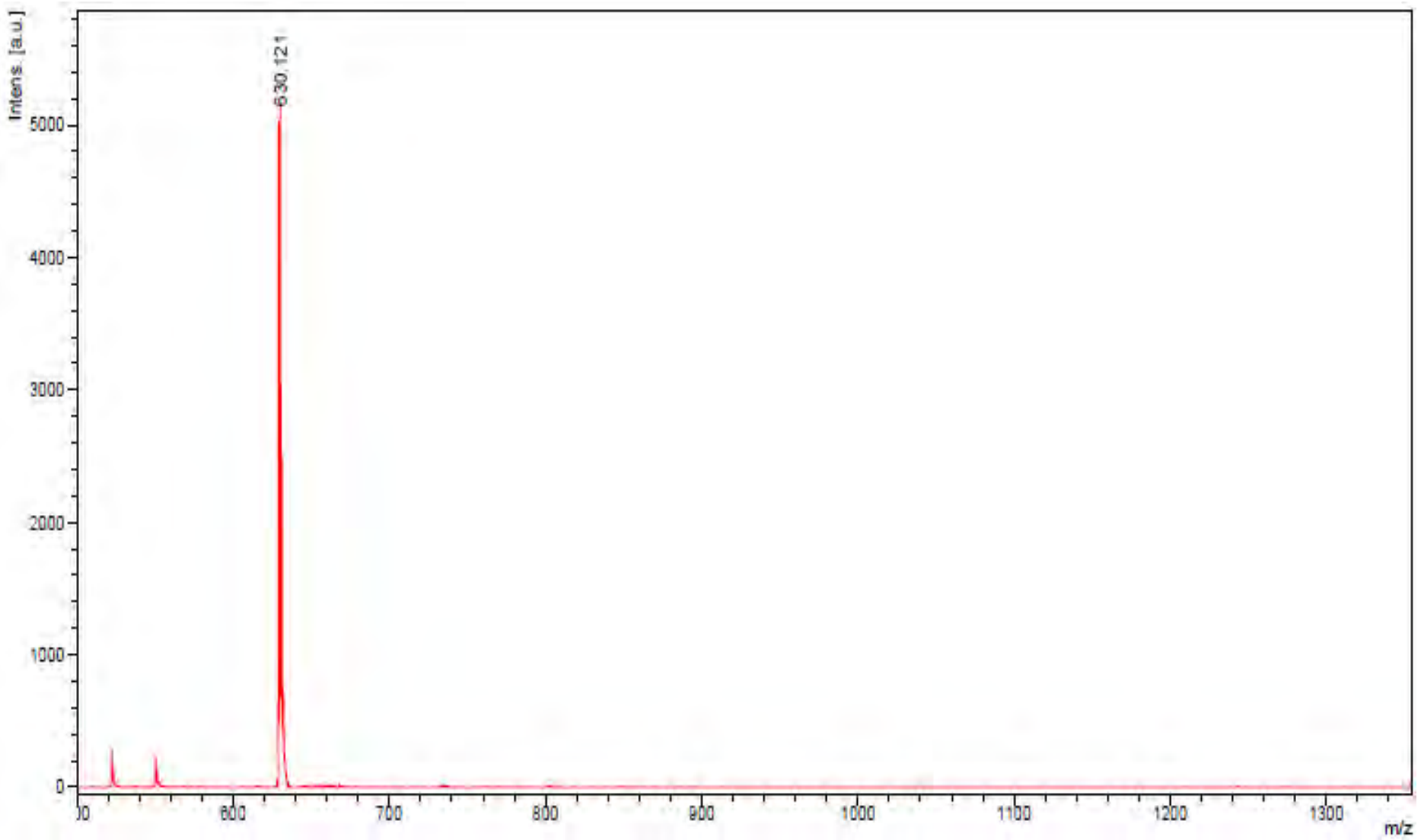

Figure 6. MALDI-TOF mass spectrum of compound **6**.

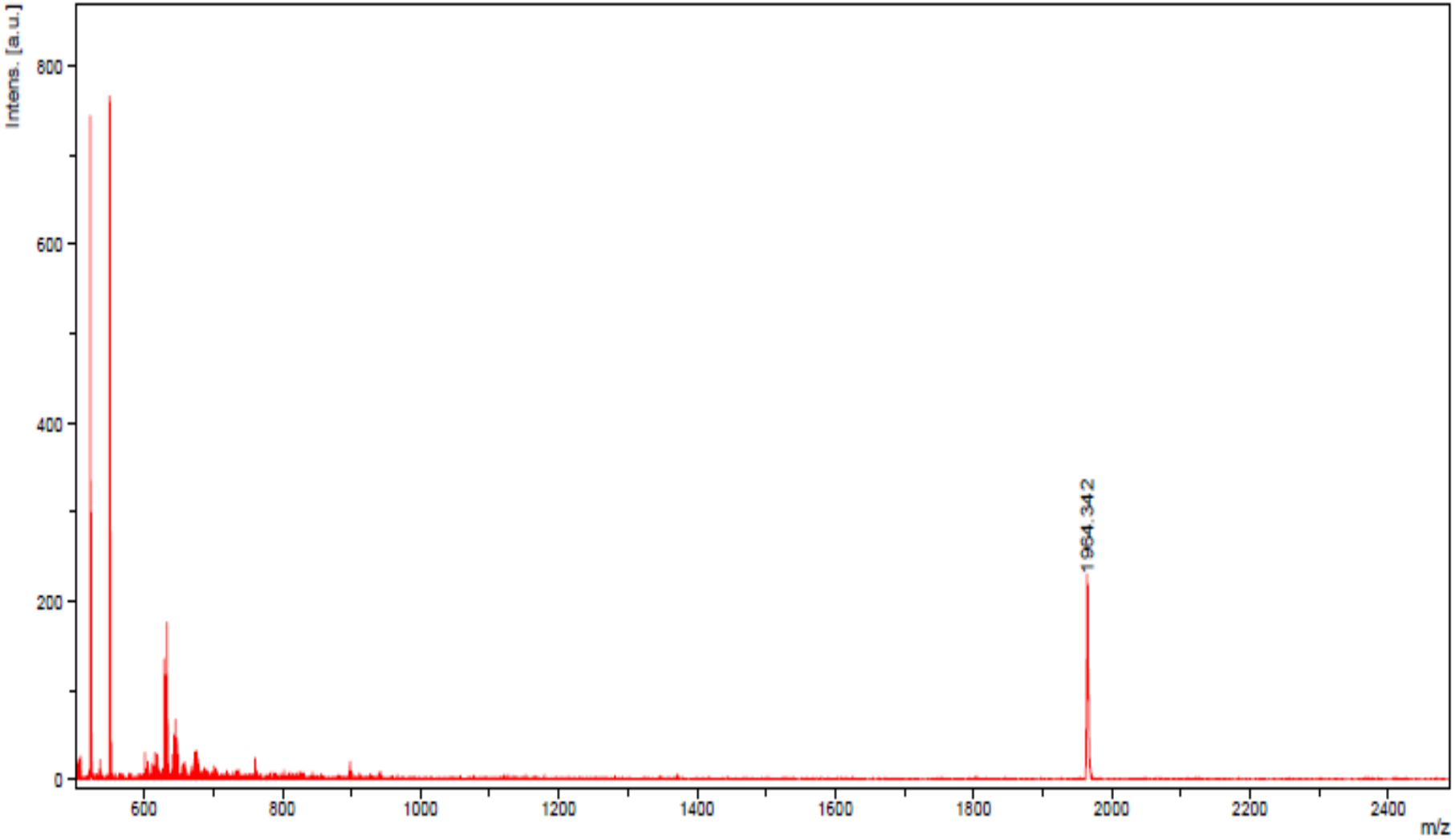

Figure 7. MALDI-TOF mass spectrum of compound **7**.

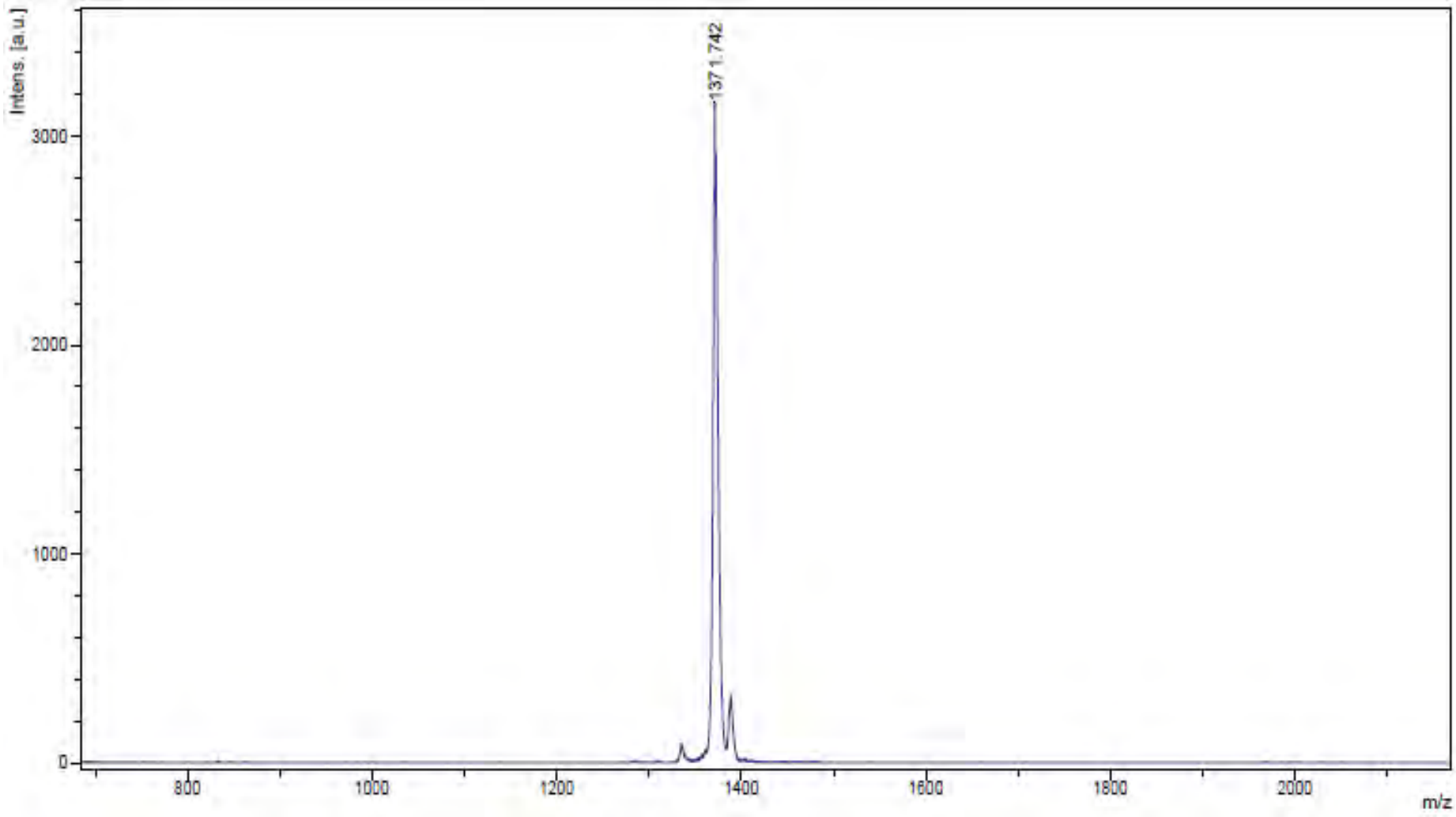

Figure 8. MALDI-TOF mass spectrum of compound **8**.

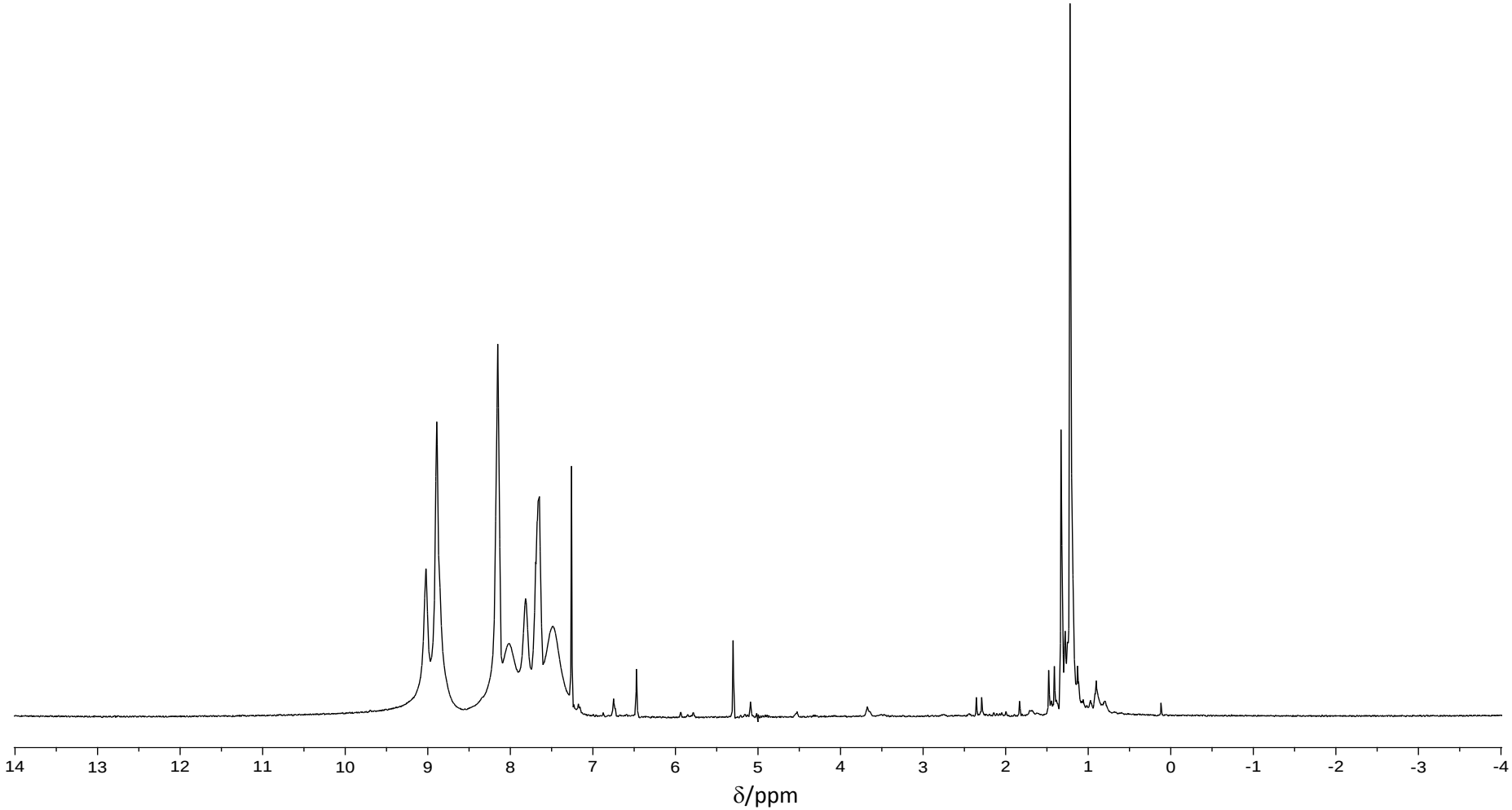

Figure 9. ^{1}H-NMR spectrum of compound **Zn-1**.

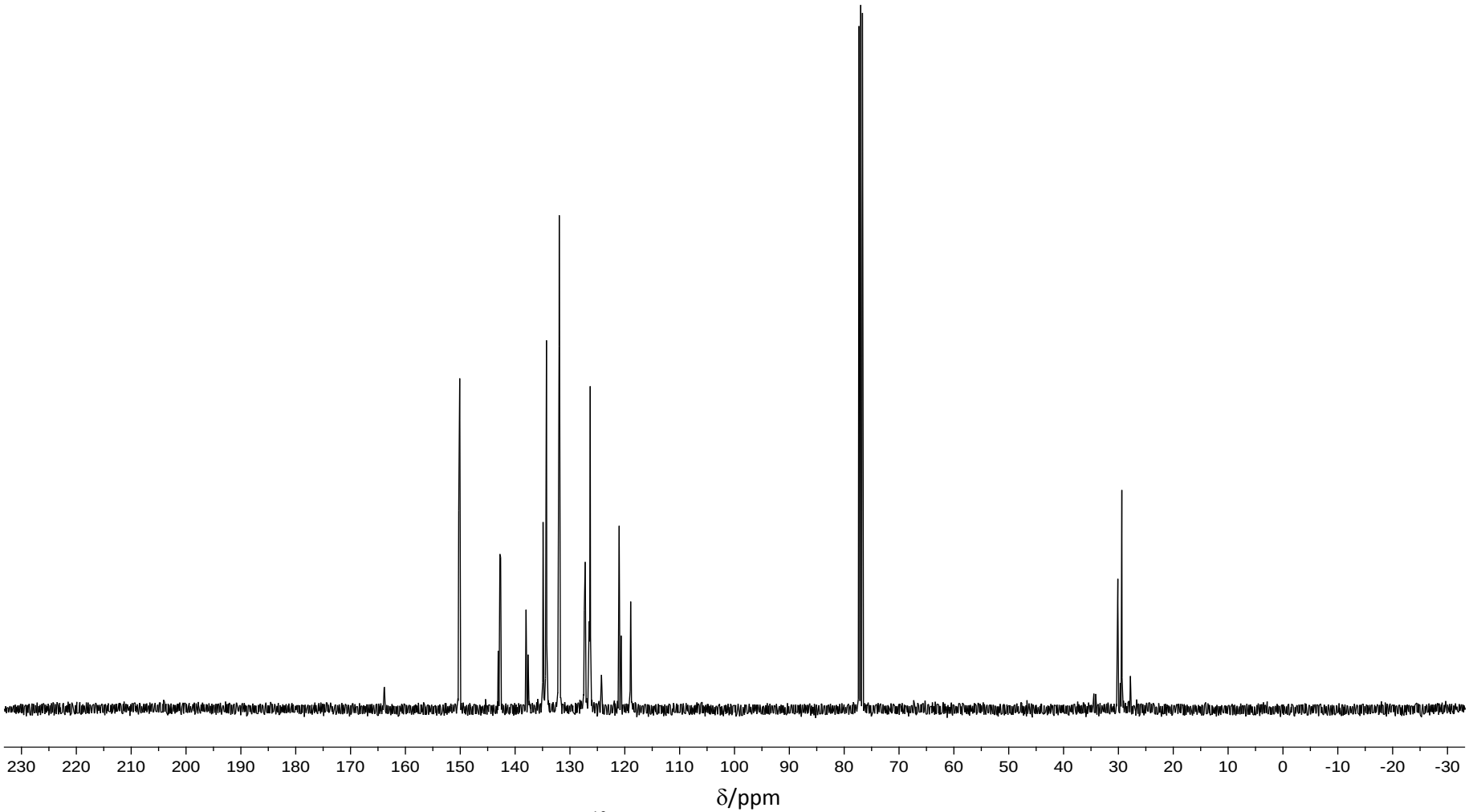

Figure 10. ^{13}C-NMR spectrum of compound **Zn-1**.

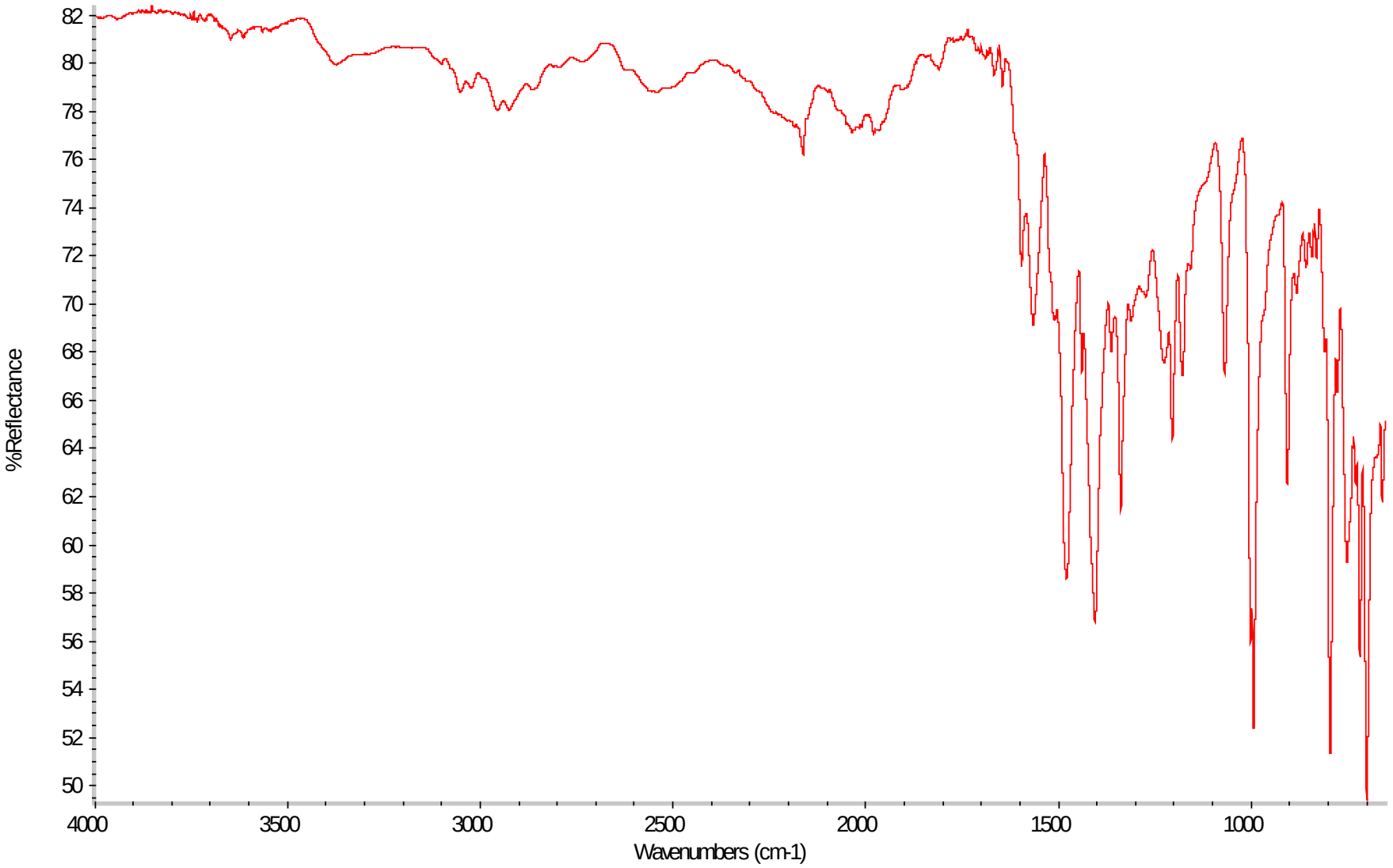

Figure 11. IR spectrum of compound **Zn-1**.

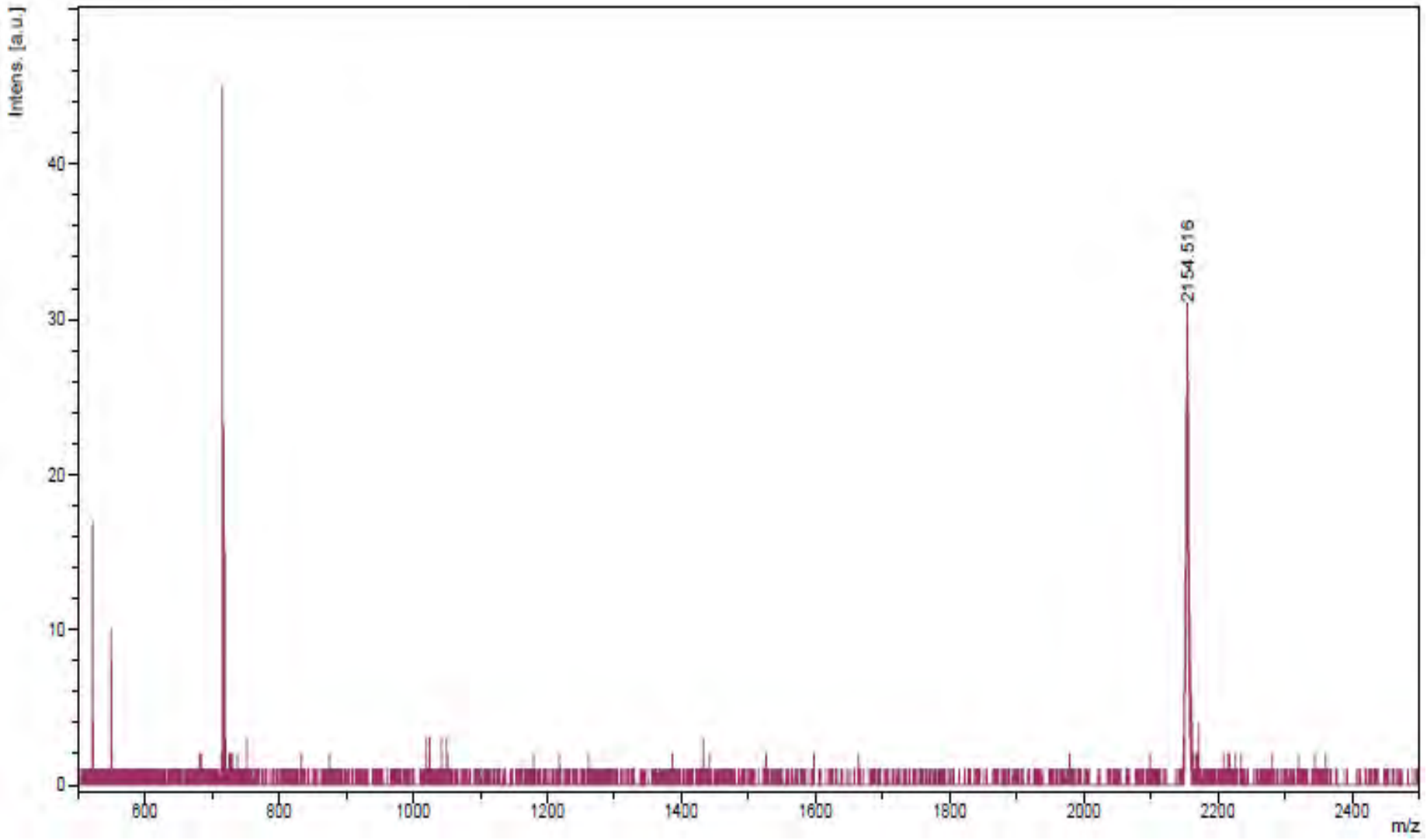

Figure 12. MALDI-TOF mass spectrum of compound **Zn-1**.

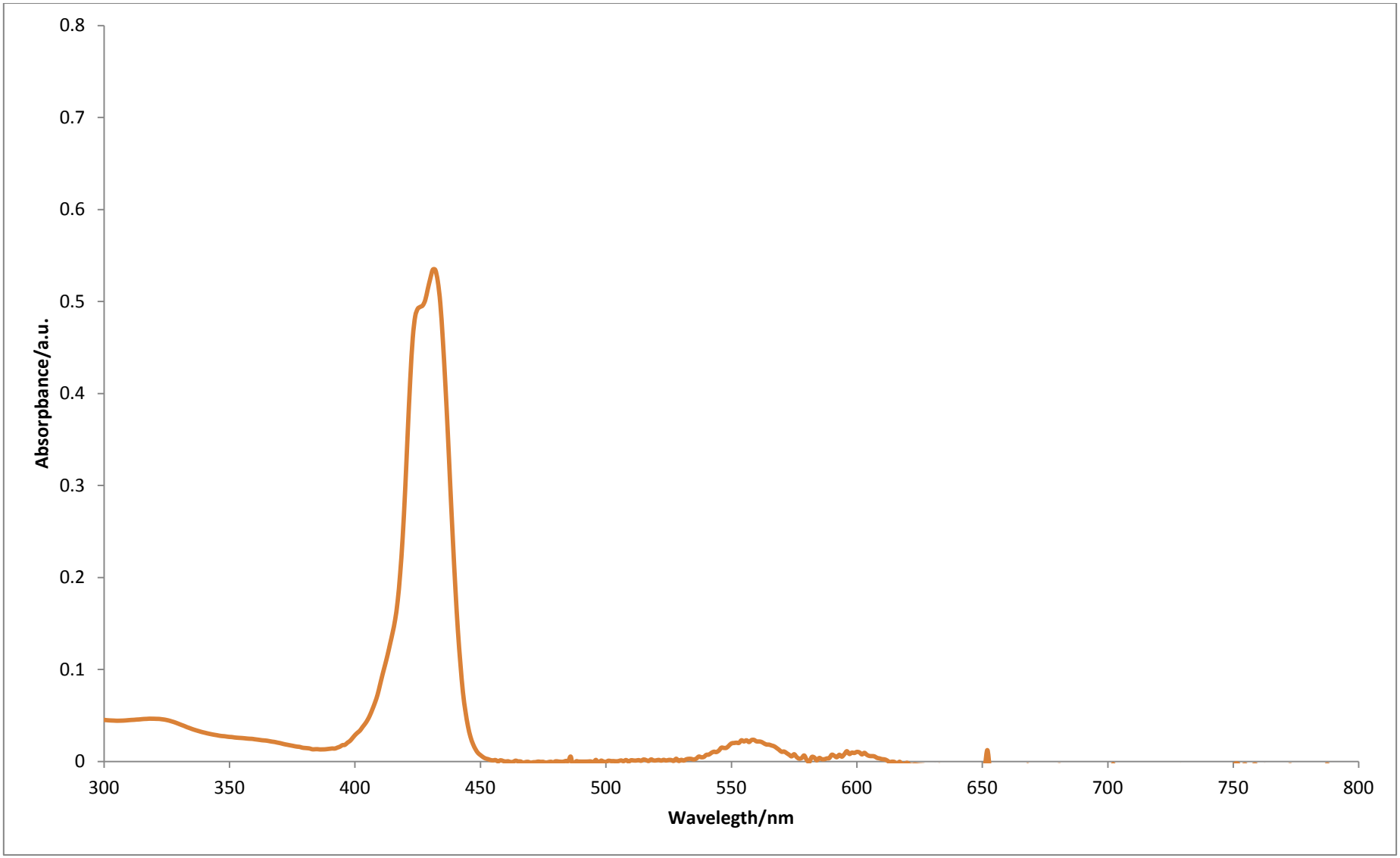

Figure 13. UV-Vis spectrum of compound **Zn-1**.

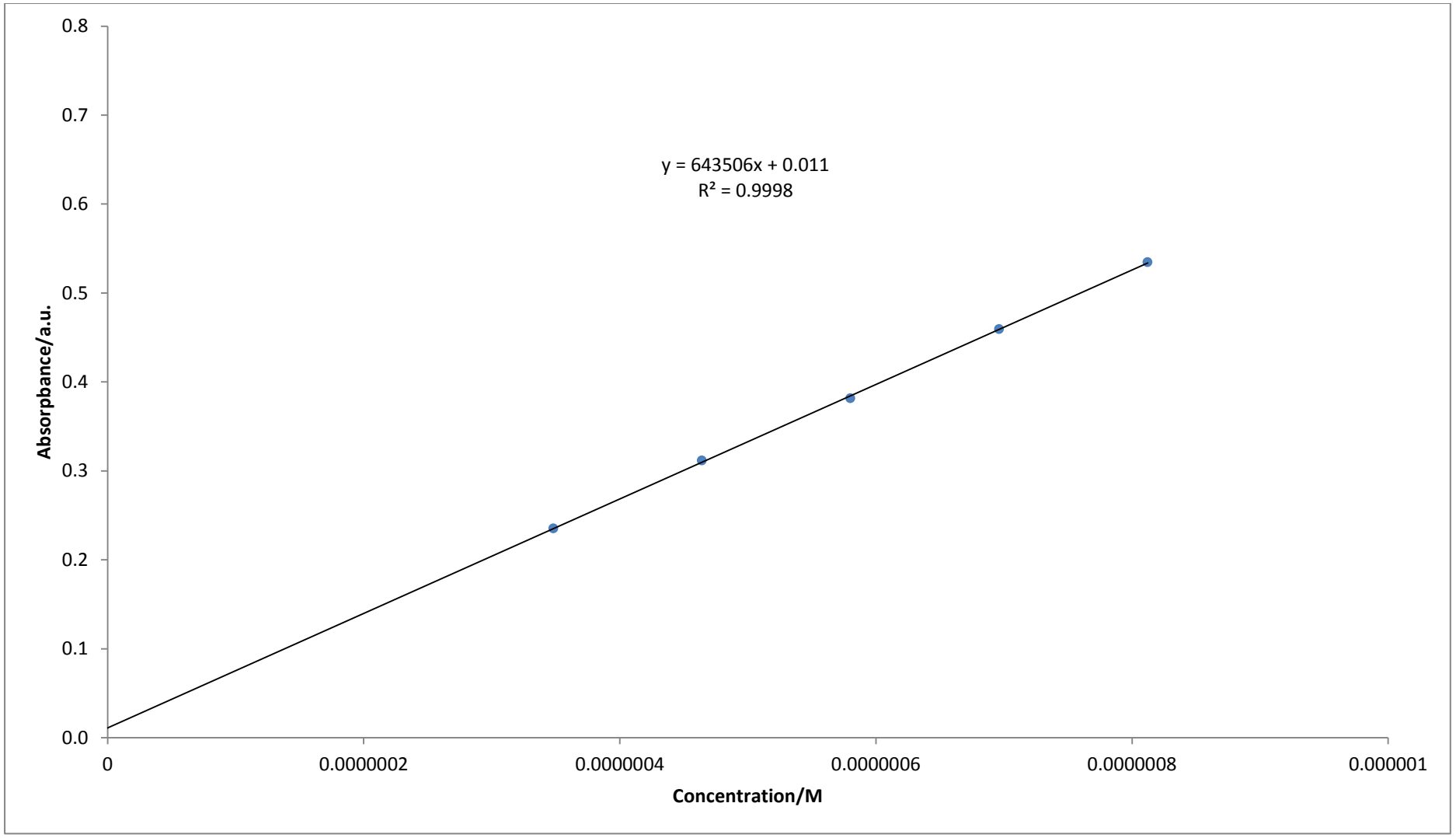

Figure 14. Calibration curve for quantitative determination of compound **Zn-1** in toluene (λ_{abs} = 431 nm).

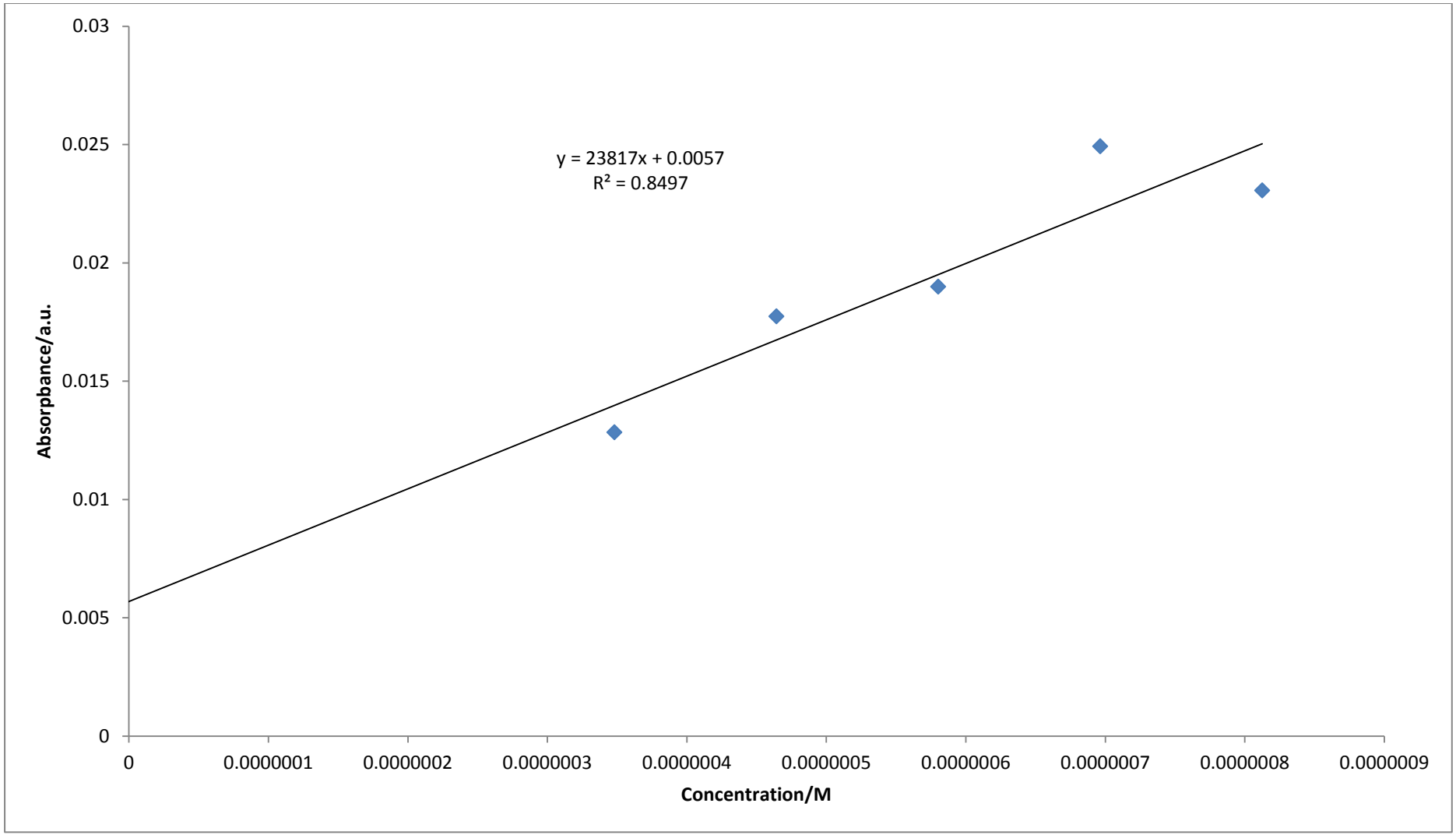

Figure 15. Calibration curve for quantitative determination of compound **Zn-1** in toluene (λ_{abs} = 552 nm).

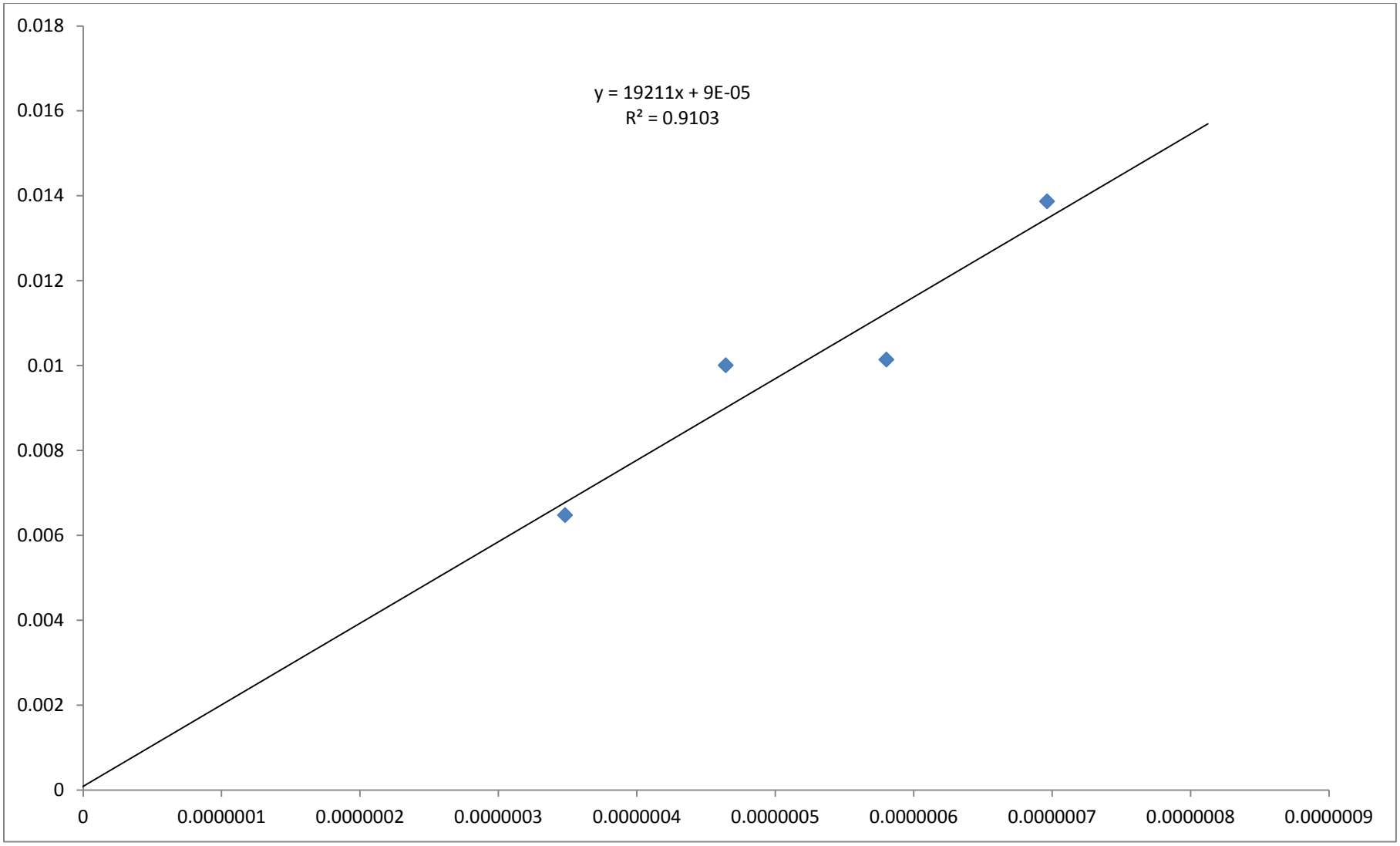

Figure 16. Calibration curve for quantitative determination of compound **Zn-1** in toluene (λ_{abs} = 601 nm).

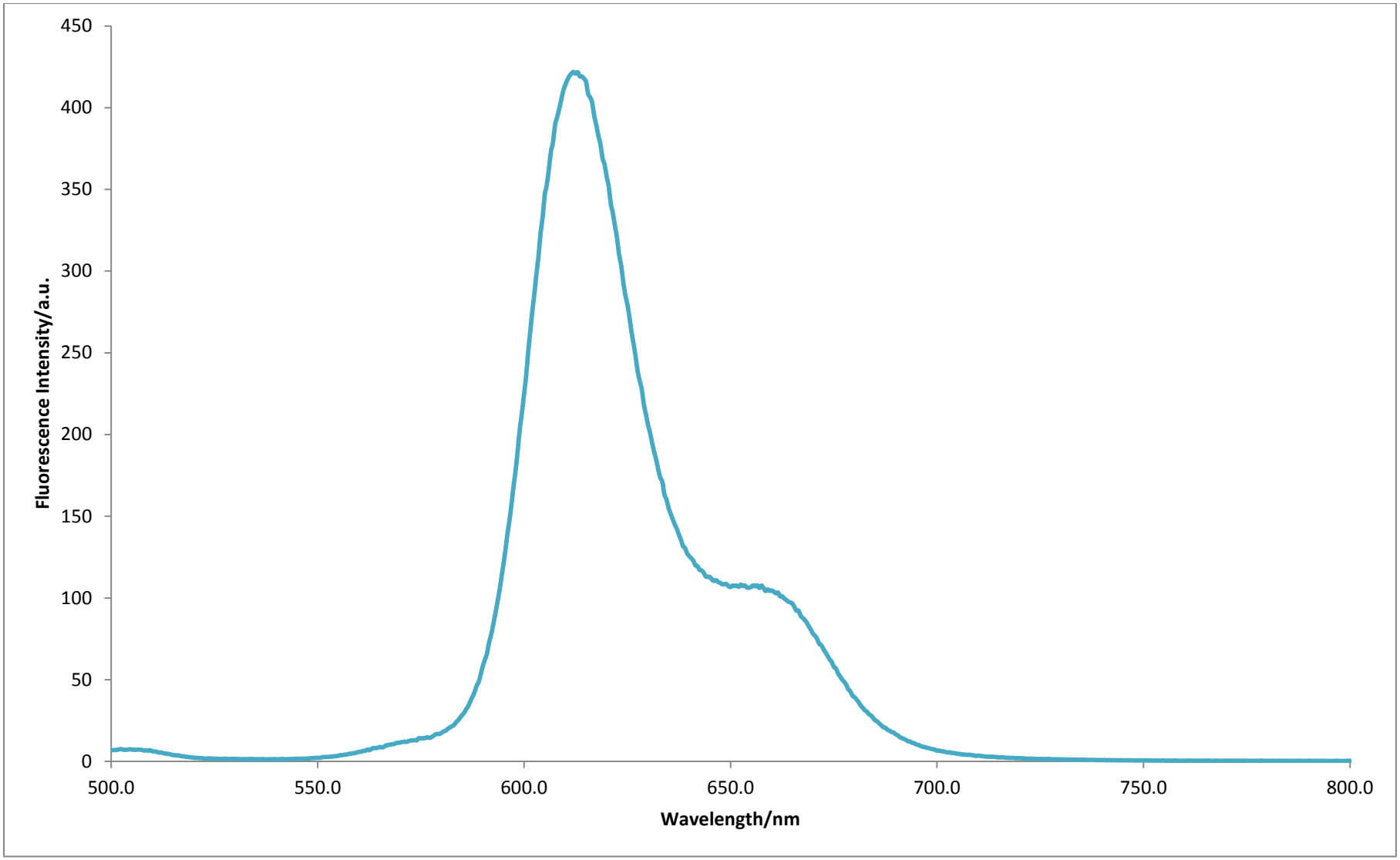

Figure 17. Fluorescence spectrum of compound **Zn-1**.

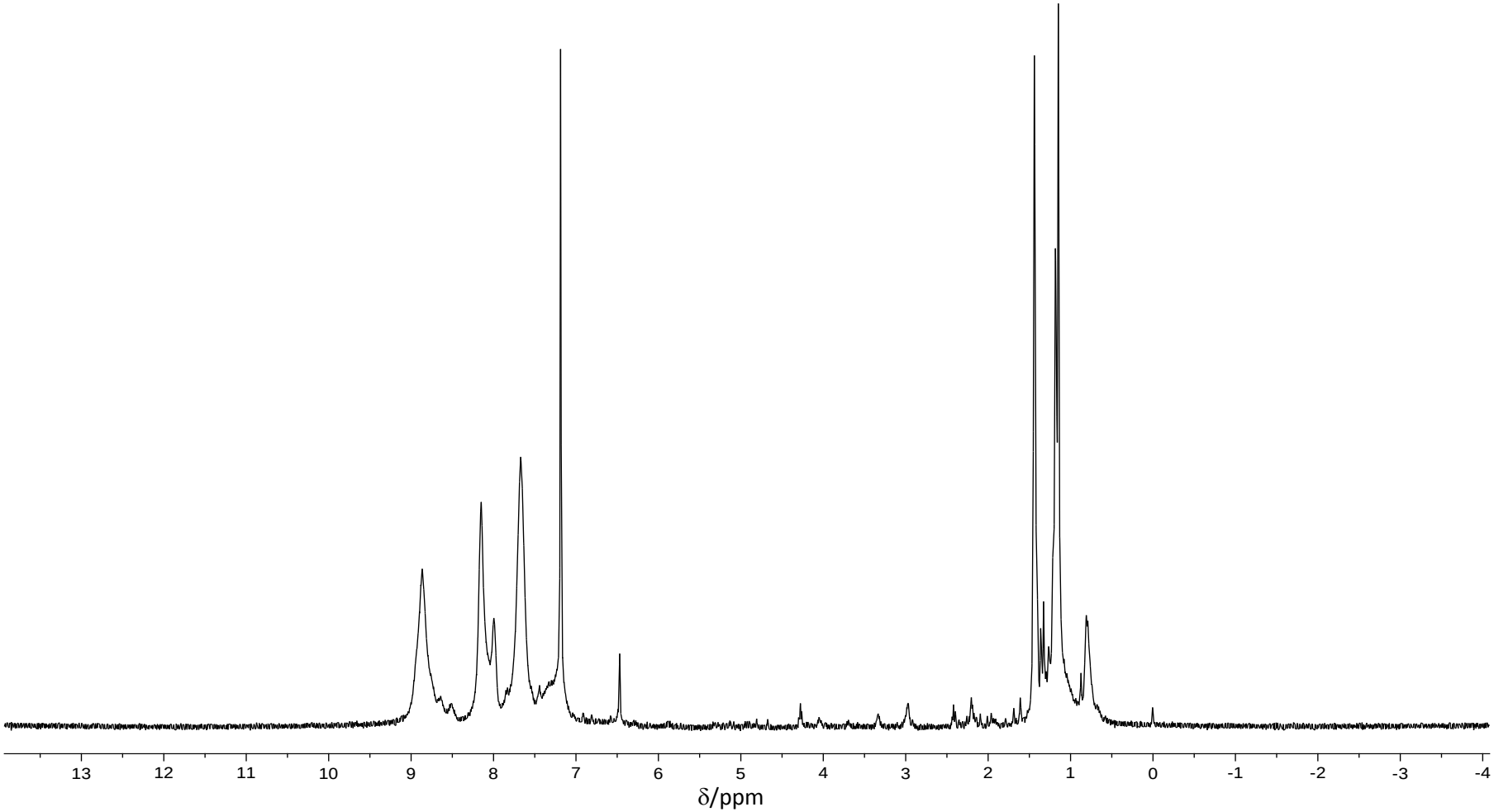

Figure 18. ^{1}H-NMR spectrum of compound **Zn-8**.

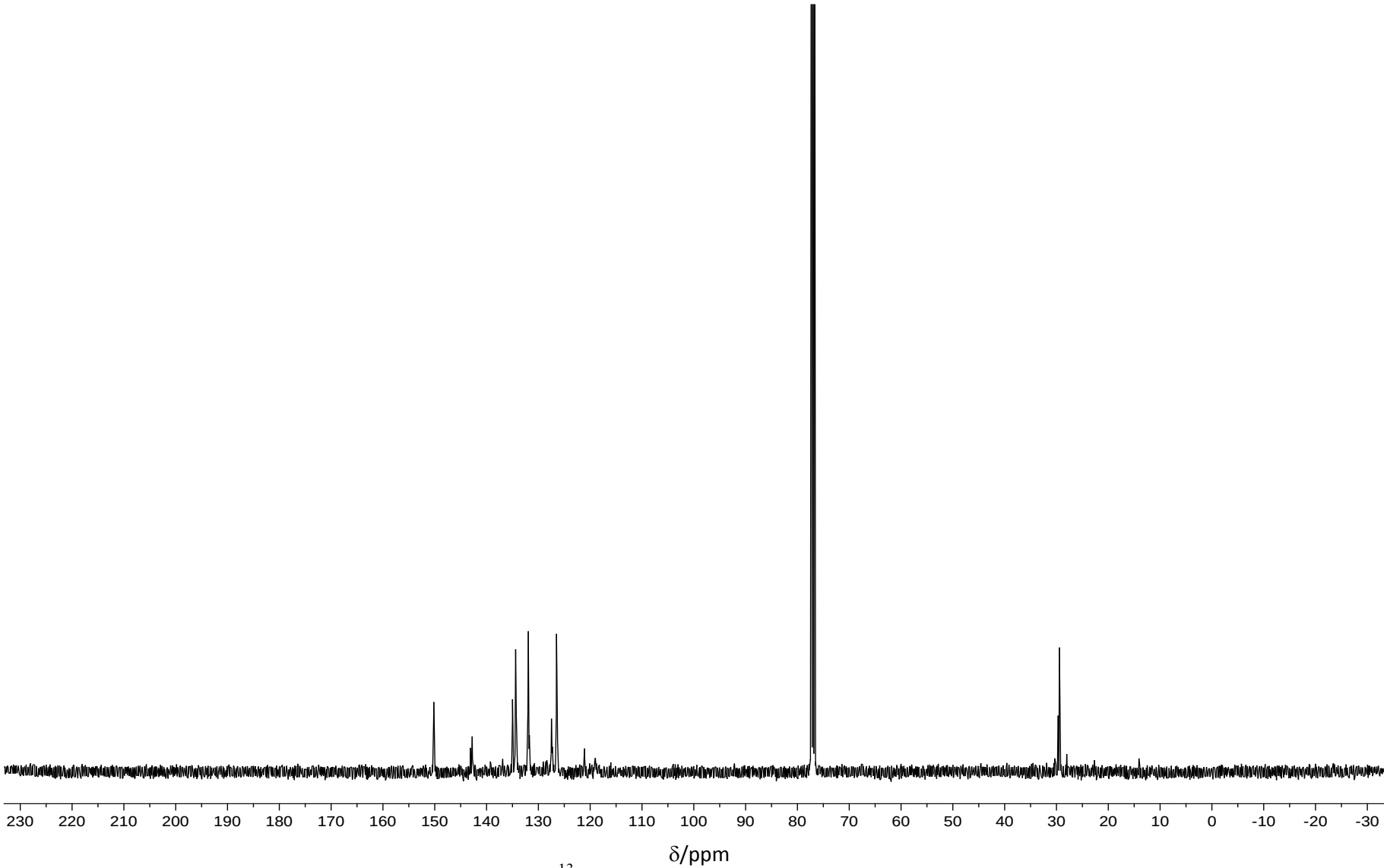

Figure 19. ^{13}C-NMR spectrum of compound **Zn-8**.

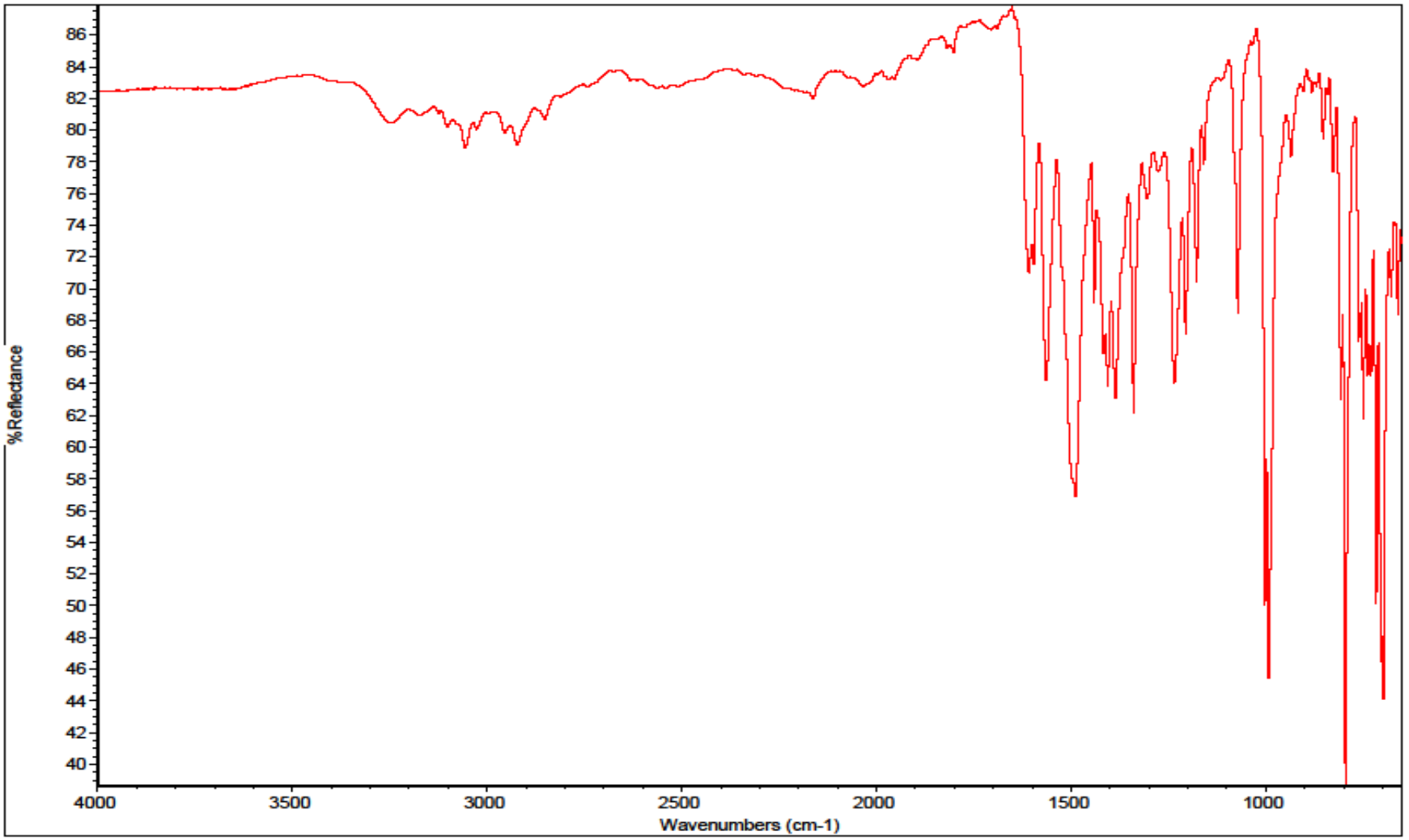

Figure 20. IR spectrum of compound **Zn-8**.

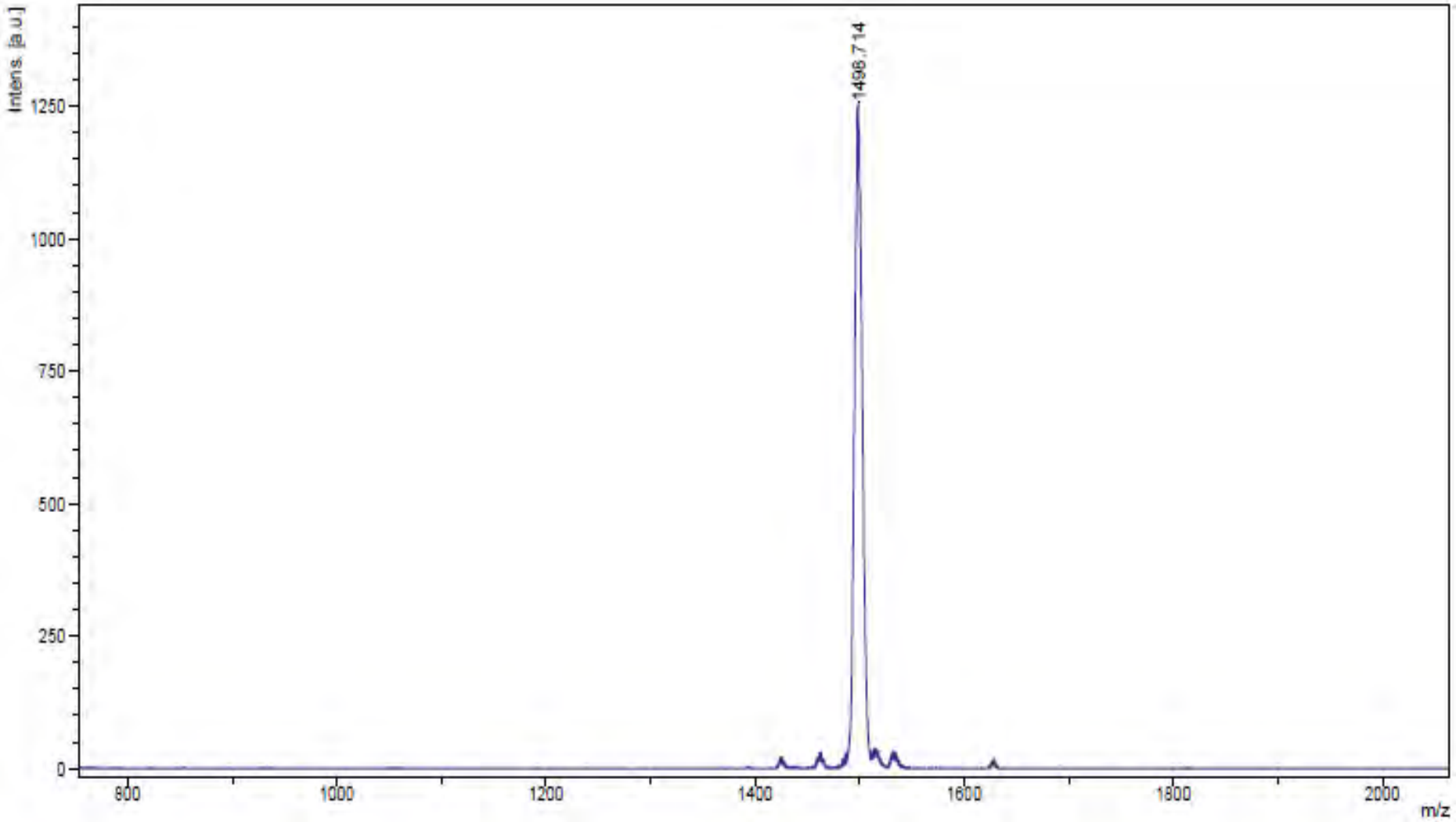

Figure 21. MALDI-TOF mass spectrum of compound **Zn-8**.

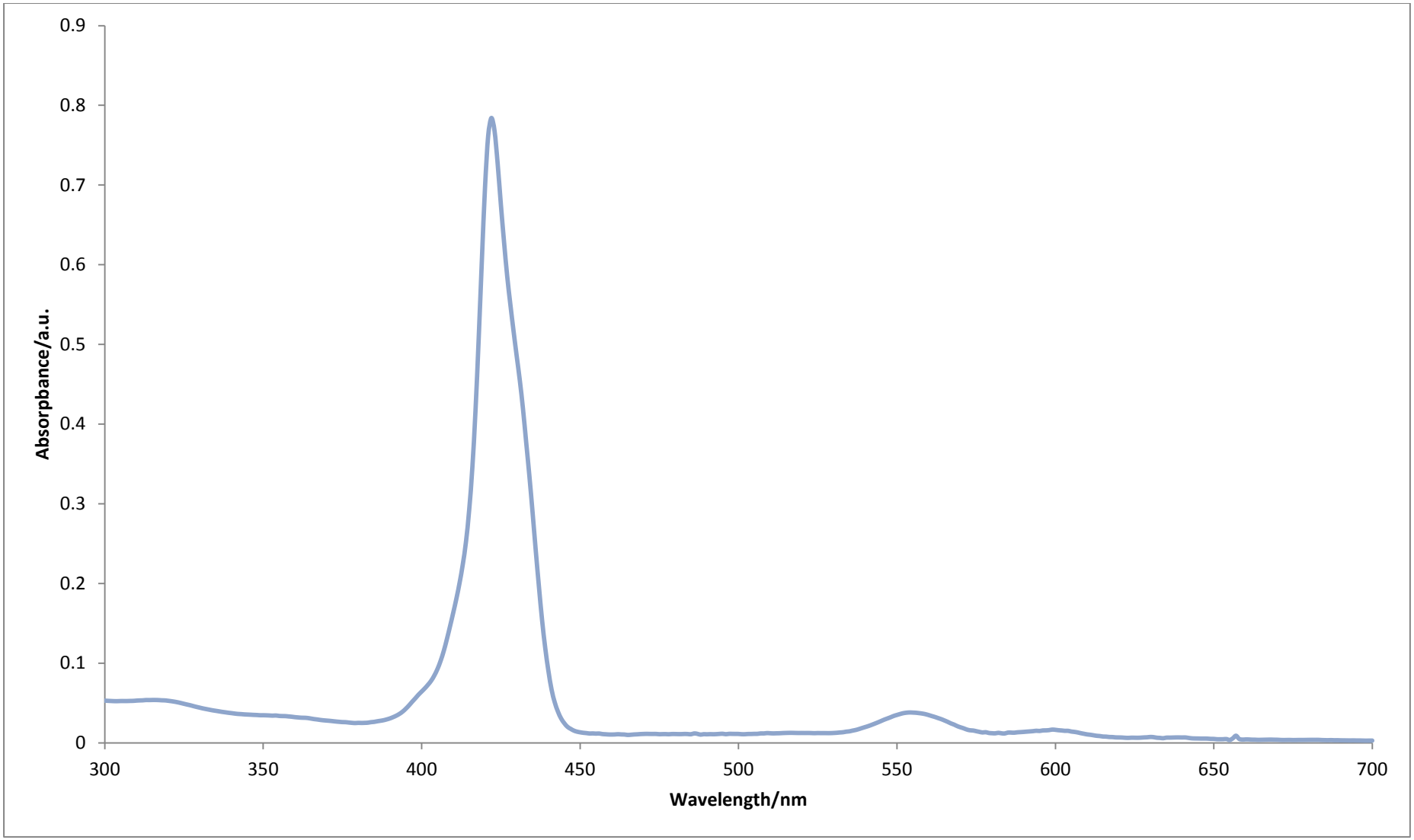

Figure 22. UV-Vis spectrum of compound **Zn-8**.

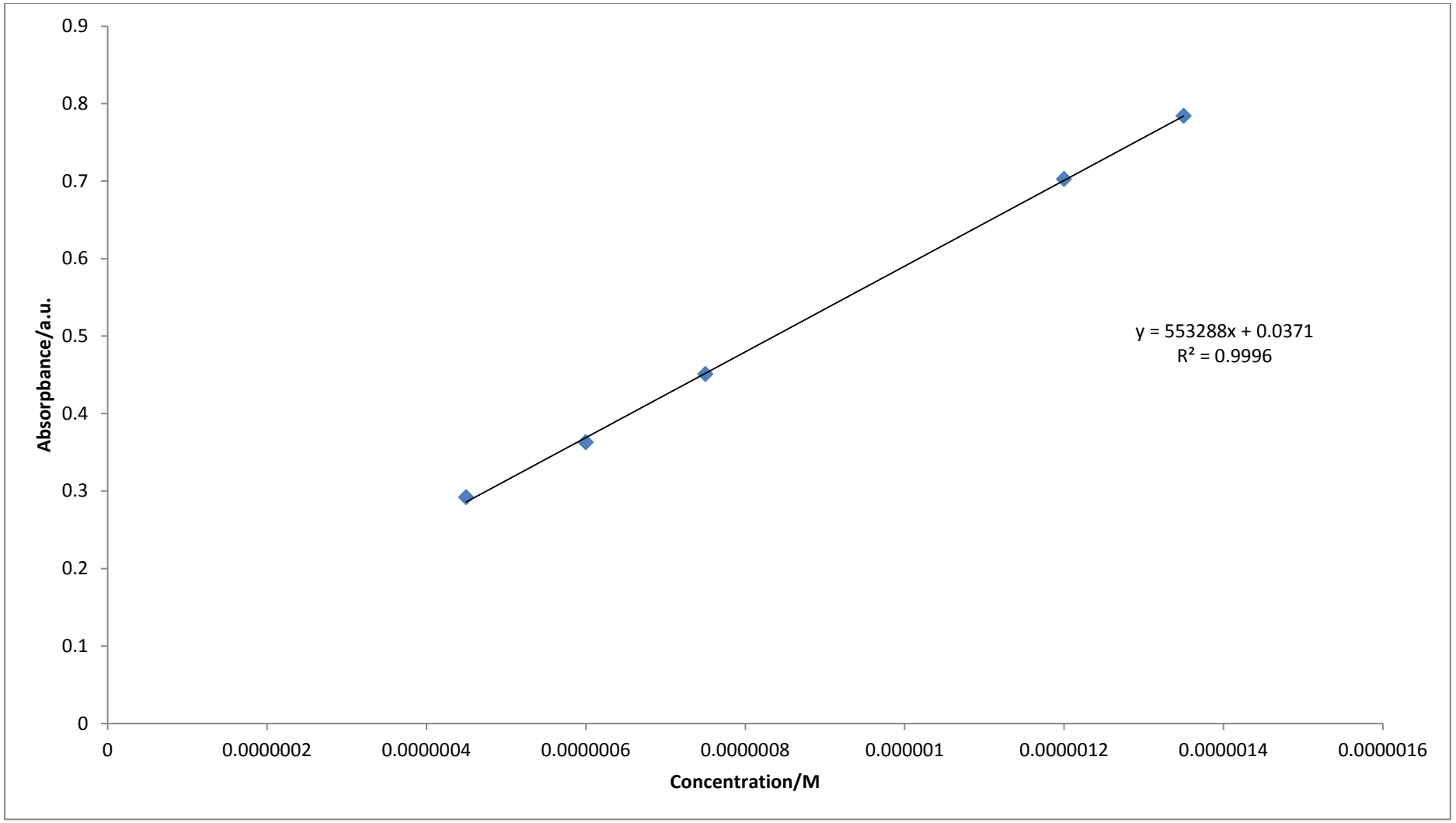

Figure 23. Calibration curve for quantitative determination of compound **Zn-8** in toluene (λ_{abs} = 422 nm).

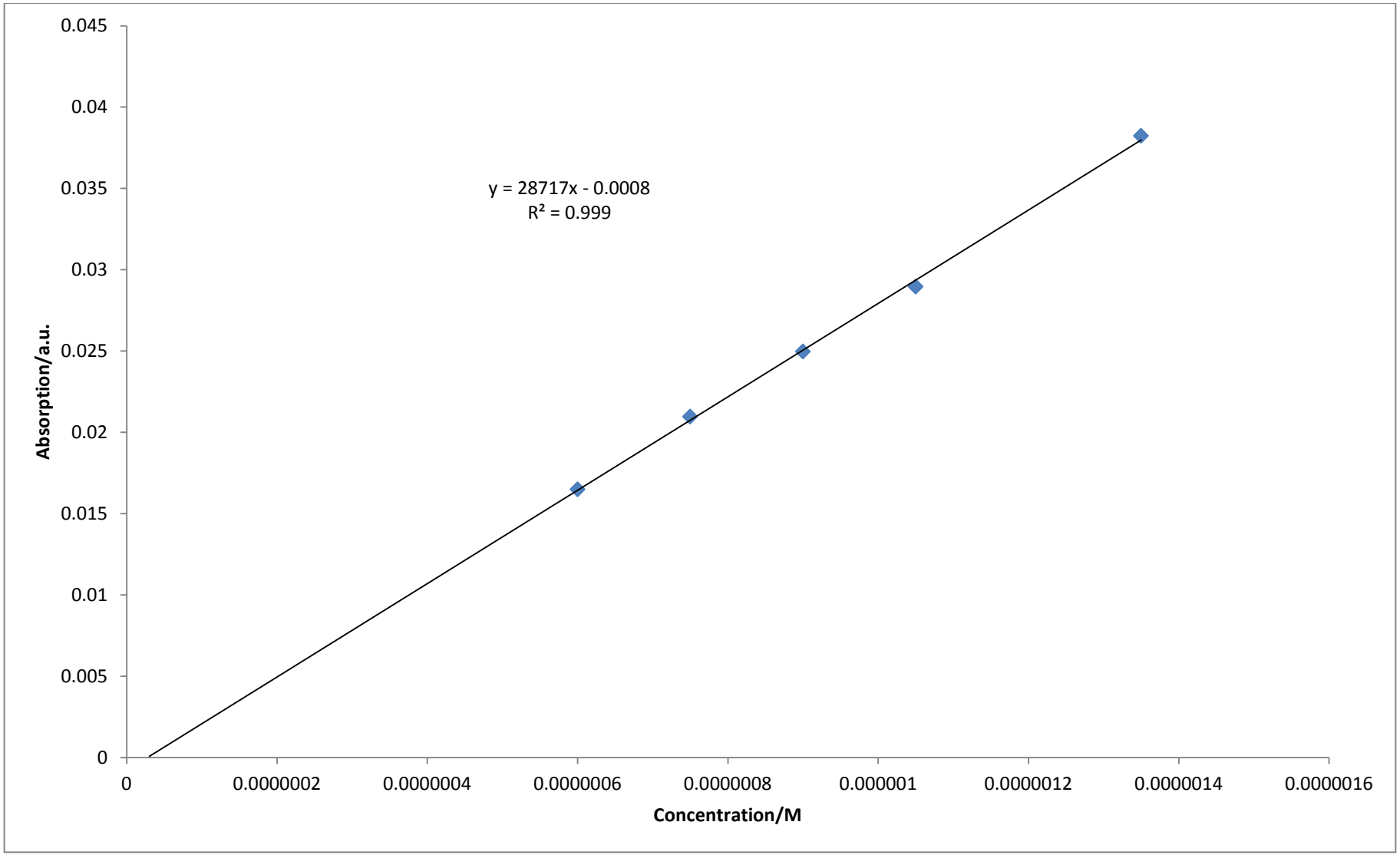

Figure 24. Calibration curve for quantitative determination of compound **Zn-8** in toluene (λ_{abs} = 554 nm).

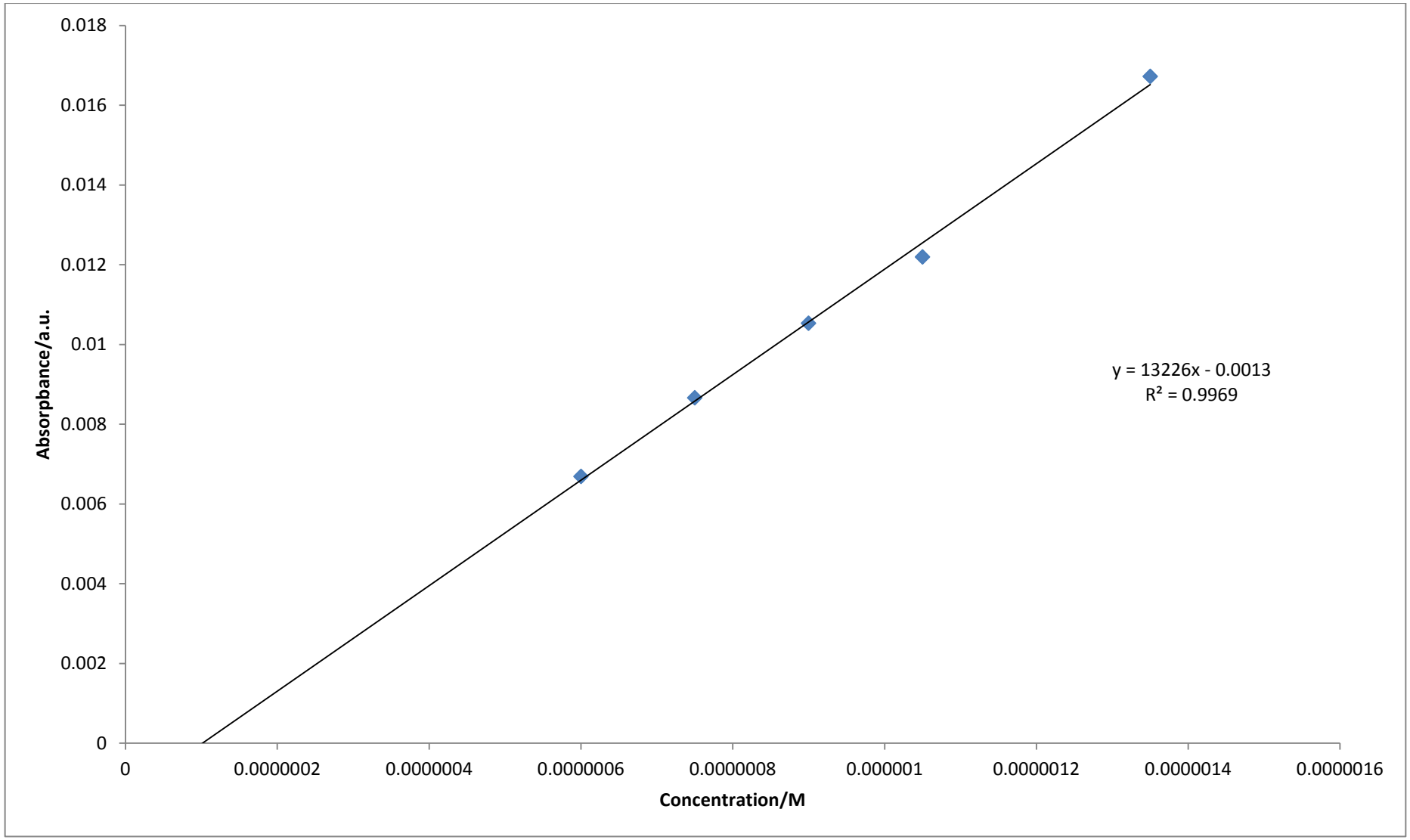

Figure 25. Calibration curve for quantitative determination of compound **Zn-8** in toluene (λ_{abs} = 599 nm).

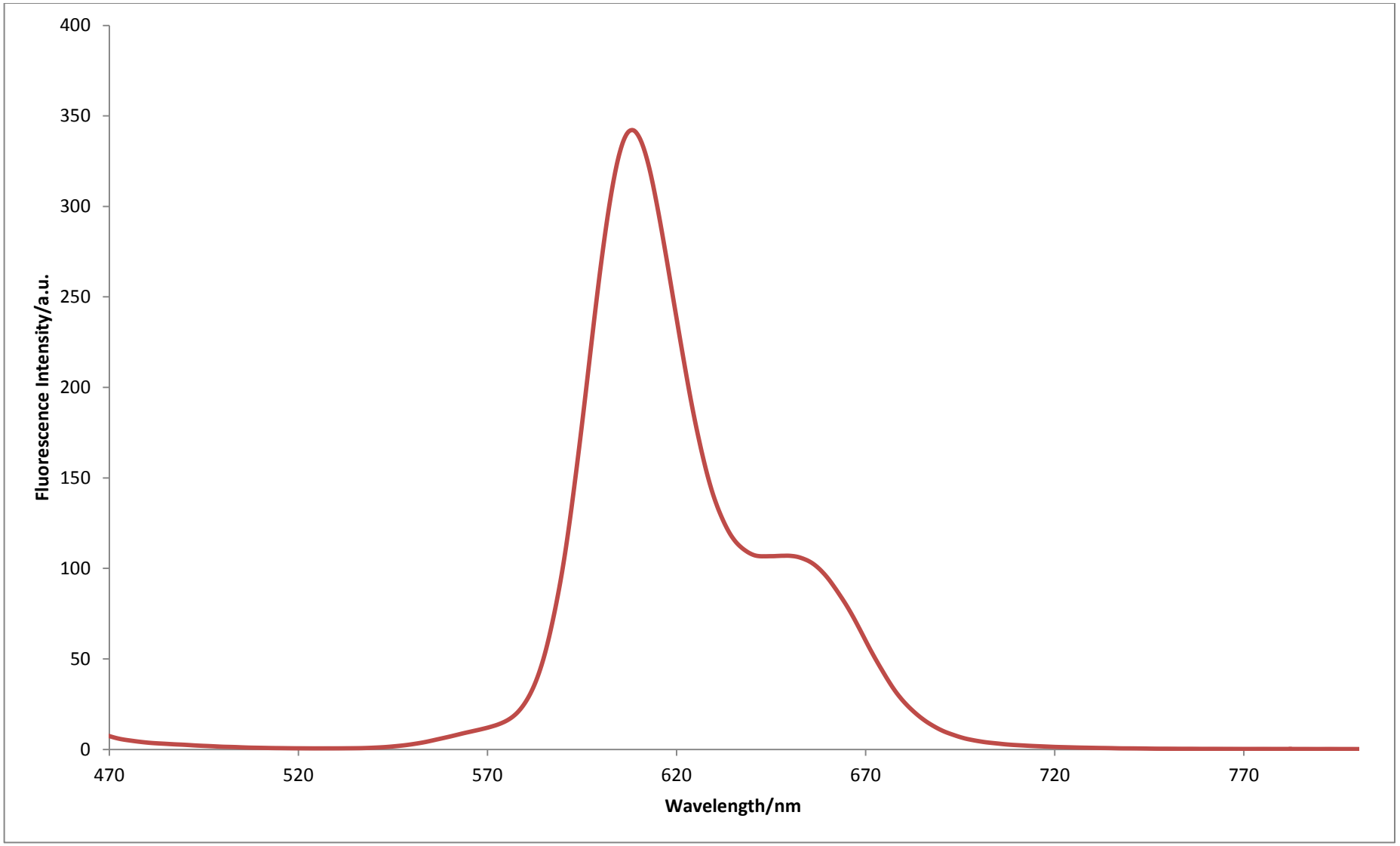

Figure 26. Fluorescence spectrum of compound **Zn-8**.

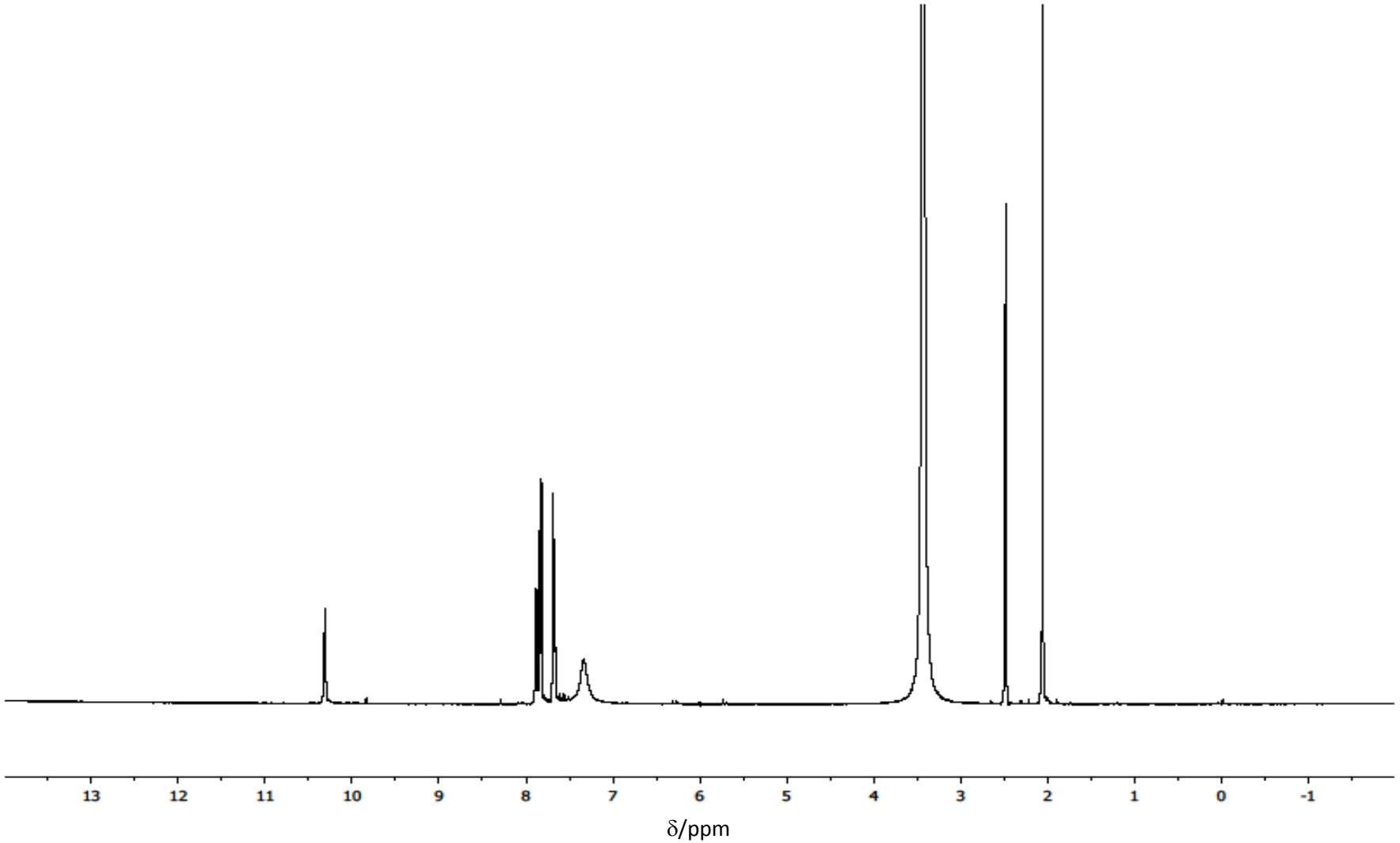

Figure 27. ^{1}H-NMR spectrum of 3-(4-aminophenyl)-2-cyano acrylic acid (**10**).

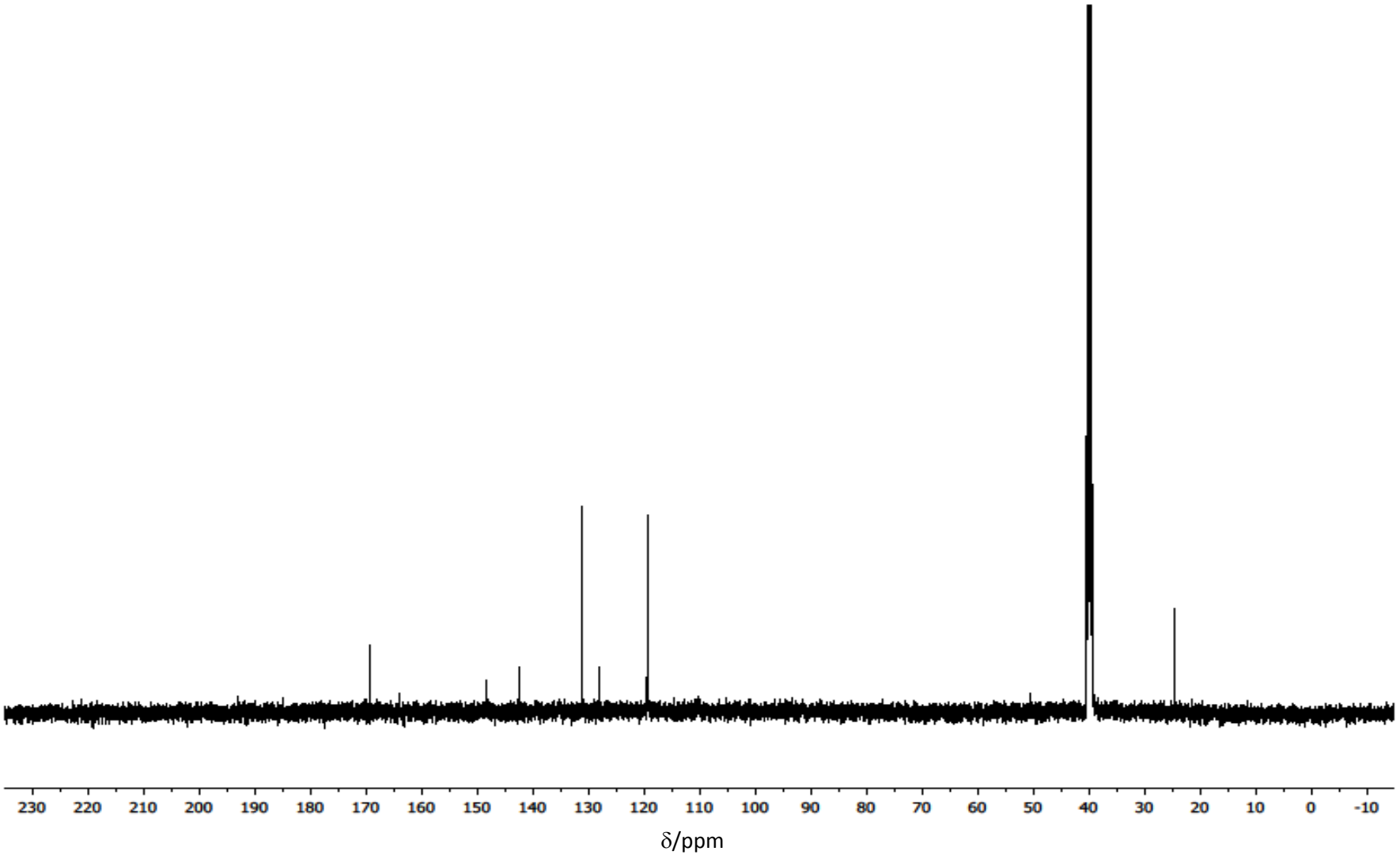

Figure 28 ^{13}C-NMR spectrum of 3-(4-aminophenyl)-2-cyano acrylic acid (**10**).

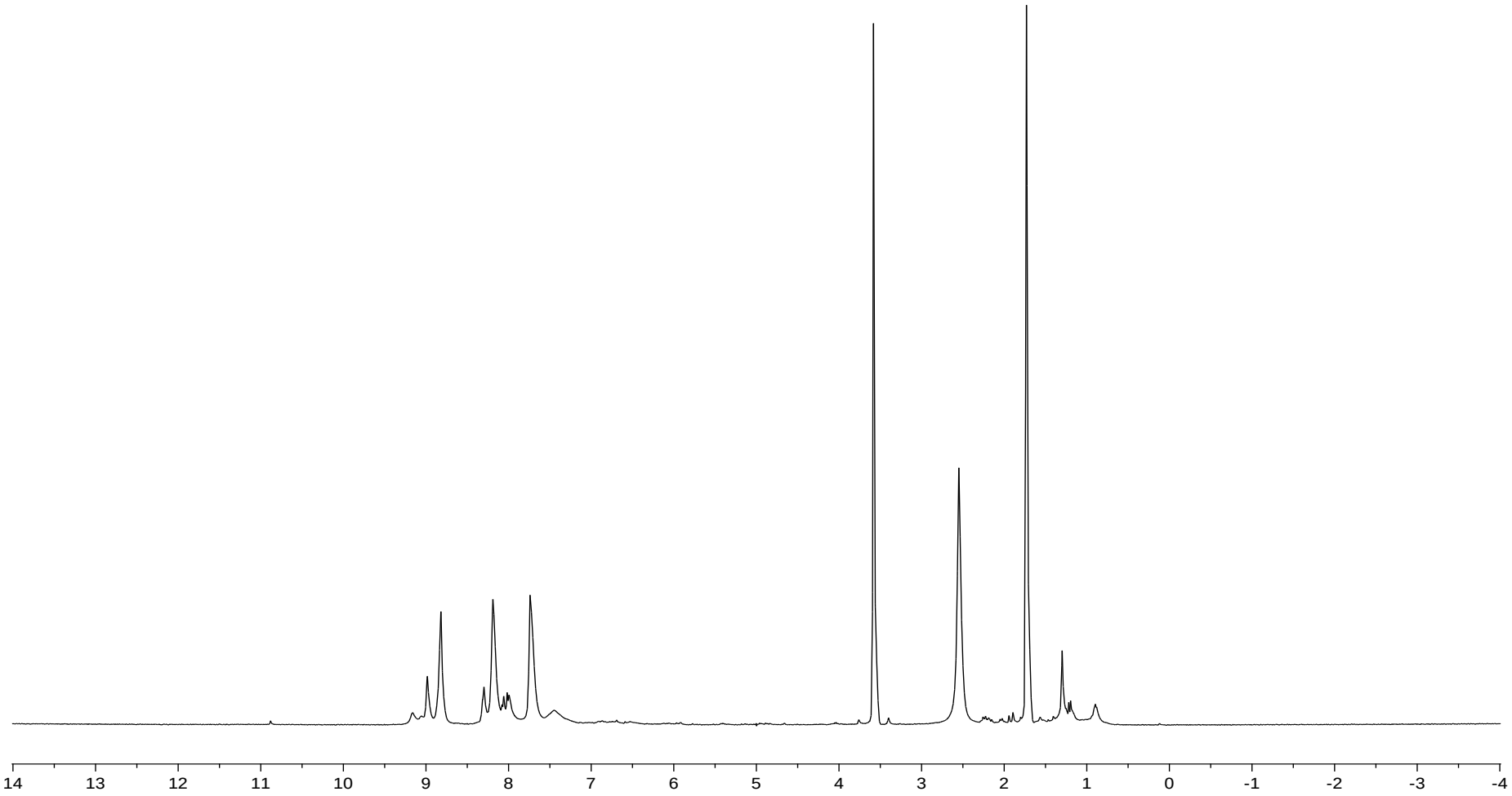

Figure 29. ^{1}H-NMR spectrum of compound **Zn-2**.

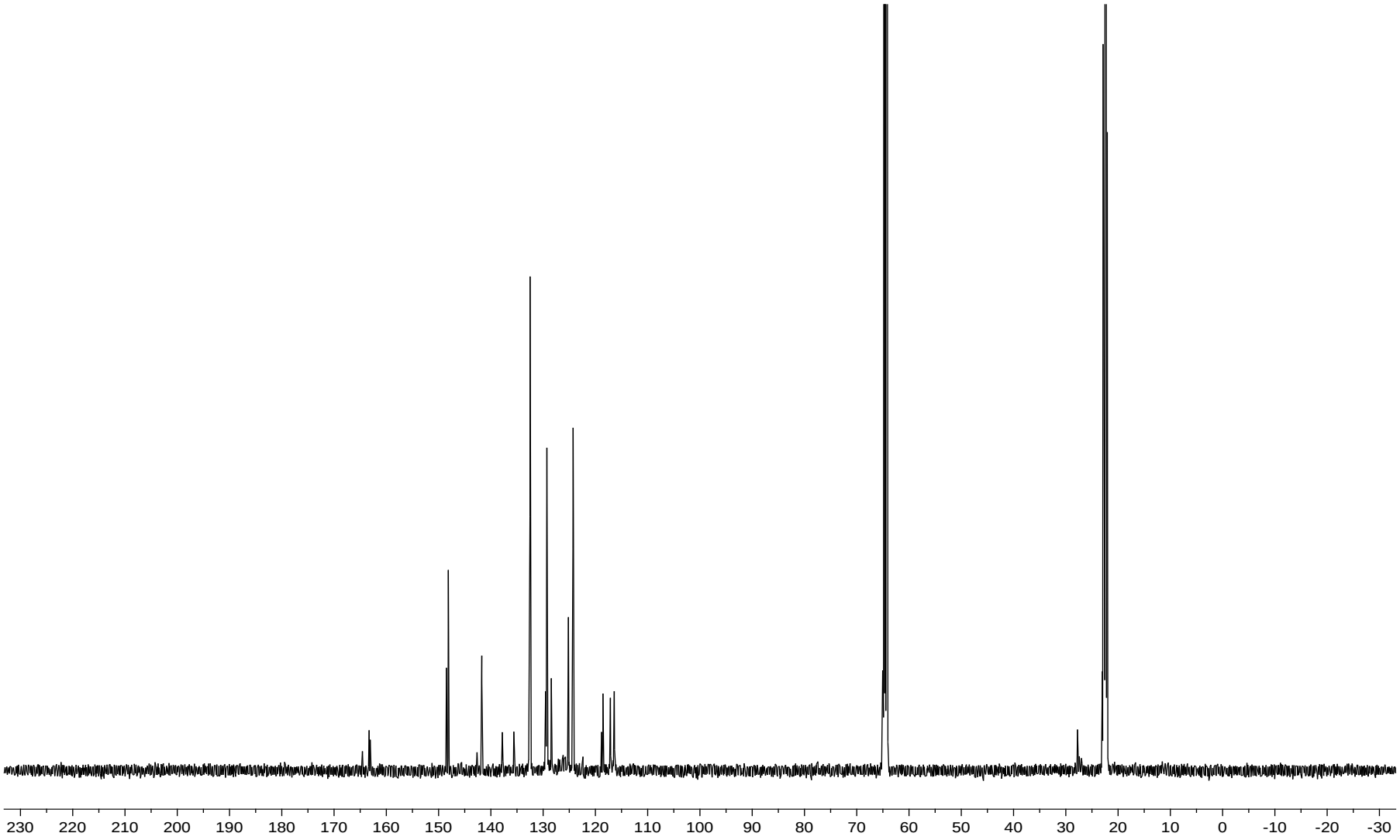

Figure 30. ^{13}C-NMR spectrum of compound **Zn-2**.

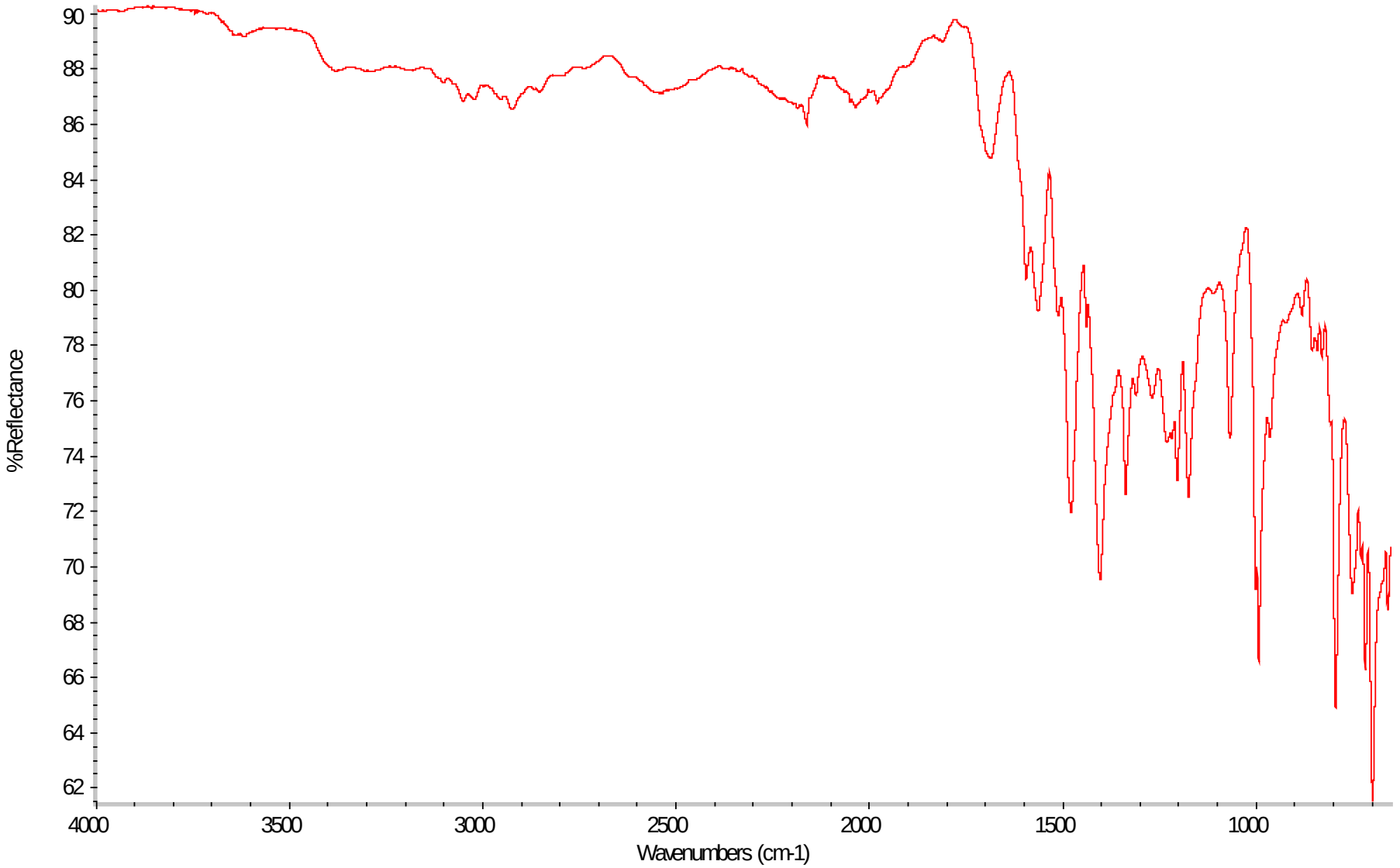

Figure 31. IR spectrum of compound **Zn-2**.

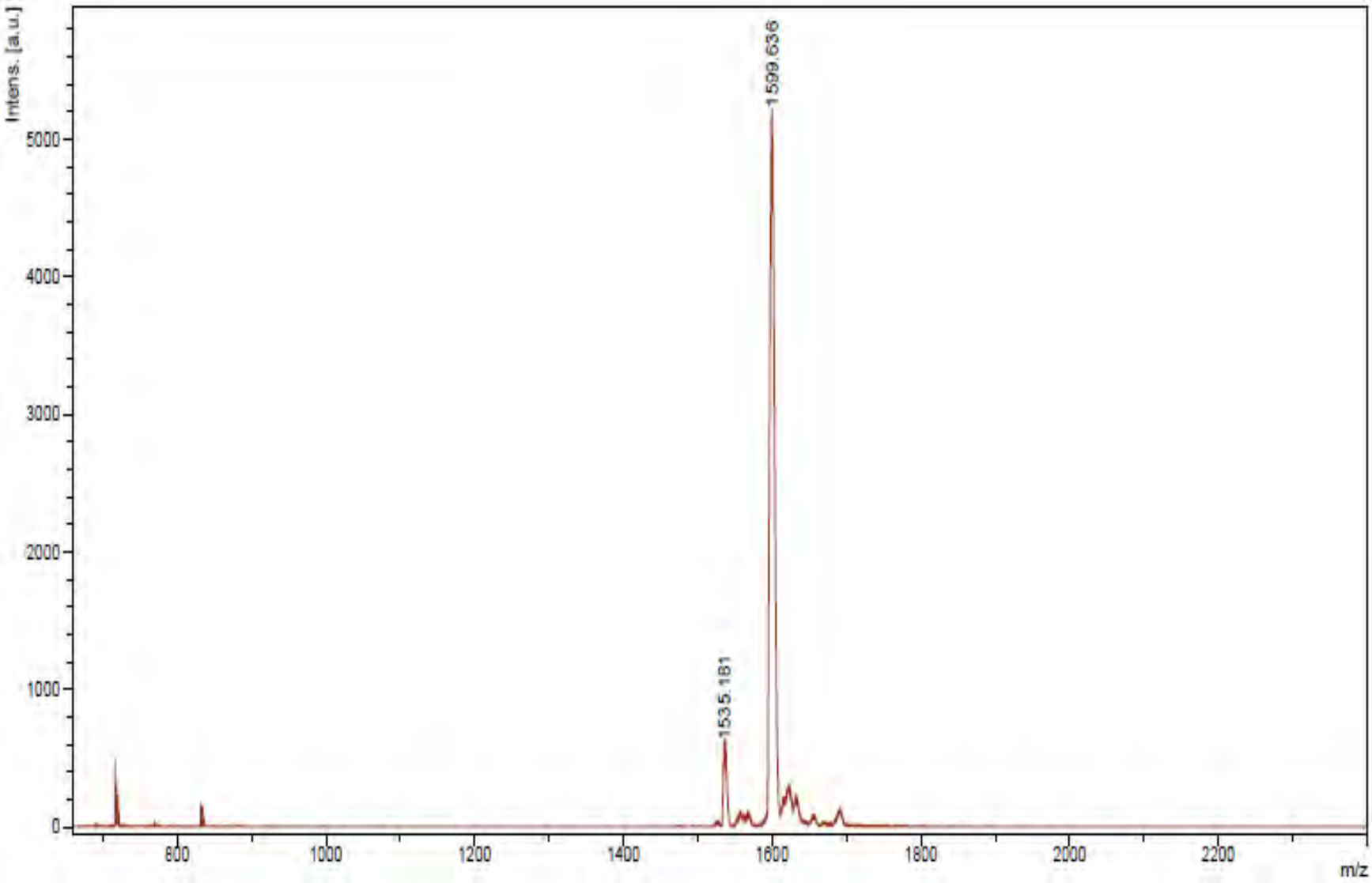

Figure 32. MALDI-TOF mass spectrum of compound **Zn-2**.

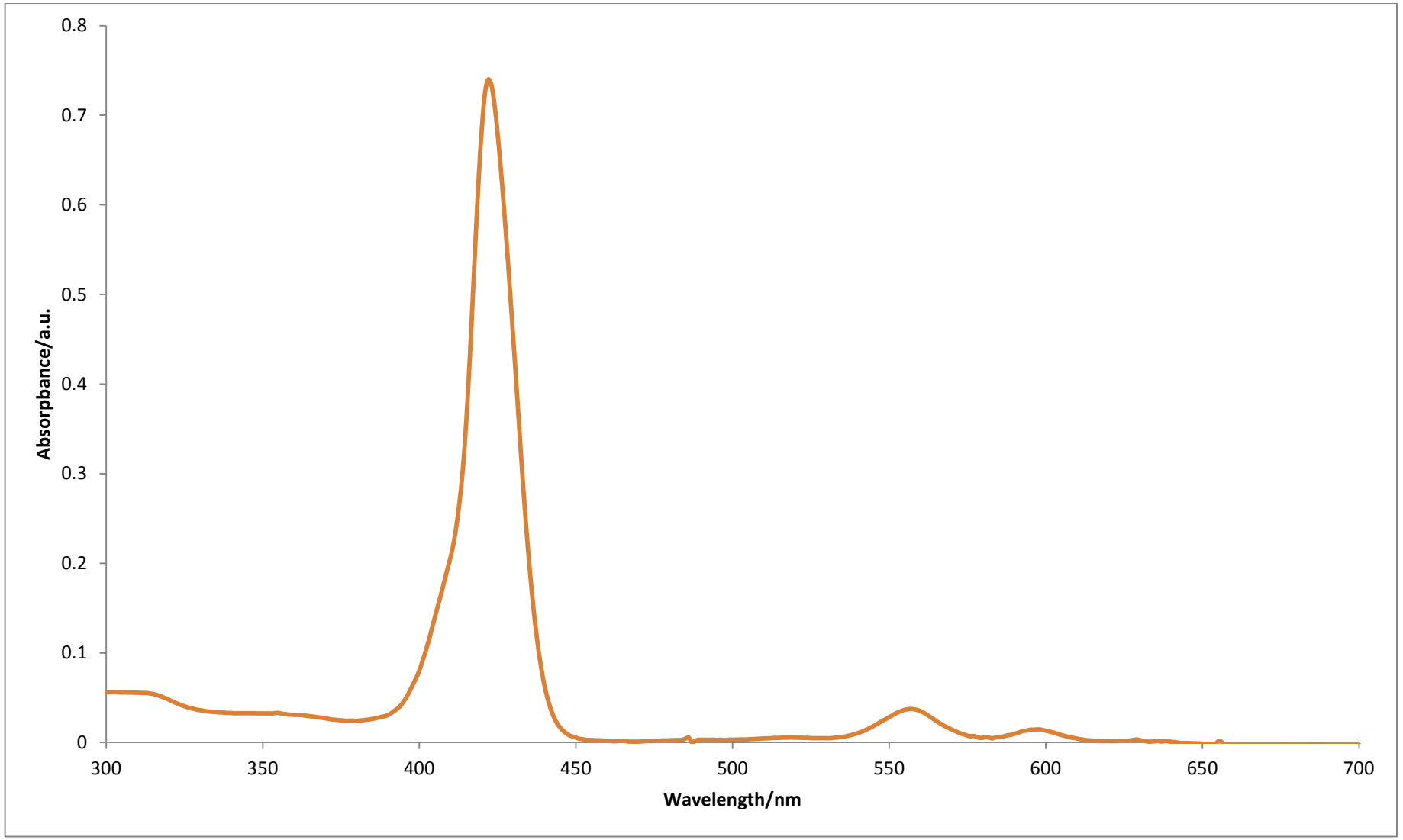

Figure 33. UV-Vis spectrum of compound **Zn-2**.

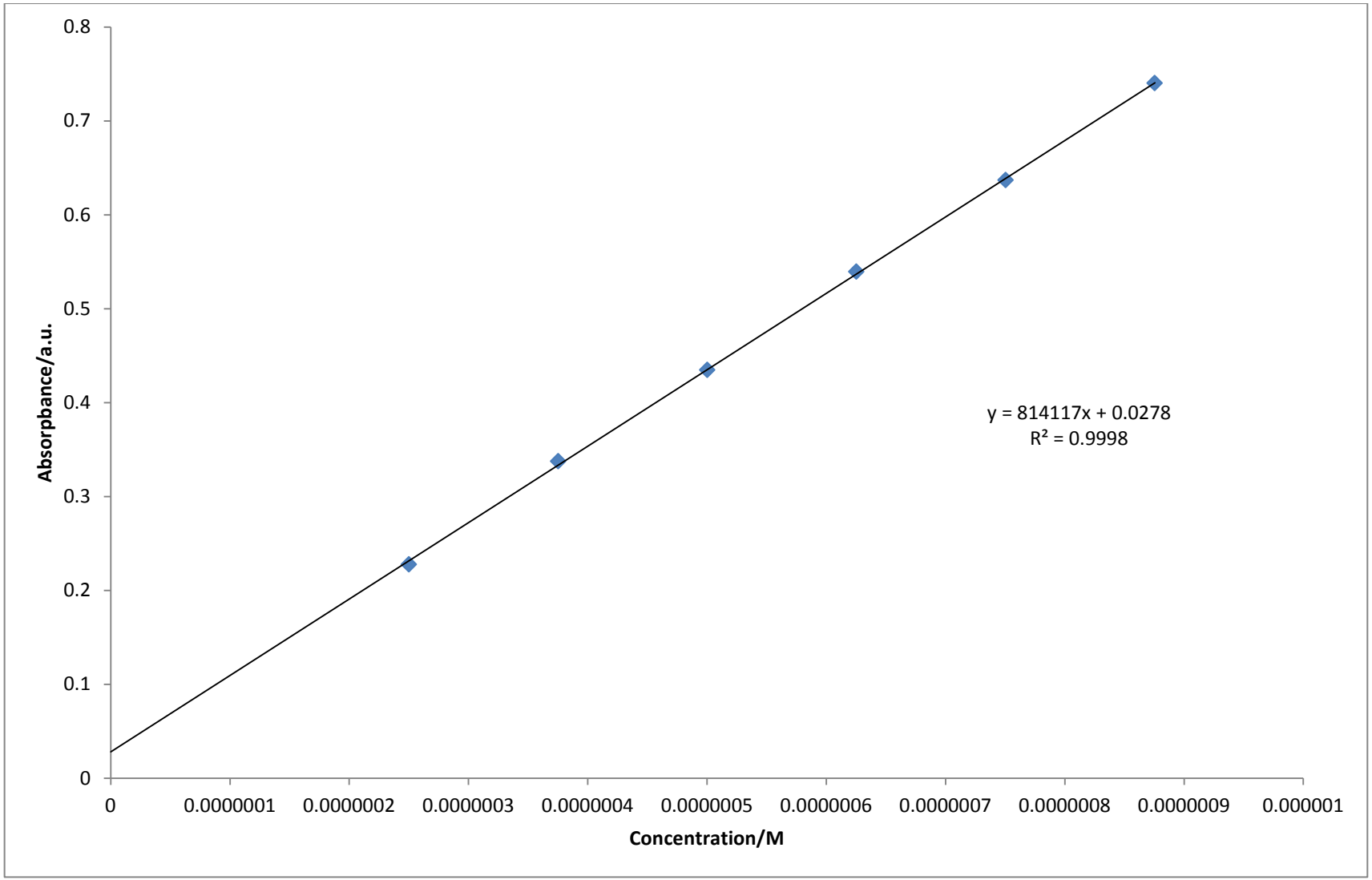

Figure 34. Calibration curve for quantitative determination of compound **Zn-2** in THF (λ_{abs} = 422 nm).

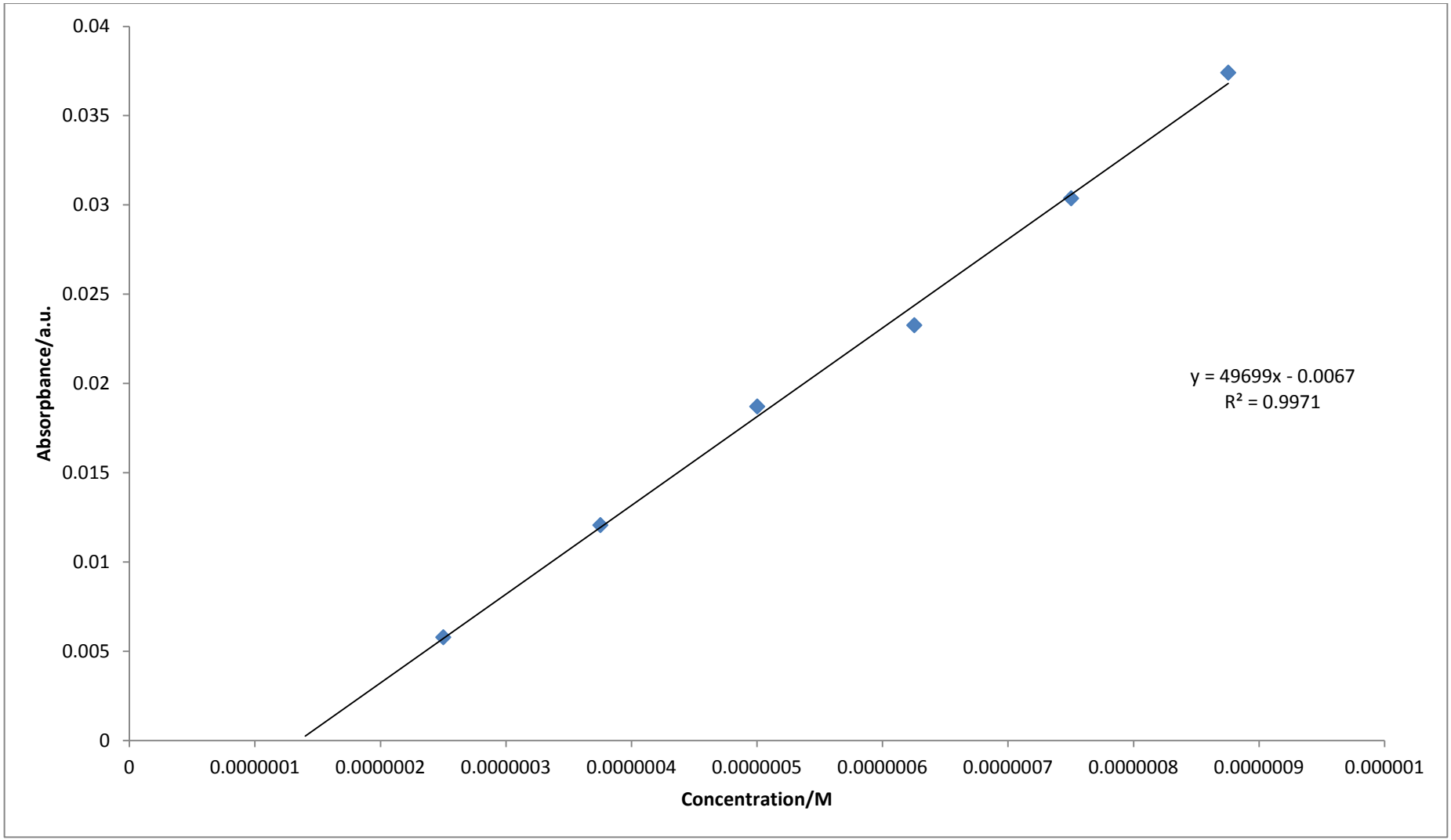

Figure 35. Calibration curve for quantitative determination of compound **Zn-2** in THF (λ_{abs} = 557 nm).

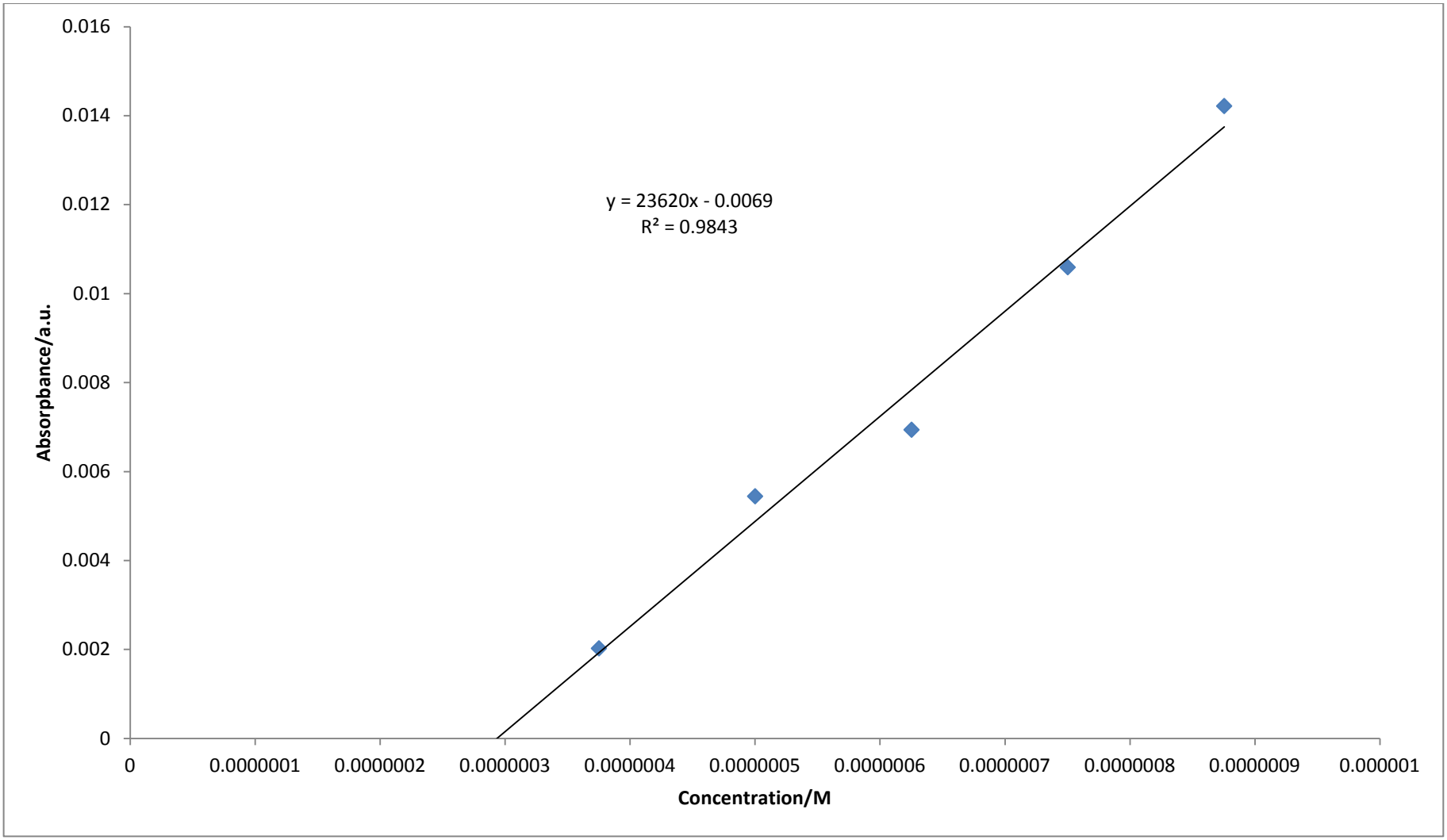

Figure 36. Calibration curve for quantitative determination of compound **Zn-2** in THF (λ_{abs} = 595 nm).

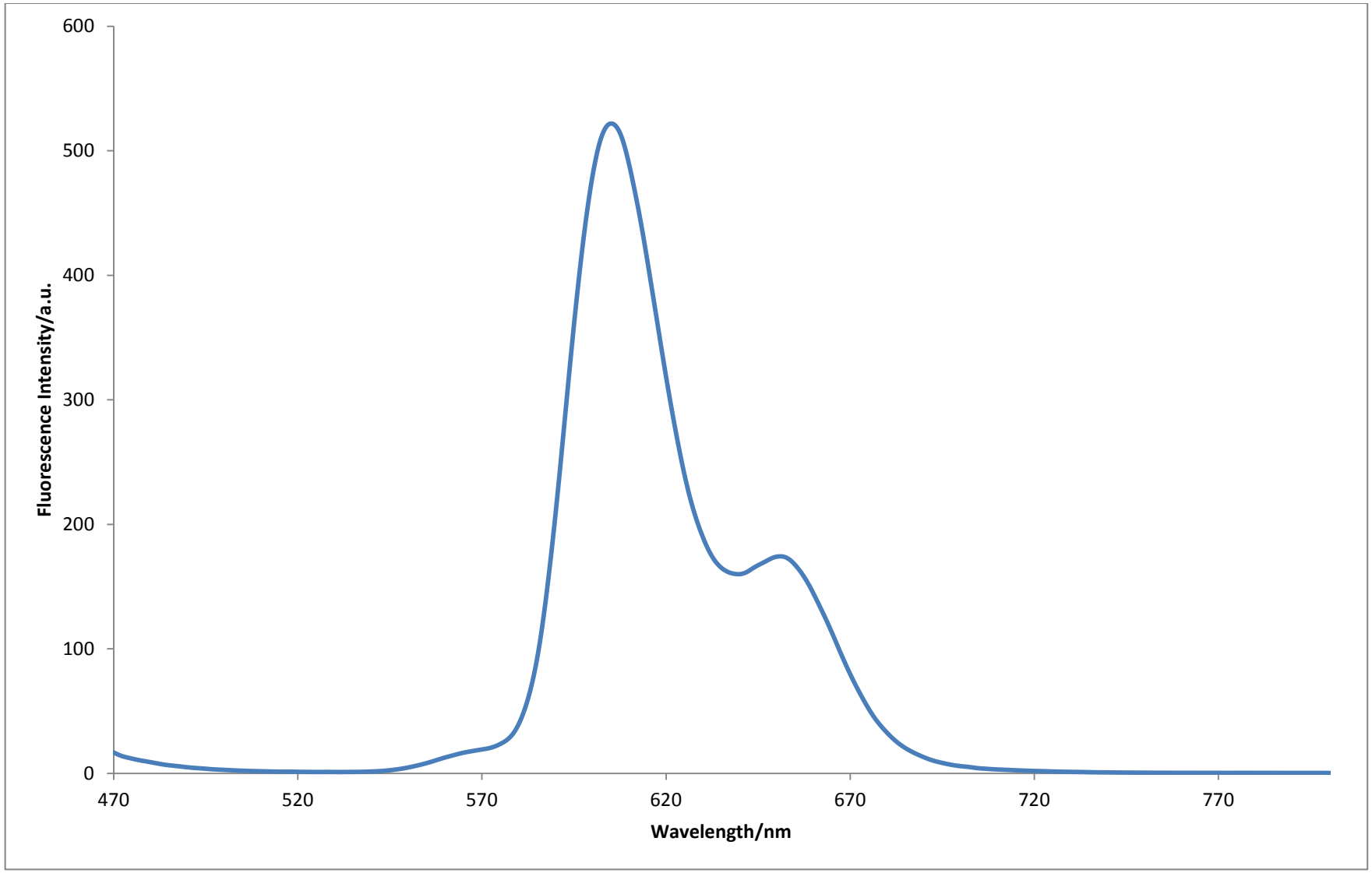

Figure 37. Fluorescence spectrum of compound **Zn-2**.

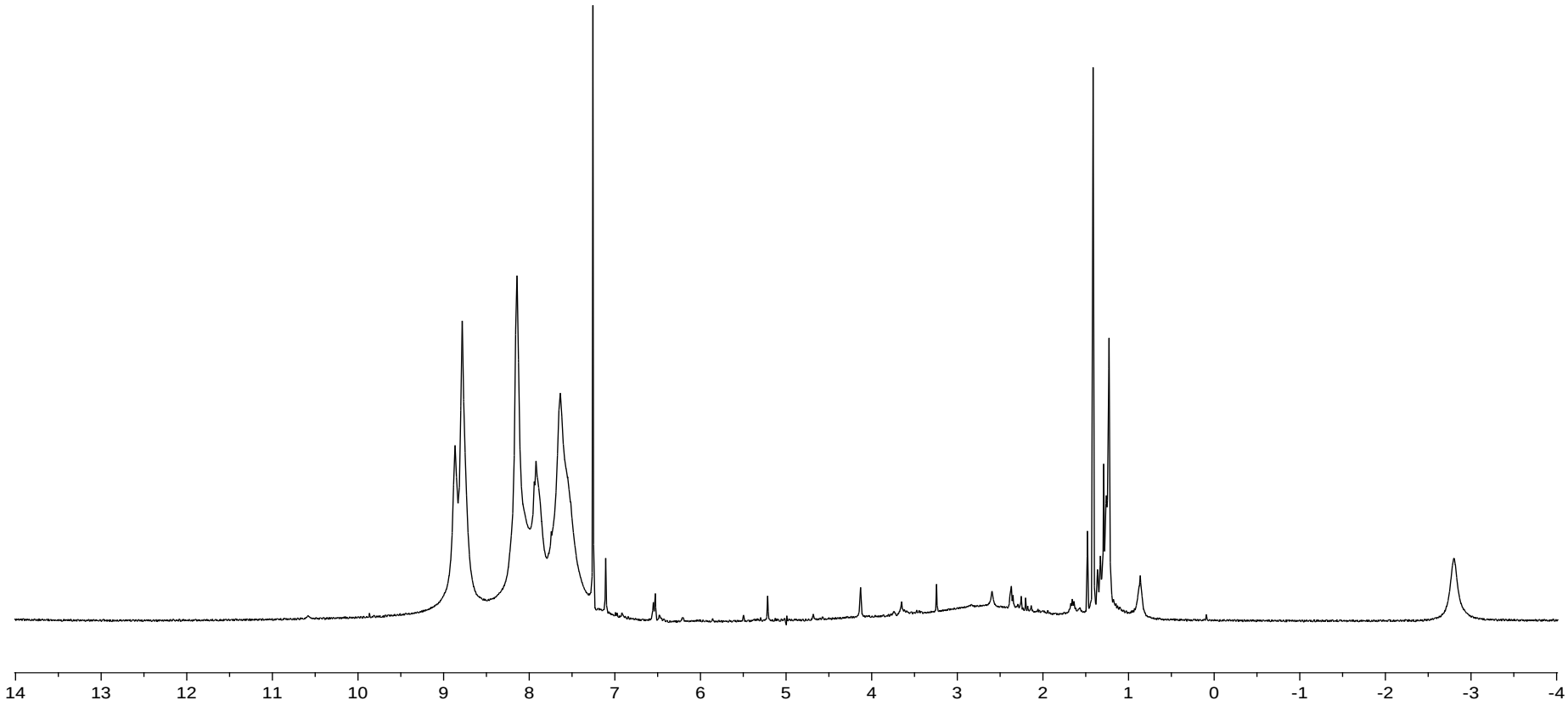

Figure 38. ^{1}H-NMR spectrum of compound **2**.

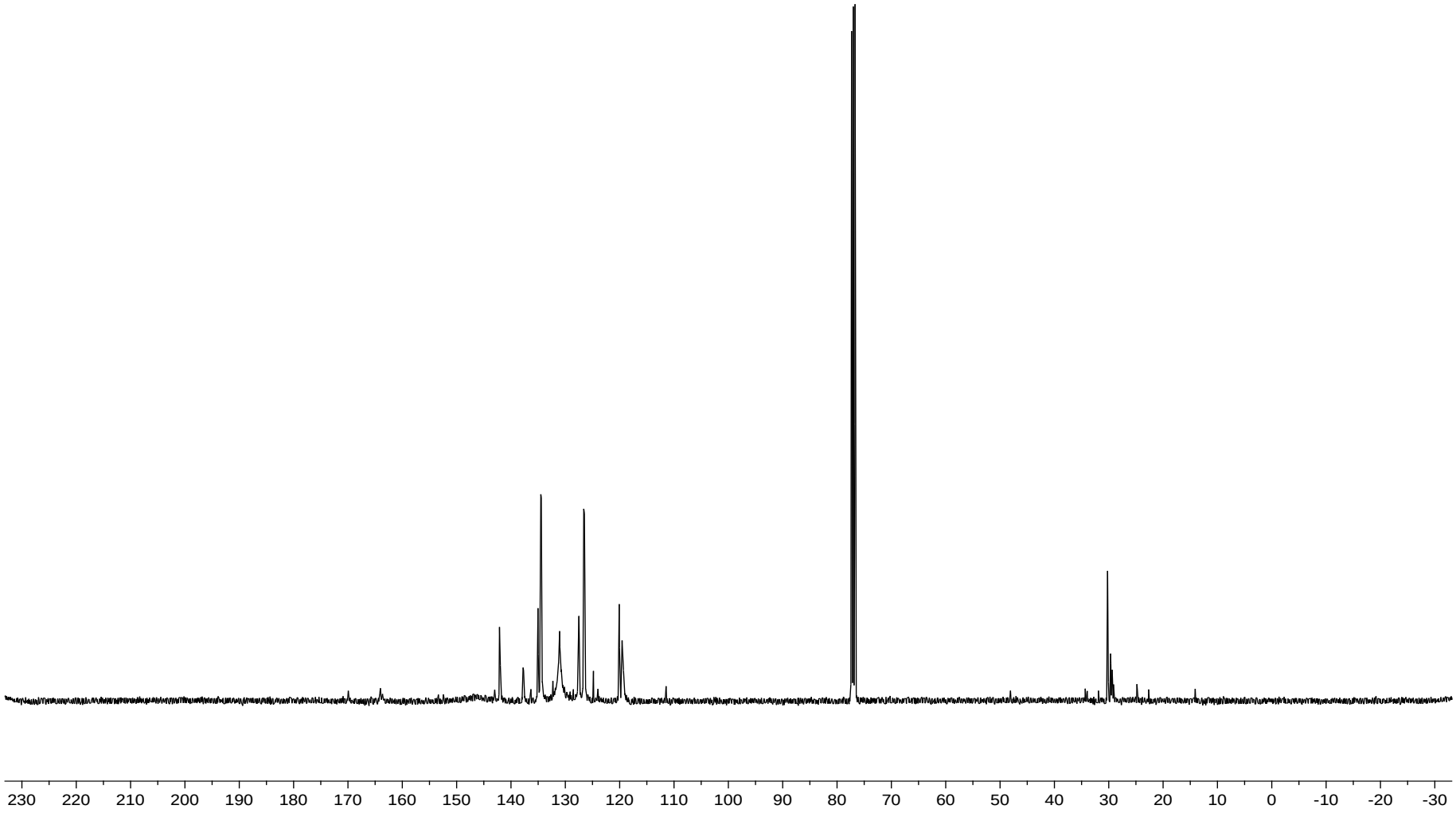

Figure 39. ^{13}C-NMR spectrum of compound **2**.

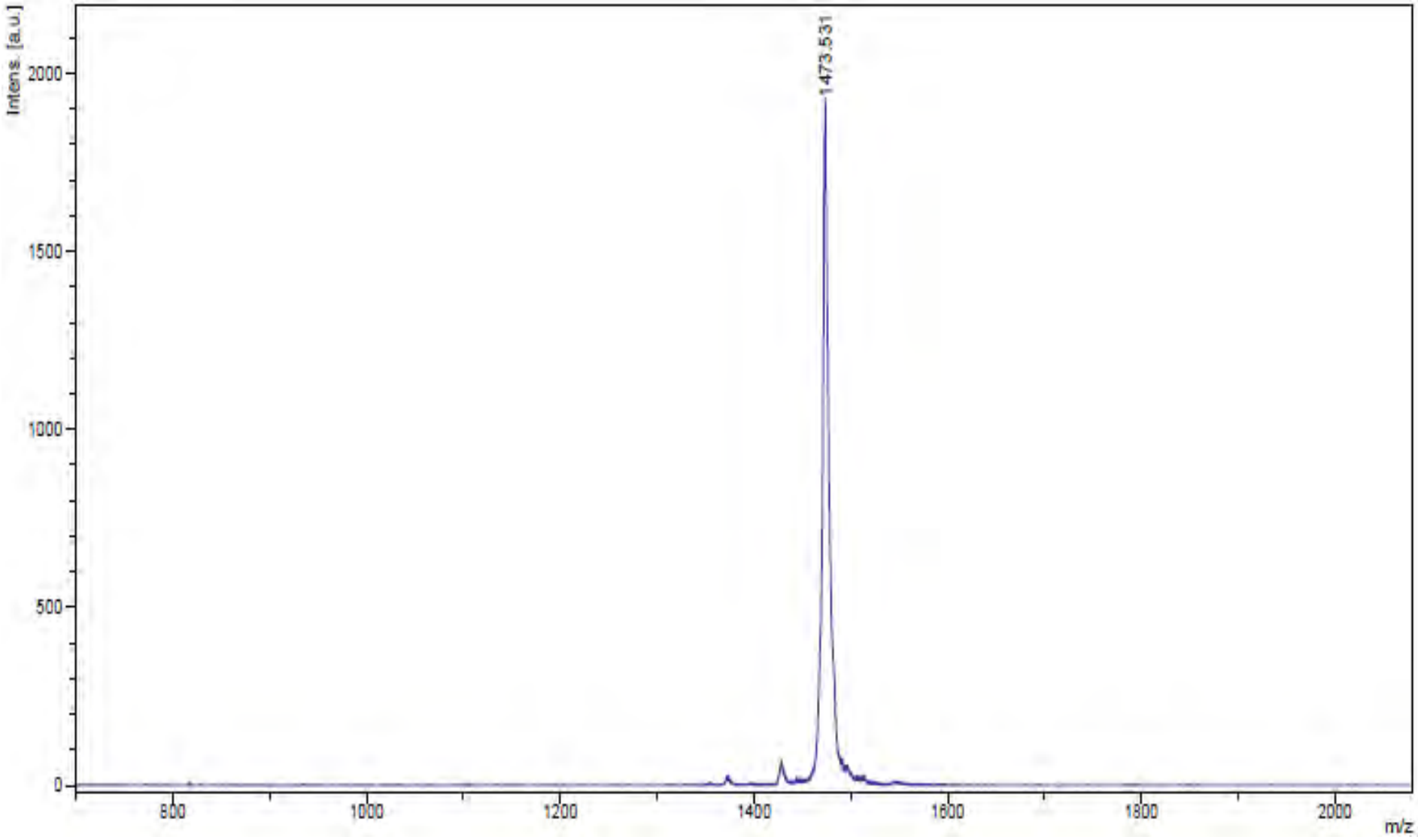

Figure 40. MALDI-TOF mass spectrum of compound **2**.

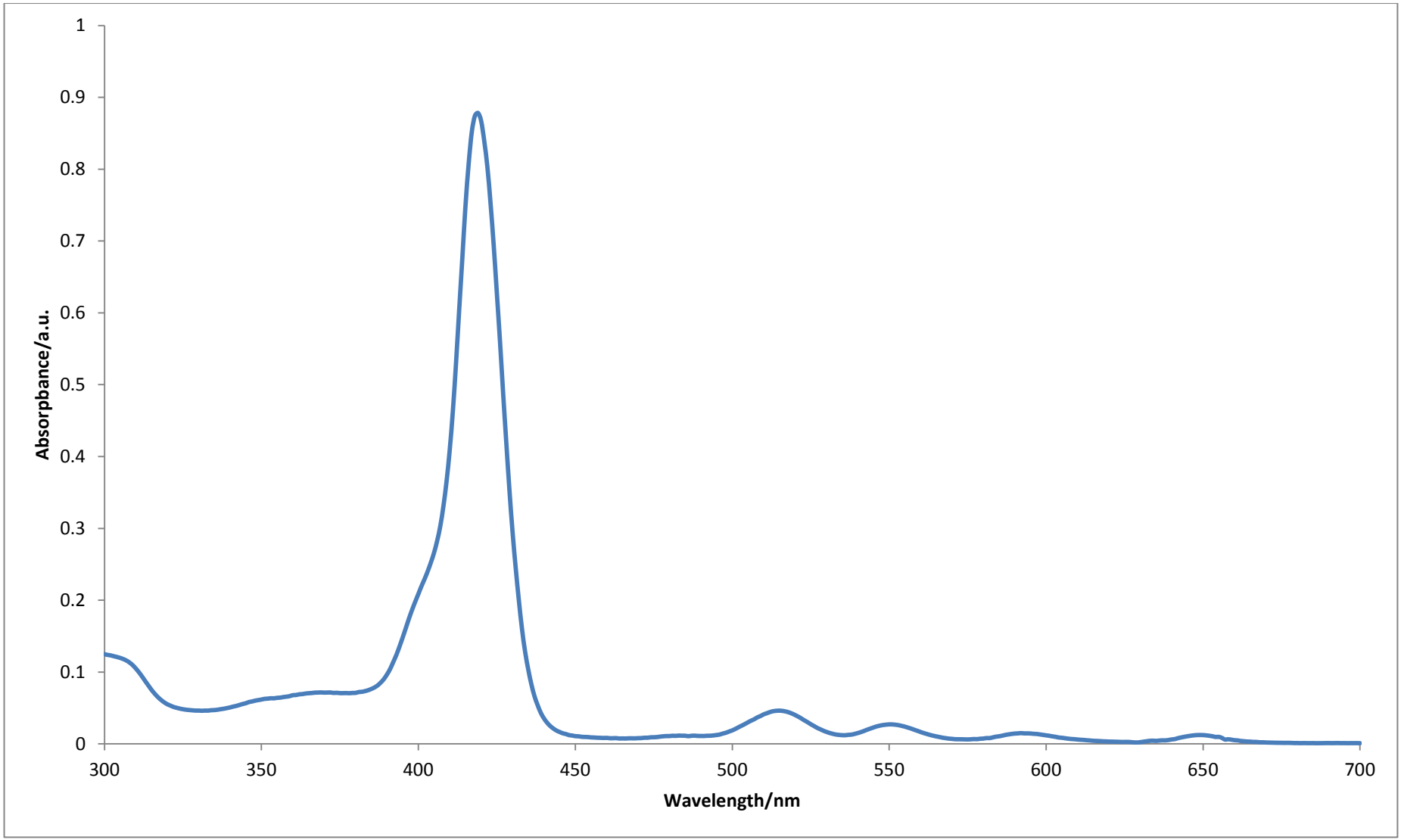

Figure 41. UV-Vis spectrum of compound **2**.

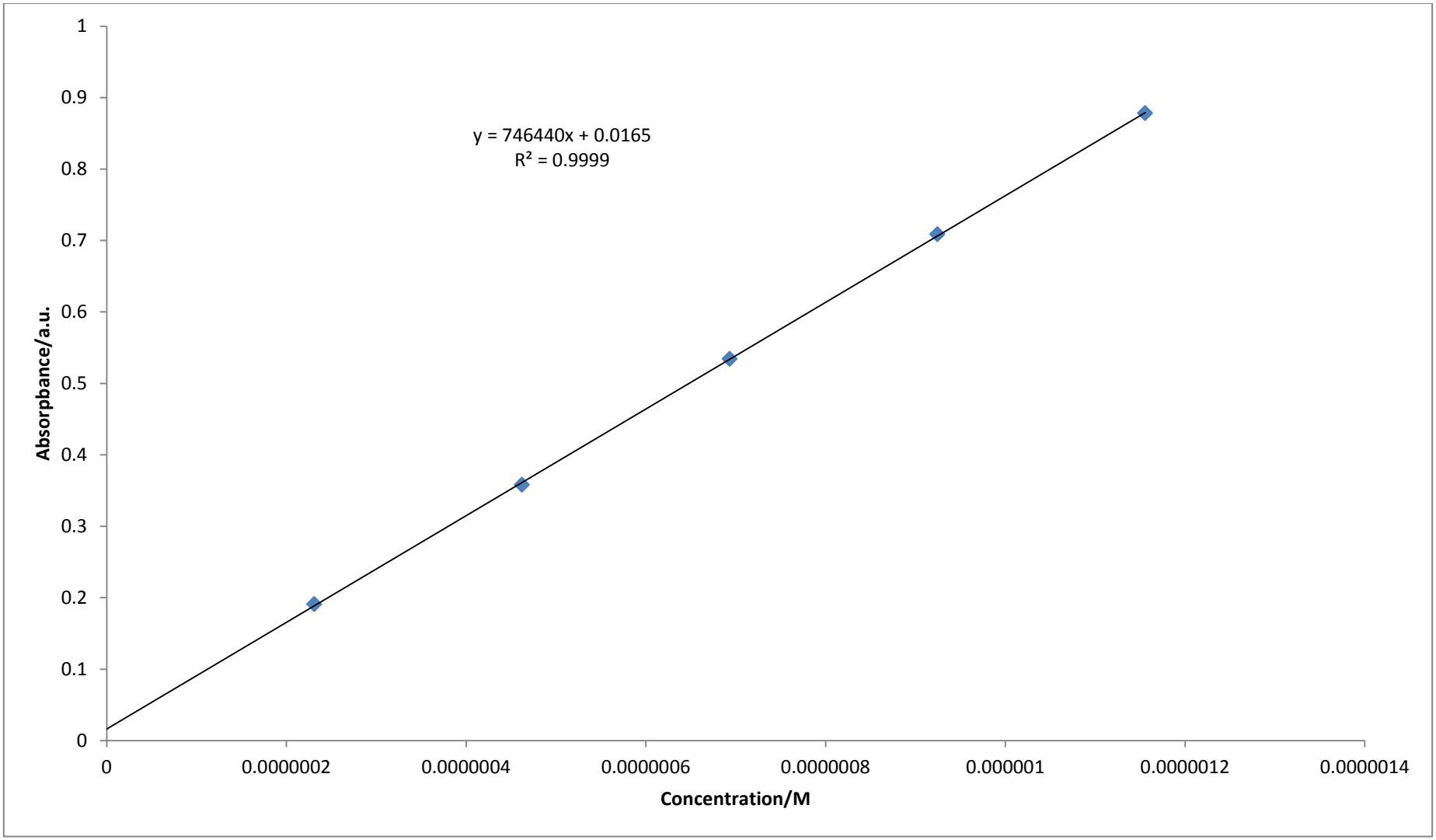

Figure 42. Calibration curve for quantitative determination of compound **2** in THF (λ_{abs} = 419 nm).

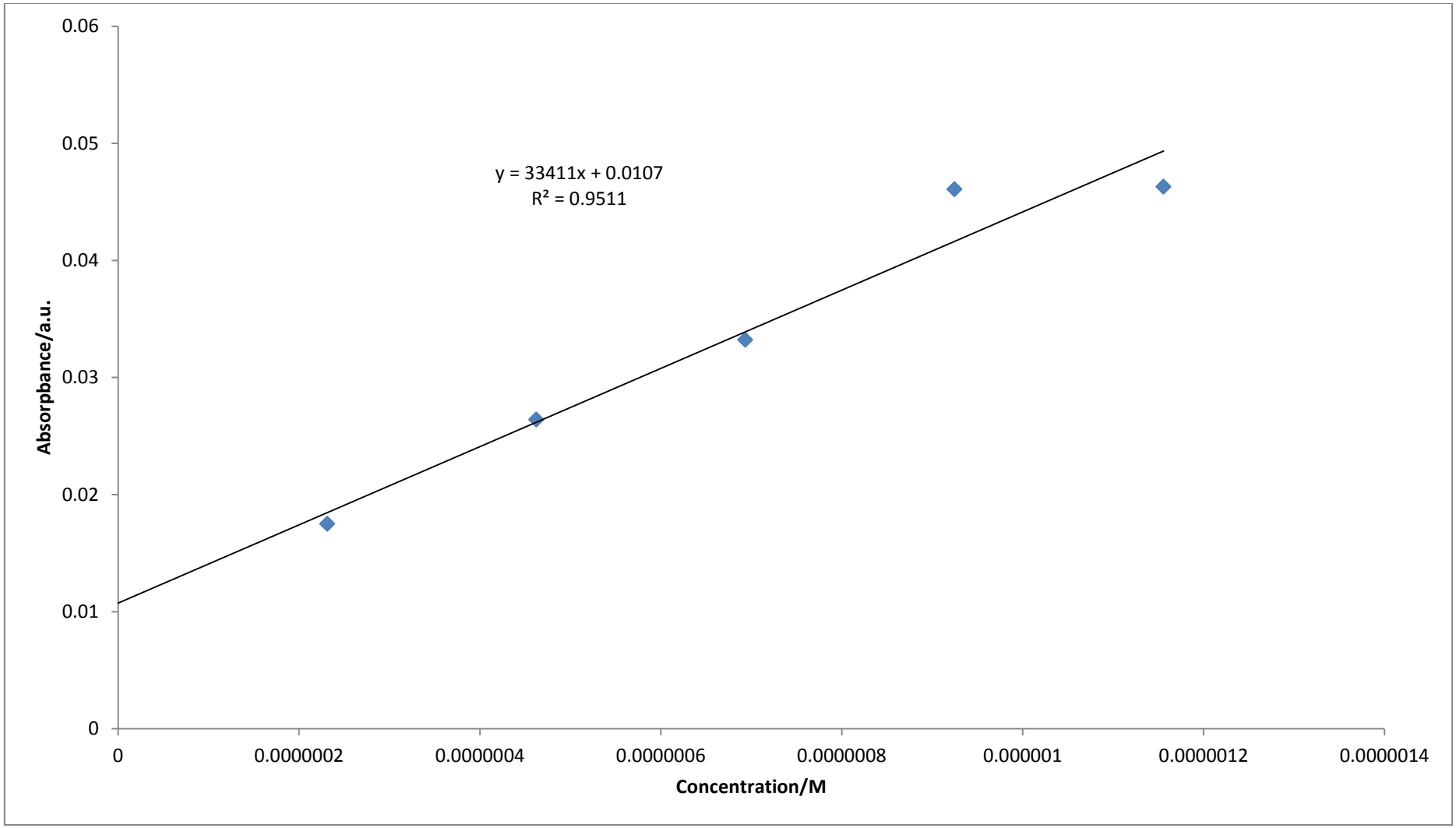

Figure 43. Calibration curve for quantitative determination of compound **2** in THF (λ_{abs} = 515 nm).

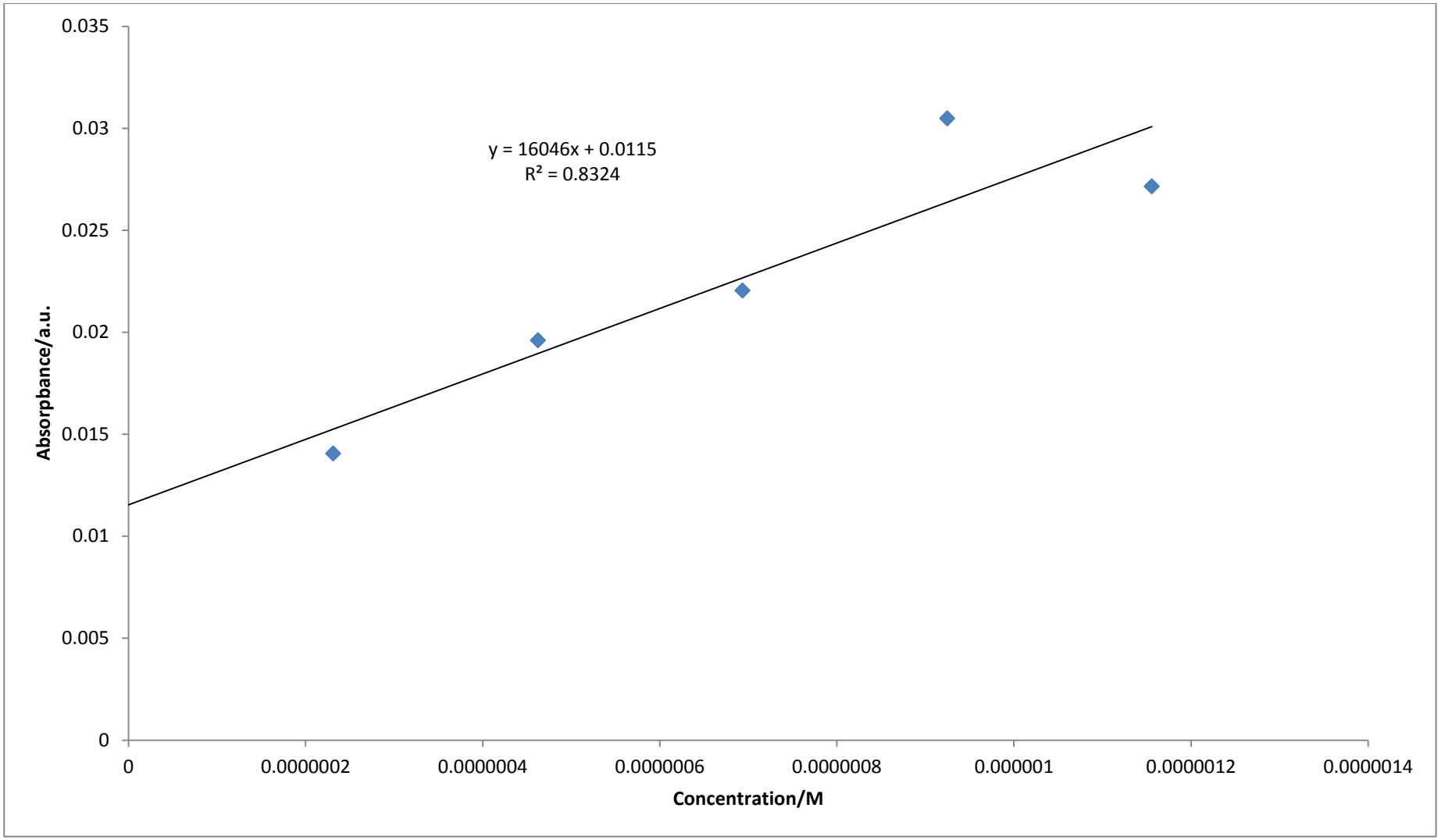

Figure 44. Calibration curve for quantitative determination of compound **2** in THF (λ_{abs} = 550 nm).

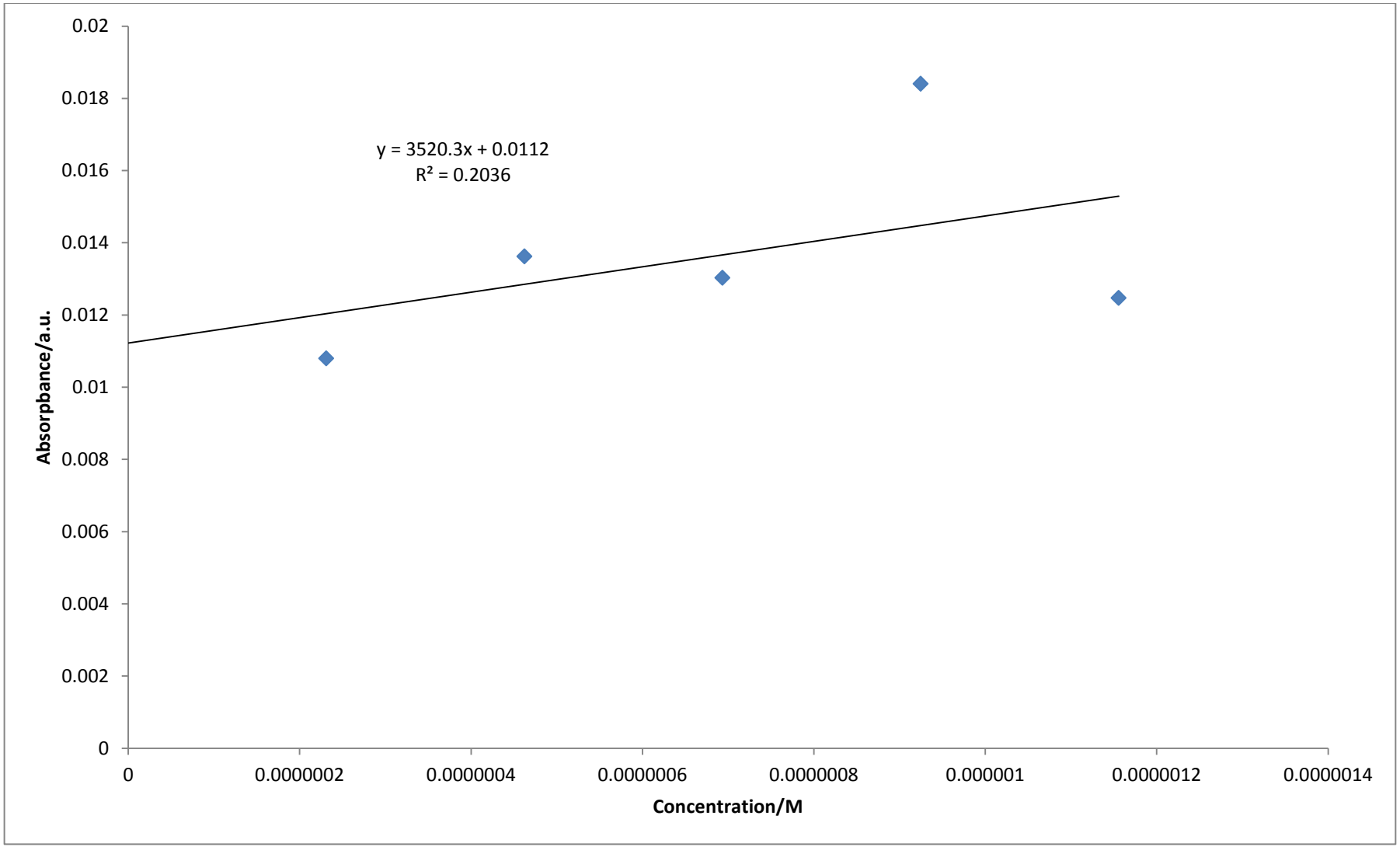

Figure 45. Calibration curve for quantitative determination of compound **2** in THF (λ_{abs} = 587 nm).

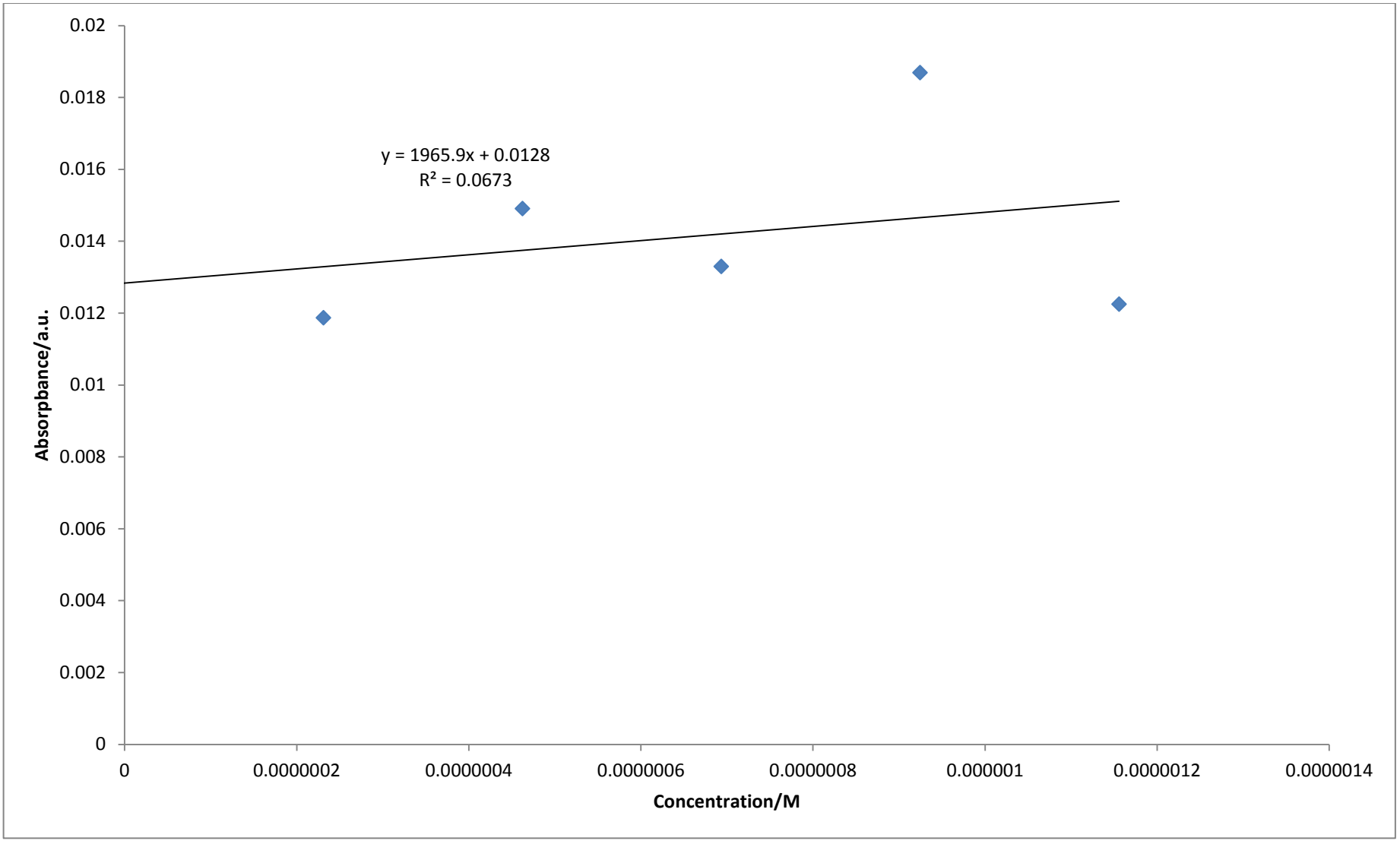

Figure 46. Calibration curve for quantitative determination of compound **2** in THF (λ_{abs} = 650 nm).

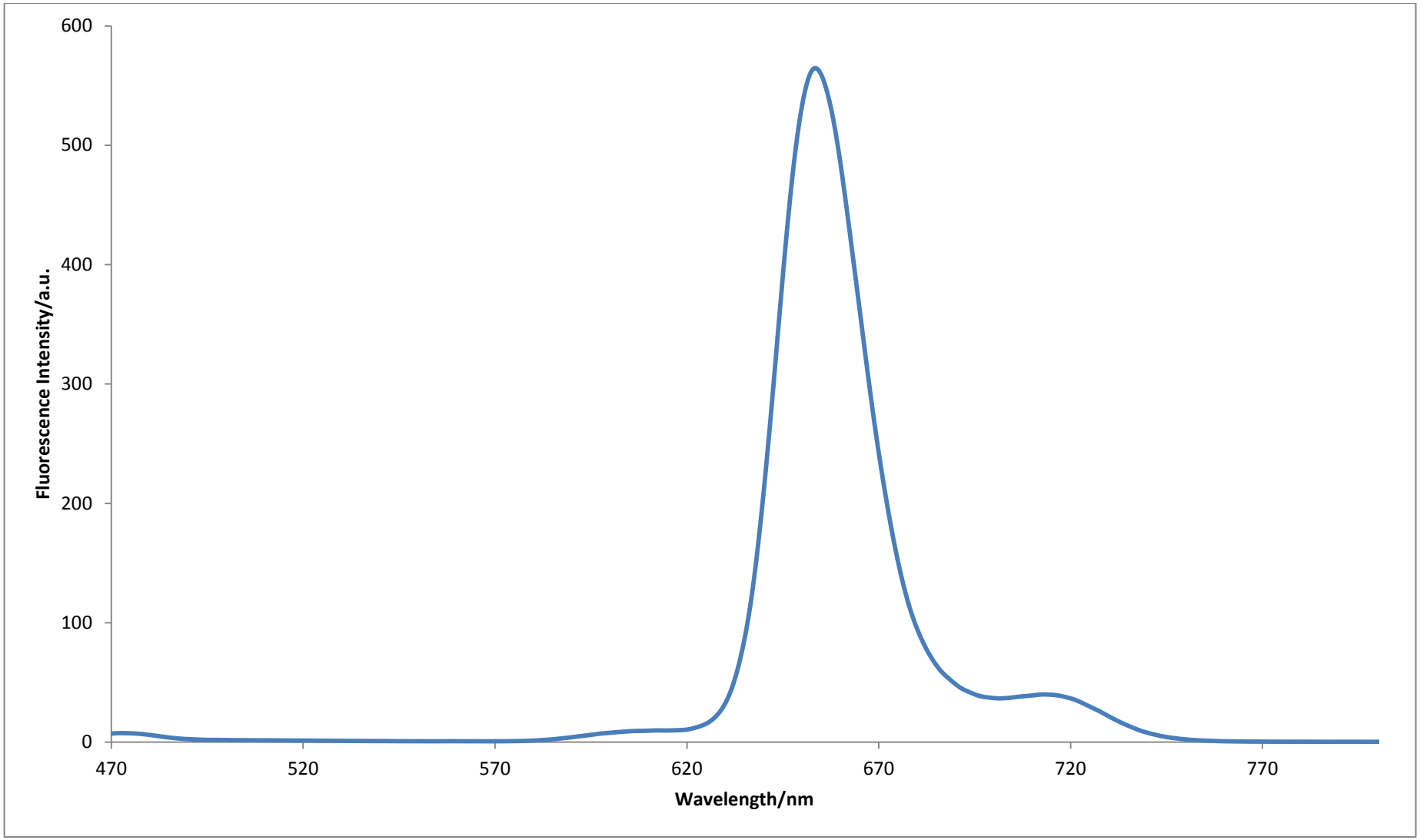

Figure 47. Fluorescence spectrum of compound **2**.

VITA

Mr. Arithat Luechai was born on December 4, 1985 in Prachuap Khiri Khan Province, Thailand. He got a Bachelor's Degree of chemistry in Faculty of Science at Silpakorn University, Nakorn Pathom in 2008. After that, he was admitted into a Master Degree program in Petrochemistry and Polymer Science, Faculty of Science, Chulalongkorn University, Bangkok in 2008 and completed the program in 2011.